

Aqueous extracts of *Dodonaea viscosa* var. *angustifolia* induce potent and selective cytotoxicity against diffuse large B cell lymphoma.

By

Babalwa Yekelo

YKLBAB001

SUBMITTED TO THE UNIVERSITY OF CAPE TOWN

In fulfillment of the requirements for the degree:

MSc (Med) in Haematology

Faculty of Health Sciences

UNIVERSITY OF CAPE TOWN



12 February 2024

Supervisor: A/Prof Shaheen Mowla

Division of Haematology, Department of Pathology, Faculty of Health Sciences, University of Cape Town.

The copyright of this thesis vests in the author. No quotation from it or information derived from it is to be published without full acknowledgement of the source. The thesis is to be used for private study or non-commercial research purposes only.

Published by the University of Cape Town (UCT) in terms of the non-exclusive license granted to UCT by the author.

Declaration

Name: Babalwa

Surname: Yekelo

Student Number: YKLBAB001

MSc Med by dissertation: MM095PTY11-Haematology

I, **Babalwa Yekelo**, hereby affirm that the research presented in this dissertation (MSc (Med)) is my original work (except where acknowledgments indicate otherwise) and that no part of it has been, is being, or will be submitted for another degree at this or any other university.

I have adhered to the Harvard convention for citation and referencing. Each contribution and quotation from the works of others in this MSc (Med) Dissertation has been appropriately attributed, cited, and referenced. I authorize the university to reproduce, in any manner necessary, either the entire contents or any portion thereof for research purposes.

Signature:

Date: 12 June 2024

Preface

The experimental work, which is detailed in this thesis, was conducted in the Department of Pathology (Division of Haematology) at the University of Cape Town, located in Observatory, Cape Town. This research project spanned from January 2022 until February 2024, making it a comprehensive and extensive project. Throughout this period, the author had the privilege of being under the expert guidance and supervision of A/Prof Shaheen Mowla, a renowned Figure in the field, and received invaluable support from Dr. Aaliyah Saferdien.

The findings presented in this thesis are entirely original and have not been previously submitted in any form for any degree or diploma at any University. Moreover, the author has ensured that proper acknowledgment is given to any external sources or references used in this research, thereby maintaining the integrity and credibility of the work.

Babalwa Yekelo (MSc candidate)

Associate Professor Shaheen Mowla (supervisor)

Dedication

I dedicate this endeavour to my mother, Nomvuyo Yekelo, who brought me into this world and loves me unconditionally.

Acknowledgments

“When you focus on the good, the good gets better.” – Abraham Hicks

During the past two years of my MSc degree, I have experienced significant growth in all areas of my life. One of the main contributors to this progress has been A/Prof Shaheen Mowla, who has served as my source of inspiration throughout this journey. With her guidance and assistance, I have gained renewed self-assurance in my academic pursuits. Furthermore, I have cultivated wholesome friendships and experienced a heightened sense of satisfaction and harmony with my goals. Thanks to A/Prof Shaheen Mowla's mentorship, I have changed my mindset and now prioritize becoming the best version of myself while consistently pursuing fresh and captivating opportunities. I now firmly believe in the authenticity of my dreams and strive to become an exceptional scientist who can bring not only scientific breakthroughs but also love and positivity to the world.

I would like to express my heartfelt gratitude to A/Prof Mowla as she has been my greatest inspiration. The way you have established a positive and healthy work atmosphere, along with your kindness and empathy, has truly influenced my personal growth. Thank you. I would also like to express my sincerest gratitude to the organizations and individuals mentioned below:

- The National Research Foundation, the University of Cape Town, and the Baxter Healthcare Bursary for their financial support.
- To Dr Aaliyah Saferdien for her invaluable support, love, friendship, and assistance with the experiments during this study.
- To Dr. Leonardo Alves De Souza Rios and Dr. Beatrice Ramorola for their assistance and valuable constructive feedback on the results of this work.
- To my lab mates Zahra Latib, Lungile Mapekula, Thando Khubeka, Lincon Mafokane, and everyone else within the Department of Pathology for their incredible support, love, friendship, and understanding.
- Department of Pathology and Prof Kamola Pillay for financial assistance.

- To the IDM Flow cytometry team, especially Dr. Tim Reid, for their assistance in analysing some of the results of this study.
- To my mother for her unconditional love, and support.
- To all my friends and family for the profound conversations, laughter, and memorable adventures we have shared.
- To my ancestors AmaDabane, AmaTshawe, Amampondo, AmaZangwa, AmaNqarhwane, OoJola. Camagu! May the darkness give way to Light!
- And lastly, to God for the precious gift of life.

Table of Contents

Declaration	i
Preface	ii
Dedication	iii
Acknowledgments	iv
Table of Contents	vi
List of Figures	ix
Chapter 1	ix
Chapter 2	ix
Chapter 3	ix
List of Tables	x
Chapter 1	x
Chapter 2	x
Abbreviations	xi
Abstract	xiv
Chapter 1	1
Background	1
1.1 The burden of cancer.	1
1.2 Haematological cancers.	1
1.3 Non-Hodgkin lymphoma.	2
1.3.1 Diffuse large B cell lymphoma.	3
1.4 The healing properties of traditional medicine.	5
1.4.1 Herbal natural compounds as anti-cancer agents.	5
1.4.2 Phytochemical compounds as anti-cancer agents.	6

1.5	<i>Dodonaea viscosa</i> , a traditional herbal medicine.	8
1.5.1	Known therapeutic characteristics of <i>Dodonaea viscosa</i>	8
1.5.2	Anti-cancer properties of <i>D. viscosa</i>	10
1.6	Preliminary data and Rationale of the proposed research.	10
1.6.1	Aims of the study.	11
Chapter 2		12
Materials and Methods.....		12
2.1	Cell lines and culture conditions.	12
2.2	Cryopreservation for long-term storage of cell lines.	12
2.3	Preparation of aqueous <i>Dodonaea viscosa</i> extract.	13
2.4	Cell treatments.	13
2.5	WST-1 cell viability assay.....	13
2.6	Determination of selectivity index (SI).	14
2.7	CellTrace proliferation assay.	14
2.8	Colony forming assay using MethoCult-based semi-solid media.	15
2.9	Cell cycle profiling.	15
2.10	Assessment of cell morphology using light microscopy.	16
2.11	Annexin V incorporation assay.	16
2.12	Caspase-Glo [®] 3/7 assay.....	17
2.13	Protein extraction and quantification.	17
2.14	SDS-PAGE and western blotting.....	18
2.14.1	Antibody incubation and protein detection.	20
2.14.2	Membrane stripping.....	20
2.15	Statistical analyses.....	21
Chapter 3.....		22
Results.....		22

3.1	Aqueous extract of <i>Dodonaea viscosa</i> exhibits selective cytotoxicity against diffuse large B cell lymphoma cells, relative to non-cancerous lymphoblastoid cells.	22
3.2	The proliferation and viability of DLBCL cells are inhibited by DVE as demonstrated by proliferation-tracking.	24
3.3	DVE inhibits the proliferation of DLBCL cells in a semi-solid medium.	26
3.4	DVE does not modify the cell cycle profile of DLBCL cells and induces cell death.	28
3.5	DLBCL cells exposed to DVE display typical apoptotic morphological features.	30
3.6	Annexin V assay shows widespread cell death of DVE-treated DLBCL cells, relative to LCLs.	33
3.7	DVE potently induces the activity of early-stage executioner caspase-3/7.	35
3.8	DVE modulates the expression of apoptotic markers caspase-3 and PARP-1.	37
Chapter 4		40
Discussion		40
Conclusion		45
References		47
Appendix A		79
Appendix B		81
Appendix C		87
Appendix D		88

List of Figures

Chapter 1

Figure 1.1. The most common types of lymphoma diagnosed in patients who underwent bone marrow biopsy (BMB), at Groot Schuur Hospital, between 2004 and 2014 (inc.), per HIV status. 3

Figure 1.2. DLBCL subtypes are distinguished by their cellular origins and genetic lesions..... 4

Chapter 2

Figure 2.1. Diagram illustrating the “Western Blot Sandwich” cassette orientation for protein transfer.. 19

Chapter 3

Figure 3.1. Determination of IC50 and SI values for the aqueous extract of *D. viscosa* (DVE) using the WST-1 viability assay. 23

Figure 3.2. DVE slows down the proliferation of DLBCL cells in comparison to LCLs and induces cell death. 25

Figure 3.3. DVE inhibits the proliferation of DLBCL cells in a semi-solid medium..... 27

Figure 3.4. DVE does not modify the cell cycle profile of DLBCL cells and induces cell death..... 29

Figure 3.5. Morphological analysis of cells treated with DVE..... 32

Figure 3.6. DVE induces apoptosis in DLBCL cells. 35

Figure 3.7. DVE potently induces the activity of early-stage executioner caspase-3/7.. 36

Figure 3.8. DVE modulates the expression of apoptotic markers caspase-3 and PARP-1..... 39

List of Tables

Chapter 1

Table 1.1. Summary of selected approved phytochemical compounds used as anti-cancer agents to treat diffuse large B cell lymphoma 7

Table 1.2 Summary of selected reported therapeutic characteristics of *D. viscosa*. 9

Chapter 2

Table 2.1. Components of protein samples loaded onto SDS-PAGE gels 19

Abbreviations

7-AAD	7-Amino-Actinomycin
ABC-DLBCL	Activated B Cell-like Diffuse Large B Cell Lymphoma
AgNPs	Silver nanoparticles
AIDS	Acquired Immunodeficiency Syndrome
ALT	Alanine aminotransferase
ANOVA	Analysis of Variance
AST	Aspartate aminotransferase
ART	Antiretroviral therapy
BCA	Bicinchonic acid
BCR	B cell receptor
BL	Burkitt Lymphoma
BSA	Bovine Serum Albumin
CAM	Complementary and Alternative Medicine
CANSA	Cancer Association of South Africa
CD	Cell debris
CFSE	Carboxyfluorescein Succinimidyl Ester
CO ₂	Carbon dioxide
CNS	Central Nervous System
CS	Cell Swelling
COO	Cell of origin
CT	Computed tomography
CVB3	Coxsackievirus B3
DLBCL	Diffuse Large B Cell Lymphoma
DMSO	Dimethyl sulfoxide
DTT	Dithiothreitol
DV	<i>Dodonaea viscosa</i>
DVE	<i>Dodonaea viscosa</i> extract

EBV	Epstein-Barr virus
EPOCH	Etoposide, prednisone, vincristine, cyclophosphamide, and doxorubicin
FBS	Foetal Bovine Serum
GC	Germinal Centre
GCB-DLBCL	Germinal Centre B Cell-like Diffuse Large B Cell Lymphoma
HAART	Highly active antiretroviral therapy
HIV	Human Immunodeficiency Virus
HL	Hodgkin lymphoma
HRP	Horseradish peroxidase
HTLV-1	Human T-Cell Leukaemia virus type-1
IC ₅₀	Drug concentration can inhibit cell viability by 50%.
IHC	Immunohistochemistry
LCL	Lymphoblastoid Cell Line
LDH	Lactose dehydrogenase
MB	Membrane Blebbing
M.tb	<i>Mycobacterium tuberculosis</i>
MTT	3-[4,5-dimethylthiazol-2-yl]-2,5 diphenyl tetrazolium bromide
MRI	Magnetic resonance imaging
NCI	National Cancer Institute
NF	Nuclear fragmentation
NF-κB	Nuclear Factor kappa B
NOS	Not otherwise specified
P1	Parental cell generation
P2	Daughter cell generation
PAGE	Polyacrylamide Gel Electrophoresis
PARP-1	Poly ADP-ribose Polymerase
PBS	Phosphate Buffered Saline
PBST	Phosphate Buffered Saline and 0.1% Tween-20
PET	Positron emission imaging

PI	Protease Inhibitor
P/S	Penicillin/Streptomycin
R-CHOP	Rituximab-cyclophosphamide, doxorubicin, vincristine, and prednisone
RPMI	Roswell Park Memorial Institute
RTK	Receptor Tyrosine Kinases
RVSA-11	Rotavirus SA-11
SA	South Africa
SDS	Sodium Dodecyl Sulphate
SDS-PAGE	Sodium Dodecyl Sulphate Polyacrylamide Gel Electrophoresis
SEM	Standard Error of the mean
SI	Selectivity Index
TB	Tuberculosis
TBS	Tris Buffered Saline
TBST	Tris Buffered Saline and 0.1% Tween-20
TCM	Traditional Chinese medicine
TEMED	Tetramethyl ethylenediamine
TM	Traditional medicine
UICC	Unions for International Cancer Control
UT	Untreated
T	Treated
WHO	World Health Organisation
WST-1	2-(4-iodophenyl)-3-(4-nitrophenyl)-5-(2,4-disulfophenyl)-2H-tetrazolium

Abstract

Cancer is a major cause of death globally, with approximately 10 million deaths in 2020. In South Africa, the number of new cancer cases is expected to double by 2030. Non-Hodgkin lymphoma (NHL), which represents a group of cancers originating from lymphoid tissues, was ranked the 11th most common cancer globally, accounting for 544,000 new cases and 260,000 deaths in 2020. In South Africa, NHL ranks among the top five invasive cancers among both males and females. Diffuse large B cell lymphoma (DLBCL), an aggressive B-cell derived cancer is the most prevalent cancer within the NHL group of cancers. DLBCL can be grouped into two main subtypes, namely the germinal-centre B cell (GCB) and the activated-B cell (ABC) subtypes, with the ABC subtype reported to have a more aggressive clinical course than the GCB subtype. Additionally, DLBCL is an HIV-associated cancer and is, thus, highly overrepresented among HIV-infected individuals. Currently, 30-40 % of DLBCL patients relapse or develop refractory disease following treatment with the standard DLBCL therapy. This figure is worse among HIV-infected DLBCL patients. There is therefore a need to develop more effective therapeutic regimens to treat this cancer.

In recent years there has been increasing focus, by cancer sufferers, on the use of alternative therapies for treating their disease. An estimated 80% of the South African population seek health care from traditional healers. Medicinal plants form a major part of the repertoire of tools that these traditional healers use to treat their patients. Many plant species have already been the source of bioactive compounds used to develop currently approved cancer drugs. In the current research, the anti-cancer potential of aqueous extracts of *Dodonaea viscosa* (DVE), a plant commonly used by traditional healers in the Western Cape region of South Africa, against DLBCL cells, is being investigated. Previously published reports showed that extracts of *Dodonaea viscosa* can inhibit the growth of several types of cancer cells, including breast, prostate, and colon cancer. There are currently no published reports on the effects of DVE on DLBCL cells.

The IC₅₀ of DVE against two DLBCL cell lines (HBL-1 and SU-DHL-4) was determined, relative to a non-cancerous lymphoblastoid cell line (LCL) (PB-LCL-B95-8H) using viability assays. Thereafter, the effect of DVE on proliferation was investigated using proliferation-tracking and colony formation in a semi-solid medium. The effect of DVE on the cell cycle was also investigated. Lastly, induction of apoptosis was determined using microscopy, Annexin V incorporation assay, caspase activity assay, and western blotting to assess the expression of apoptotic markers.

Viability assays showed that DVE could potently and selectively inhibit the proliferation of two DLBCL cell lines, namely the GCB cell line SU-DHL-4, and the ABC cell line HBL-1, relative to the non-cancerous lymphoblastoid cell line PB-B95-8H. This converted into a favorable selectivity index of 2.25 for SU-DHL-4 and 3 for HBL-1, demonstrating that DVE preferentially triggers cell death in the cancer cells. The cell-Trace proliferation assay, which tracks live cell proliferation over time, showed a 2.3-fold and 1.3-fold reduction of daughter cells (P2 generation) in the DVE-treated SU-DHL-4 and HBL-1 cells relative to untreated SU-DHL-4 and HBL-1 cells respectively, with the non-cancerous cells being much less affected. The effect of proliferation was further confirmed through a colony-forming assay, which showed potent inhibition of colony formation over 7 days, by DVE, for both cancer cell lines. No notable changes in the phases of the cell cycle (G1, S, G2/M) were observed in all cell lines when exposed to DVE. However, an increase in the sub-G1 population, which is indicative of cell death, was evident in the DVE-treated DLBCL cells.

The induction of apoptosis was investigated firstly through microscopy, to assess for the presence of cellular morphological features typical of this mode of cell death. Membrane blebbing, nuclear fragmentation, the presence of apoptotic bodies, and cell shrinkage were observed for both DLBCL cell lines while slight cell swelling was observed for the PB-B95-8H cells. Using the Annexin V incorporation assay, a majority of late apoptotic (64%) and non-viable/necrotic (15%) cells were detected in DVE-treated SU-DHL-4 cells, while mostly early apoptotic cells (49%) were observed for HBL-1. The non-cancerous cell lines were left mostly unaffected. These findings were further supported by the caspase-3/7 activity assay and western blot analysis, which demonstrated that DVE treatment induces the expression of the apoptotic markers PARP-1 and caspase-3 in DLBCL cells, with the SU-DHL-4 cells displaying traces of necrosis, as evidenced by smaller cleaved PARP-1 fragments (74 kDa and below).

Overall, the study shows that aqueous extract of *D. viscosa* is selectively cytotoxicity towards DLBCL cells, and significantly less toxic towards a corresponding non-cancerous B cell line. Additionally, at the same concentration as DVE, and under the same treatment conditions, the GCB DLBCL cell line was more sensitive to DVE than the ABC DLBCL cell line. This is in line with reports on the more aggressive and resistant nature of the ABC subtype. While this research is the first to demonstrate that extracts of the medicinal plant *D. viscosa* are cytotoxic toward DLBCL cells, more research is needed to further understand the mechanisms of cell death, as well as to demonstrate these findings in an *in vivo* model. Additionally, biochemical studies should be done to identify the bioactive compounds responsible for the cytotoxic effects observed.

Chapter 1

Background

1.1 The burden of cancer.

Cancer is a leading cause of mortality worldwide, accounting for around 10 million deaths in 2020, or one-sixth of all fatalities (World Health Organization, 2022). Furthermore, the occurrence of cancer in South Africa is on the rise, with projections indicating that the number of new cases will nearly double from 2019 to 2030, amounting to just over 120,000 new cases in 2023 (Finestone and Wishnia, 2022). The distinctive features of cancer cells are uncontrolled cell division, evasion of growth suppressors and cell death, ability to metastasize, and promotion of angiogenesis (Hanahan and Weinberg, 2011). Cancer cells have also developed the ability to evade the immune system and promote inflammation which aids tumour growth (Hanahan and Weinberg, 2011). Research in cancer biology has enhanced our understanding of why “normal” cells become cancerous and how they grow uncontrollably, which has been critical in the development of therapeutic strategies to combat the progression of this disease. However, cancer is not one disease but a group of many related diseases, which can occur almost anywhere in the body, each with its own genetic and molecular characteristics, risk factors, causes, and treatments. In many cases, treatment is suboptimal, and therefore, the quest to enhance our knowledge about the biology of cancer, and the development of new and more effective treatments, continues.

1.2 Haematological cancers.

Haematological malignancies encompass a diverse group of cancers that originate in cells of the immune system and affect the blood, bone marrow, and lymphatic systems (Novak and Rego, 2012). Approximately 1.24 million cases of haematological malignancies are diagnosed annually on a global scale, constituting approximately 6% of total cancer cases (GLOBOCAN, 2018). Additionally, GLOBOCAN (2018) provided estimations that indicate the mortality rate of blood cancer patients surpasses 720,000 individuals every year, accounting for more than 7% of all

cancer-related deaths. Infection with the human immunodeficiency virus (HIV) has been shown to significantly increase the incidence of certain types of haematological malignancies, and this is attributable to several factors including immunosuppression, immunological dysregulation, prolonged antigenic stimulation, and direct viral activity (Mowla and Ahmed, 2022; De Martel *et al.*, 2012; Dolcetti *et al.*, 2016; Carbone *et al.*, 2021). Various types of blood cancers include leukemia, lymphoma, myelodysplastic syndromes, myeloproliferative disorders, and multiple myeloma.

Individuals who are living with HIV or AIDS face an elevated susceptibility to Hodgkin's and certain subtypes of non-Hodgkin lymphoma in comparison to those who are HIV-negative (Black *et al.*, 2023). In the Southern African region, which has the highest prevalence of HIV infection globally, HIV-associated cancers represent a major healthcare challenge (Dhokotera *et al.*, 2019). While the utilization of combination antiretroviral therapy (antiretrovirals and chemotherapy) has significantly improved the incidence and outcome of individuals with HIV-associated cancers, morbidity, and mortality remain high within this group, especially in low-resource settings such as many regions within Southern Africa (Kimani *et al.*, 2020; World Health Organization, 2018; Mbulaiteye *et al.*, 2003).

1.3 Non-Hodgkin lymphoma.

Non-Hodgkin lymphoma (NHL), which constitutes a large group of cancers of lymphocytes (white blood cells), was ranked the 11th most common cancer globally, accounting for 544,000 new cases and 260,000 deaths in 2020 (Sung *et al.*, 2021). Furthermore, NHL is responsible for approximately 3% of the overall cancer burden in both females and males across the globe. NHL exhibits a higher prevalence within the age group of 65 to 74 years and is also the fifth most frequently encountered diagnostic entity among pediatric malignancies affecting children under the age of 15 years (Sapkota and Shaikh, 2023). In South Africa, NHL ranks among the top five invasive cancers among both males and females (CANSAs, 2019). Among all NHL subtypes, of which there are more than 60, diffuse large B cell lymphoma (DLBCL) is the most common, accounting for 20%-30% of all NHL cases diagnosed (Susanibar-Adaniya *et al.*, 2021). A study conducted at the University of Cape Town, reporting on data collected between 2004 and 2014

(inclusive), reveals that, among HIV-infected patients, DLBCL is the most prevalent, which is in line with several studies both in South Africa and elsewhere in the world (Figure 1) (Phillips and Opie, 2018; Dhokotera *et al.*, 2019; Wang *et al.*, 2021).

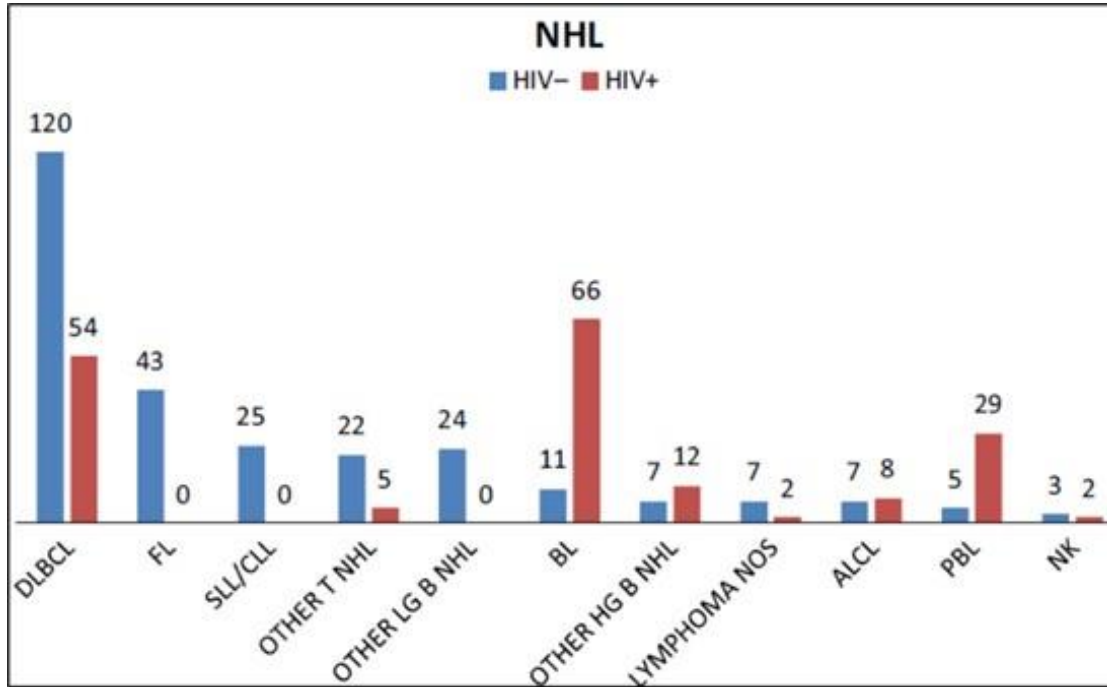


Figure 1.1. The most common types of lymphoma diagnosed in patients who underwent bone marrow biopsy (BMB), at Groot Schuur Hospital, between 2004 and 2014 (Inc.), per HIV status (Phillips and Opie, 2018). The abbreviations are DLBCL – diffuse large B cell lymphoma, FL – follicular lymphoma, SLL/CLL – small lymphocytic lymphoma/chronic lymphocytic leukaemia, OTHER T NHL – other T non-Hodgkin Lymphoma, OTHER LG B NHL – other low-grade B non-Hodgkin lymphoma, BL – Burkitt lymphoma, OTHER HG B NHL – Other high-grade B non-Hodgkin, LYMPHOMA NOS – lymphoma not otherwise specified, ALCL – anaplastic large cell lymphoma, PBL – plasmablastic lymphoma, NK -natural killer cell lymphoma, HIV- - HIV negative, HIV+ - HIV positive.

1.3.1 Diffuse large B cell lymphoma.

DLBCL is an aggressive cancer, displaying high heterogeneity at both the molecular and genetic levels (Pasqualucci, 2013). It is typically classified into distinct subtypes based on molecular and genetic characteristics as well as cell-of-origin (Frontzek and Lenz, 2019). DLBCL not otherwise specified (DLBCL NOS) is the most common type of DLBCL, which constitutes two main categories or phenotypes, namely Activated B-cell-like Diffuse Large B-cell Lymphoma (ABC-DLBCL) and Germinal Centre B-cell-like Diffuse Large B-cell Lymphoma (GCB-DLBCL). These subtypes exhibit notable differences in terms of their cellular origins, genetic characteristics, and clinical

behaviour (Figure 1.2) with the ABC subtype generally associating with worse prognosis and poorer overall survival compared to the GCB subtype in response to standard first-line therapy (Frontzek and Lenz, 2019). Although the 5-year survival rate, with first-line therapy, is approximately 60%, up to 50% of patients become refractory to treatment, or relapse (Watanabe *et al.*, 2018). Generally, these patients are then placed on more intense therapeutic regimens, which are often accompanied by adverse events and poor quality of life.

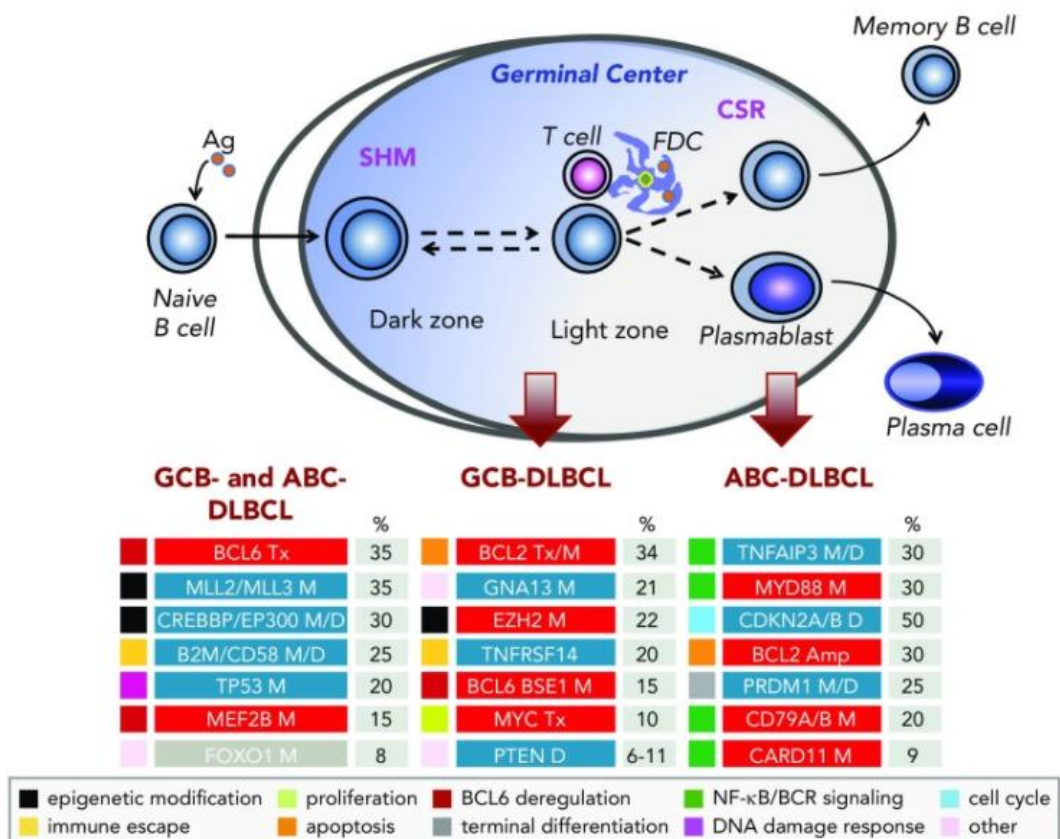


Figure 1.2. DLBCL subtypes are distinguished by their cellular origins and genetic lesions. This diagram depicts the germinal centre (GC) reaction and its relationship to the two molecular subtypes of DLBCL NOS, GCB-DLBCL, and ABC-DLBCL. The most common, functionally characterized gene mutations defined in this disease are shown in the bottom frames, where blue represents impairment events and red represents gain-of-function events; color codes on the left represent distinct groups, according to the infiltrated biological pathway (Pasqualucci and Dalla-Favera, 2018).

In addition to the sub-optimal efficacy of certain chemotherapy treatments, the toxicity of anti-cancer medications presents a significant challenge for both patients and doctors. The risk of adverse events increases with the patient's age, as well as the immune-compromised state. In

regions of South Africa where health resources are sub-optimal, the already inadequate patient outcomes are further aggravated by limited access to healthcare providers due to infrastructure and socio-economic barriers. This, in turn, leads to inconsistent ART therapy and unequal access to treatment in public healthcare facilities (Economist Impact, 2023). This speaks to a clear need to not only enhance current cancer treatment protocols but also to identify new drugs that are accessible and affordable for the relevant patient groups.

Research shows that the use of complementary and alternative medicine (CAM) among cancer patients has increased in the last decades. CAM refers to a broad set of non-mainstream practices, which includes the use of mind-body therapies, entire medical systems such as acupuncture, as well as natural products (Wode *et al.*, 2019).

1.4 The healing properties of traditional medicine.

Traditional medicine (TM) is described as diverse health practices, approaches, expertise, and beliefs incorporating plant/animal/mineral base medicine, spiritual therapies, and exercises applied singularly or in combination, to maintain well-being, as well as to treat, diagnose, or prevent illnesses that are not incorporated into primary healthcare systems (WHO, 2019). Herbal medicine includes plant parts or combinations of active ingredients in herbal materials. These medications are used to treat or prevent disease as well as to restore, correct, or modify biological functions (WHO, 2019). Most importantly, traditional medicine also has a sizable economic impact, with its contribution to the South African economy alone amounting to about R2.9 billion (Kasilo *et al.*, 2013). A sizeable portion of the population in Sub-Saharan Africa is presumed to rely on TM to maintain their health or to prevent and treat both communicable and non-communicable diseases and has long been thought to be widespread in this region (Mander *et al.*, 2007).

1.4.1 Herbal natural compounds as anti-cancer agents.

Plants and their derivatives have played a crucial role in the development of effective anti-cancer drugs. For instance, vincristine and vinblastine, which are utilized in treating various types of cancer such as lymphomas and leukemias, were obtained from the leaves of the Madagascar

periwinkle plant (Asma *et al.*, 2022). Another example is etoposide, derived from the mandrake plant, which is utilized in the treatment protocols for both Hodgkin and non-Hodgkin lymphomas (Reyhanoglu and Tadi, 2020).

South Africa is home to an estimated 68,000 to 300,000 practicing Traditional Medical Practitioners (TMPs) (full-time and part-time), and thus, the use of Complementary and Alternative Medicine (CAM) is prevalent (Street *et al.*, 2018). These traditional healers are highly regarded by their communities and within which they play an important role in healthcare provision, which cannot be overlooked (Gqaleni *et al.*, 2007; Street *et al.*, 2018). Many communities in South Africa heavily rely on TMPs for their primary healthcare needs due to their cultural significance, availability, and accessibility. Importantly, traditional medicine also has a sizable economic impact, with its contribution to the South African economy amounting to approximately R2.9 billion (Kasilo *et al.*, 2013). Therefore, TMPs are an essential component of healthcare provision in South Africa, and efforts are being made to explore various models for integrating this practice into the national healthcare delivery system. These models are currently being considered and developed by researchers and experts in the field (Moshabela *et al.*, 2015; Mothibe and Sibanda, 2016; Pinkoane *et al.*, 2012; Street *et al.*, 2018).

1.4.2 Phytochemical compounds as anti-cancer agents.

Phytochemicals are compounds that are found in plants and are commonly referred to as secondary metabolites. Numerous studies have provided evidence supporting the utilization of these phytochemical compounds in the treatment of various diseases, including cancer, through their ability to modulate the immune system, as well as having anti-cancer properties (Egbuna *et al.*, 2019). Carotenoids, phenolics, glucosides, monoterpenes, and flavonoids are among the major therapeutic phytochemicals that have been derived from plants (Kerr *et al.*, 2013). Table 1.1 lists some of the studies reporting on anti-cancer phytochemical compounds currently used to treat DLBCL. Plants used by traditional healers therefore hold valuable potential for the discovery of novel phytochemicals that can be used in the treatment of cancer.

Table 1.1. Summary of selected approved phytochemical compounds used as anti-cancer agents to treat diffuse large B cell lymphoma.

Anticancer agent	Derived from:	Description and Mechanism of action
Paclitaxel (Taxol)	<i>Taxus brevifolia</i> (Pacific Yew)	Paclitaxel (Taxol) belongs to a group of compounds called Taxanes and is commonly used to treat a variety of tumours, including lung cancer, breast cancer, ovarian cancer, Kaposi sarcoma, and DLBCL (Barreca et al, 2020). The primary mode of action of paclitaxel is its capacity to stabilize and inhibit microtubule depolymerization, which results in cell cycle arrest during the G2/M phase and cell death (Barreca et al, 2020).
Vincristine	<i>Catharanthus roseus</i> (Madagascar periwinkle)	Vincristine is a component of R-CHOP (Rituximab-cyclophosphamide, doxorubicin, vincristine, and prednisone), which is the first-line therapy for DLBCL (Wei et al, 2021). It belongs to a group of alkaloids called vinca alkaloids. Vincristine inhibits mitotic spindle structure. Vincristine also exerts immunomodulatory effects on tumour cells, increasing PD-L1 expression. Vincristine enhances the expression of PD-L1, which increases the immune response against cancer cells (Wei et al, 2021).
Vinblastine	<i>Catharanthus Roseus</i> (Madagascar periwinkle)	Vinblastine is a vinca alkaloid and is beneficial against a variety of cancers, including monozygotic leukaemia, breast cancer, liver cancer, ovarian cancer, head and neck cancer, testicular cancer, solid sarcoma, malignant melanoma, and DLBCL (Vari et al, 2018). In DLBCL cell lines, it has been shown to increase the expression of PD-L1, an immune regulatory protein. Upregulation of PD-L1 can boost the antitumour immune response by activating effector T cells (Vari et al., 2018).
Etoposide and Teniposide	<i>Podophyllum genus</i> (Mayapple)	Etoposide and Teniposide are inhibitors of topoisomerase II and have been demonstrated to target DNA topoisomerase II activities, resulting in DNA breaks, and influencing different aspects of DLBCL cell metabolism (Kancherla et al., 2001). Teniposide disrupts cell cycle progression by preventing mitosis and inducing apoptosis in DLBCL cells both <i>in vitro</i> and <i>in vivo</i> (Kancherla et al, 2001).
Topotecan	<i>Camptotheca acuminata</i> (Happy Tree)	Topotecan is an inhibitor of topoisomerase I, and thus, through inhibition of this enzyme, it causes DNA strand breaks, leading to cell death. It has demonstrated therapeutic success in diffuse large B cell lymphoma (DLBCL) and other haematological cancers (Tomicic et al, 2005).

1.5 *Dodonaea viscosa*, a traditional herbal medicine.

Dodonaea viscosa var. *angustifolia* is a flowering shrub (Figure 1.3) thought to have originated in Australia but can be found all over the world in the tropics and subtropics including on the continents of Africa (including South Africa), Asia, Australasia, Northern America, and Southern America (USDA, 2022). Common names for this medicinal plant in South Africa include Gansies, bossidokter, Kankerbos (Afrikaans), and English common names (hopbush, Florida hopbush, gigantic hopbush, sticky hopbush, and hopshrub) (USDA, 2022). *D. viscosa* is commonly prescribed by indigenous Rastafarian healers in the Western Cape area of South Africa for a range of illnesses including gout, skin infections, diarrhea, hepatitis or splenic pains, vaginal colic, ulcers, and muscle aches. Additionally, it is also prescribed as an antipruritic agent for dermatitis and eczema (Rojas *et al.*, 1992, Alanazi *et al.*, 2023; Siddiqui *et al.*, 2023).



Figure 1.1. *Dodonaea viscosa* var. *angustifolia* plant, an evergreen shrub or small tree that can grow up to 5 meters tall. It is described as having fissured light grey bark, drooping leaves light green on the top side, and a lighter green on the underside. It produces small yellowish-green flowers that are followed by clusters of yellow or reddish fruits with papery wings (SANBI, 2023).

1.5.1 Known therapeutic characteristics of *Dodonaea viscosa*.

Scientific studies aimed at defining the therapeutic properties of extracts of *D. viscosa* and its derivatives, as well as the mechanisms of action, have revealed several useful characteristics that can be explored. A selected list of those characteristics is summarized in Table 1.2 below.

Table 1.2 Summary of selected reported therapeutic characteristics of *D. viscosa*.

Therapeutic characteristic	A brief description of the observed effect
Antimicrobial	<p>Mice infected with <i>S. aureus</i> and treated with aqueous extracts of <i>D. viscosa</i> leaves for 30 days displayed reduced abnormal kidney histology compared to mice infected with <i>S. aureus</i> but not treated with <i>D. viscosa</i> extracts (Majeed <i>et al.</i>, 2022).</p> <p>Methanolic extracts of <i>D. viscosa</i>, and purified compounds were significantly inhibitory towards the growth of High Vaginal Strain (HVS) streptococcus species (Hossain M.A and Al Bimani B.M.H, 2000).</p>
Wound healing	<p>An ointment formulated to contain ethyl acetate fractions of <i>D. viscosa</i> leaf extract was shown to have better wound healing performance (percentage of wound closure, tensile strength, and epithelialization) compared to a control ointment, in Sprague-Dawley rats (Subramanian <i>et al.</i>, 2023).</p>
Antidiabetic	<p>Diabetic rats receiving daily oral doses of extracts of <i>D. viscosa</i> over four weeks showed a dramatic reduction in the levels of pro-inflammatory indicators in blood, kidney, and liver tissues, as well as blood glucose levels, compared to control rats. Additionally, insulin and lipid levels were restored, as well as those of other enzymes that are markers of hyperglycemia (Alanazi <i>et al.</i>, 2023).</p>
Antioxidant	<p>Methanol and chloroform extracts of <i>D. viscosa</i> were found to have protective effects against CCL₄ induced toxicity in mice. The levels of hepatic enzymes, haematological parameters, and liver antioxidant enzymes were restored in DVE-fed mice, relative to controls. Furthermore, these mice displayed improved histological characteristics of the liver, kidney, and spleen (Tong <i>et al.</i>, 2021).</p>

1.5.2 Anti-cancer properties of *D. viscosa*.

Although there are several reports on the inhibitory effects of extracts of *D. viscosa* against cancer cells, these studies have, for the most part, only generated a limited amount of data. These include the use of MTT or similar viability assays to demonstrate that extracts of *D. viscosa* can negatively impact the proliferation of various cancer cell lines (derived from colon, lung, ovarian and breast cancers) (Al-Musawi and Al-Saadi, 2021; Cao *et al.*, 2009; Herrera-Calderon *et al.*, 2020; Jayaraman *et al.*, 2021; Mossa and Al-Shawi, 2015; Ramkumar *et al.*, 2021). A notable limitation in many of these studies is that the selectivity of the extract for cancerous cells was not assessed since a non-cancerous control cell line was not included in these studies. Nevertheless, what these reports demonstrate is that *D. viscosa* is potentially a source of phytochemicals that can be used as blueprints for the development of novel and improved anti-cancer agents and should therefore be comprehensively investigated. Importantly, and to the best of our knowledge, there have been no studies to date investigating the cytotoxic effect of extracts of *D. viscosa* on the most prevalent and highly aggressive non-Hodgkin lymphoma, namely DLBCL.

1.6 Preliminary data and Rationale of the proposed research.

The cytotoxic effect of aqueous extracts of *D. viscosa* (DVE), derived from plants harvested from the wild in the Western Cape region of South Africa, was investigated on Burkitt lymphoma (BL) cell lines, in our research laboratory. Like DLBCL, BL is an aggressive non-Hodgkin B-cell lymphoma, but unlike DLBCL, BL is considered a rare cancer accounting for approximately 1% - 5% of all NHLs (WebMD, 2021). However, in HIV-endemic regions, like Southern Africa, BL is highly over-represented, due to its association with HIV infection. As can be seen the Figure 1.1 above, in that study, BL was 6 times more prevalent among HIV-infected individuals (Phillips and Opie, 2018). Our data demonstrated potent and selective toxicity against two BL cell lines, relative to a non-cancerous lymphoblastoid cell line; that DVE induces apoptosis, and that this is mediated via the PI3K pathway (Saferdien, 2023). Additionally, preclinical data using a xenograft

mouse model demonstrated that DVE had a superior safety profile compared to an established chemotherapeutic agent and that it led to retardation of tumour growth in DVE-fed mice, relative to control mice (Unpublished data). It is, therefore, hypothesized that DVE will exert similar cytotoxic effects against DLBCL cells.

1.6.1 Aims of the study.

The purpose of this research was to evaluate the cytotoxic activity of aqueous extracts of *Dodonaea viscosa* (DVE) on two diffuse large B cell lymphoma cell lines (one ABC- and one GCB-derived), relative to a non-cancerous lymphoblastoid cell line, using *in vitro* assays with the purpose to determine its potential as a source of bioactive compounds for the treatment of DLBCL.

This was achieved through the following specific objectives:

- I. To assess the cytotoxic activity of *D. viscosa* aqueous extract in DLBCL cell lines relative to a non-cancerous cell line using viability assays.
- II. To evaluate the impact of *D. viscosa* aqueous extract on proliferation in DLBCL cell lines compared to a non-cancerous cell line.
- III. To evaluate the impact of *D. viscosa* aqueous extract on apoptosis in DLBCL cell lines compared to a non-cancerous cell line.

Chapter 2

Materials and Methods

2.1 Cell lines and culture conditions.

Diffuse large B cell lymphoma cell lines SU-DHL-4 (GCB subtype) (Cellosaurus *et al.*, 2023) and HBL-1 (ABC subtype) (Cellosaurus *et al.*, 2023), as well as the non-cancerous lymphoblastoid cell line PB-B95-8H (Leopizzi *et al.*, 2024) were used in this study. SU-DHL-4 and HBL-1 cells were kindly donated by Professor Sandeep Dave (Duke University, USA), and PB-B95-8H cells were kindly donated by Professor Pankaj Trivedi (La Sapienza University, Italy). The DLBCL cell lines (SU-DHL-4, HBL-1) were cultured in Roswell Park Memorial Institute (RPMI)-1640 medium (Sigma Aldrich, Missouri, USA) supplemented with 10% Fetal Bovine Serum (FBS) and 1% Penicillin-Streptomycin solution (Sigma Aldrich, Missouri, USA) (refer to Appendix B) at a temperature of 37°C with 5% CO₂. Similarly, the Epstein Barr Virus (EBV)-immortalized control lymphoblastoid cells (PB-LCL-B95.8H) were cultured in RPMI-1640 medium supplemented with 20% FBS and 1% Pen Strep at 37°C with 5% CO₂. All cell lines were regularly tested for mycoplasma contamination which involved culturing of cells in antibiotic-free media for two days followed by fixation, DNA staining using Hoechst (14533, Sigma-Aldrich, USA), and visualization using an inverted fluorescence microscope (ZEISS Axiovert, Germany).

2.2 Cryopreservation for long-term storage of cell lines.

For long-term storage, the cells were resuspended in freezing media that consisted of a cryopreservative agent, 10% dimethyl sulfoxide (DMSO), and 10-20% FBS in RPMI. The cells were aliquoted into cryovials, each containing 1ml, and transferred into a freezing container (Nalgene® Mr. Frosty, USA) for overnight freezing at -80°C before submerging under transfer liquid nitrogen for long-term cryopreservation.

2.3 Preparation of aqueous *Dodonaea viscosa* extract.

The *Dodonaea viscosa* plant material was harvested by collaborator Professor Nokwanda Makunga (Stellenbosch University) from its natural habitat (Stellenbosch area) in the Western Cape, South Africa. The plant material, consisting of bark and leaves, was air-dried at room temperature. Aqueous extracts of *D. viscosa* (DVE) were prepared by flash-freezing the dried material using liquid nitrogen and finely grinding it into a powder using a mortar and pestle. Five (5) grams of the plant powder was transferred to an Erlenmeyer flask, and 50 ml of distilled water was added. The mixture was then subjected to sonication for 30 minutes and filtered twice using Whatman No. 1 filter paper. The resulting extract was placed in a sonicator bath for 45 minutes. Aliquots of the extract were frozen at -80°C and subsequently freeze-dried to obtain the DVE powder used in this study. The DVE powder was stored in a sealed, light-safe container containing silica beads, and was kept at room temperature. The lyophilized powder was dissolved in $1 \times$ phosphate-buffered saline ($1 \times$ PBS) solution on the day of cell treatment, at a stock concentration of 5 mg/ml.

2.4 Cell treatments.

The prepared DVE extract was added directly to the cells that had been plated the day before, by adding appropriate amounts of the freshly prepared DVE stock solution to the cell culture medium to reach the desired final concentration (1 – 200 $\mu\text{g}/\text{ml}$), ensuring that the DVE was well dissolved and resuspended within the medium. As controls, equivalent cell cultures received equivalent amounts of the diluent, i.e., $1 \times$ PBS.

2.5 WST-1 cell viability assay.

The WST-1 (2-(4-iodophenyl)-3-(4-nitrophenyl)-5-(2,4-disulfophenyl)-2H-tetrazolium) assay (Roche Applied Science, Germany) was used to determine the half-maximal inhibitory concentration (IC_{50}) of DVE for each cell line (SU-DHL-4, HBL-1, and PB-B95-8H). This assay is based on cellular mitochondrial dehydrogenases cleaving the tetrazolium salt WST-1 to formazan, leading to a colorimetric change (from a slightly red colour to dark red colour) that can

be measured using an absorbance reader (Brady *et al.*, 2007). The principle of the assay is that the more viable the cells, the higher the activity of the mitochondrial enzymes, and in turn the greater the amount of dye formed. In a 96-well plate, 1.6×10^5 cells/ml were seeded (100 μ l of cell suspension per well) and incubated overnight (approximately 16 hours) at 37°C with 5% CO₂ before treating with varying concentrations of DVE (0 – 200 μ g/ml). After 24 hours of DVE treatment, 10 μ l of WST-1 reagent was added to each well, followed by 2 hours of incubation at 37°C in the growth incubator (NuAire, USA). Thereafter, the colour change was measured using a spectrophotometer (Glo-Max®-Multi+ multi-plate reader, Promega, USA) at 450nm absorbance. Each treatment was performed in triplicate wells, and at least three independent experiments were performed.

2.6 Determination of selectivity index (SI).

The SI was calculated with the following equation:

$$SI = \frac{IC50 \text{ of the control cell line}}{IC50 \text{ of the cancer cell line}}$$

A higher SI value suggests that the biological agent is preferentially cytotoxic to cancer cells.

2.7 CellTrace proliferation assay.

The proliferation of DVE-treated DLBCL cells HLB-1 and SU-DHL-4 as well as the non-cancerous lymphoblastoid cell line PB-B95-8H were measured over time by staining live cells with a fluorescent dye and tracking proliferation using flow cytometry, and this was done using the Cell Trace™ CFSE proliferation kit (ThermoFisher Scientific, USA). The principle of the assay is that a fluorescent dye is incorporated in cells at the start of the experiment, and when these cells divide, the daughter cells will contain half the amount of dye of the parent cell (Tario *et al.*, 2012). The staining procedure was performed according to the manufacturer's instructions. Briefly, 1.6×10^5 cells per cell line was washed twice using 1 x PBS and then stained with 0.5 μ M CellTrace™ CFSE dye for 20 minutes at Room Temperature (RT) with gentle continuous mixing.

Thereafter, 5 x the original volume of complete culture media was added to the cells, after which the cells were incubated at RT for 5 minutes to quench any free dye remaining in the solution.

The samples were then centrifuged for 4 minutes at 1500 rpm before being resuspended in 2 ml of complete culture media, transferred into the culture dish (35 mm), and then treated with 40 µg/ml DVE, or received equivalent amounts of diluent (controls). Dishes were incubated at 37°C in a humidified 5% CO₂ incubator for 48 hours, in the dark. Unstained control was included, to assess background staining, as well as cells stained at the starting point of the experiment to set the baseline fluorescence. At the end of treatment, cells were fixed and processed using the Becton Dickson FACSymphony™ A5 flow cytometry instrument (Becton Dickson, USA), and the data was analysed using FlowJo v10.9. For fixation, cells were pelleted and resuspended in 1ml 1 × PBS followed by a dropwise addition of 3 ml 70% methanol while gently vortexing to avoid clumping. Thereafter, cells were transferred to 5 ml Falcon round bottom tubes, incubated on ice for 30 minutes, pelleted and washed twice in 1 × PBS, and the pellets resuspended in 200 µl 1 × PBS. At least two independent experiments were performed.

2.8 Colony forming assay using MethoCult-based semi-solid media.

The colony-forming assay was used to assess cell proliferation from a single progenitor cell, and the MATHCOUNTS™ (STEMCELL Technologies, Canada) based semi-solid medium was used as it contains cytokines and growth factors that support the growth of haematopoietic-derived cells. The cells were seeded in 35 mm culture dishes at a density of 1.6×10^5 cells/well in 1500 µL of MethoCult medium containing varying concentrations of DVE (30 µg/ml and 60 µg/ml) or without DVE (control). The cells were then incubated for seven days at 37°C with 5% CO₂ and images were captured on days 1, 3, 5, and 7, using the phase contrast filter, on the Axiovert Inverted Fluorescence Microscopy (Carl Zeiss, Germany). The images were quantified using ImageJ. At least two independent experiments were performed.

2.9 Cell cycle profiling.

The effect of DVE on the phases of the cell cycle of the cell lines (HBL-1, SU-DHL-4, PB-B95-8H) was evaluated by flow cytometry. Cells were plated (1.6×10^5 cells/mL) in duplicate 35 mm dishes, in their appropriate complete media, and treated (30 and 60 µg/ml DVE, or equivalent amounts of 1 × PBS as control), followed by incubation for 24 hours. To prepare the cells for cell

cycle profiling, the FxCycle™ PI/RNase Staining Solution was used (Invitrogen, USA), according to the manufacturer's instructions. Briefly, duplicate cell samples were pooled into 15 mL centrifuge tubes (Falcon™), and the cells were pelleted, resuspended in 1 × PBS, counted, and 1.0×10^6 cells were fixed in 70% methanol, and the tubes were incubated on ice for 30 minutes. Following this, the cells were pelleted again, washed with 1 mL of 1 × PBS, and thereafter resuspended in 500 μL of PI/RNase Staining Solution and incubated for 30 minutes. The samples were analysed using the Becton Dickson FACSCalibur™ Flow Cytometry equipment (Becton Dickinson, USA). Analyses were done with the Becton Dickson Cell Quest Pro™ software (Becton Dickson, USA). At least two independent experiments were performed.

2.10 Assessment of cell morphology using light microscopy.

The cells were seeded in duplicate wells in a 6-well plate at a concentration of 1.6×10^5 cells/well in 2000 μL culture complete medium and incubated at 37°C with 5% CO₂. The next day, cells were treated (30 and 60 μg/ml DVE, or equivalent amounts of 1 × PBS as control), followed by incubation for 24 hours. The phenotypic morphological features of the cells were observed under light microscopy using the phase contrast filter (Axiovert Inverted Fluorescence Microscopy, Carl Zeiss, Germany). To capture the images, cells were transferred onto glass microscope slides and covered with a glass cover slip, and snapshots were taken using the Zeiss AxioCam HRm camera and AxioVision software. At least three independent experiments were performed.

2.11 Annexin V incorporation assay.

The PE Annexin V apoptosis detection kit I (BD Biosciences, USA) was used to evaluate apoptosis and non-viable/necrotic cells. The components of the kit include the Annexin V protein conjugated to the fluorochrome Phycoerythrin (PE), which binds to phosphatidylserine residues on the surface of apoptotic cells, and 7-Amino-Actinomycin (7-AAD), which intercalates into DNA in the G-C rich regions. Single staining with Annexin V indicates early apoptotic cells, double staining with Annexin V and 7-AAD indicates late apoptotic cells and single staining with 7-AAD indicates non-viable/necrotic cells. The cells (HBL-1, SU-DHL-4, PB-B85-8H) were seeded in duplicate 35 mm wells (1.6×10^5 cells/well) in 2000 μL complete medium. Following incubation,

cells were treated with two different concentrations of DVE (30 or 60 µg/ml) and incubated for 24 hours. The cells were processed for Annexin V assay according to the manufacturer's instructions. Briefly, at the end of the experiment, duplicate wells were pooled within a 15 mL centrifuge tube (Falcon™), and cells were pelleted, and washed twice with cold 1 x PBS, before resuspension in 1 × binding buffer at a density of 1 × 10⁶ cells per sample. These cells were stained as appropriate (unstained, PE Annexin only, 7-AAD only, and PE Annexin and 7-AAD) and processed using the Becton Dickson FACSCalibur™ Flow Cytometer (Becton Dickinson, USA). Compensation and analysis were done with the Becton Dickson Cell Quest Pro™ software (Becton Dickson, USA).

2.12 Caspase-Glo® 3/7 assay.

The homogenous Caspase-Glo® 3/7 Assay measures the activity of caspase-3 and -7 by using luminescence (Shi, 2004). The assay contains a substrate for caspase-3/7, which contains the DEVD tetrapeptide, which is cleaved to release a light-producing substrate (aminoluciferin). The reagents also allow for cell lysis and are optimized for caspase activity. When Caspase-Glo® 3/7 Reagent is introduced in an “add-mix-measure” arrangement, it causes cell lysis, which leads to caspase-mediated cleavage of the substrate and the creation of a “glow-type” luminous signal consumed by luciferase. The quantity of luminous signal is proportional to the quantity of caspase 3/7 (Shi, 2004). The cells (HBL-1, SU-DHL-4, PB-B85-8H) were seeded into a 96-well plate at a density of 1.6 × 10⁵ cells/well in 100 µL complete medium and treated the next day with 60 µg/ml DVE (control cells received equivalent amounts of 1 × PBS, blank wells were also included as controls for this assay) and incubated for 24 hours. Thereafter, 100 µL of Caspase-Glo® 3/7 reagent was added to each well, gently mixed, and incubated at RT for 3 hours after which the luminescence was measured using the Glomax® Multi Detection System (Promega, USA).

2.13 Protein extraction and quantification.

To obtain total protein for western blotting, cells (HBL-1, SU-DHL-4, PB-B85-8H) were seeded in duplicate wells in a 6-well plate at a density of 1.6 × 10⁵ cells/well in 2000 µL of complete medium. Cells were treated the next day with DVE (30 and 60 µg/ml or untreated) and incubated for 24

hours. The cell respective duplicate samples were pooled into 15 mL centrifuge tubes (Falcon™), the cells pelleted, washed twice in 1 × PBS, and then resuspended in Radio-Immunoprecipitation Assay (RIPA) buffer including 1× cOmplete™, Mini, EDTA-free Protease Inhibitor Cocktail (Roche, Germany) (Appendix B). The extract was incubated overnight at -80°C to maximize cell lysis, and thereafter, centrifuged at 12000 rpm at 4°C for 20 minutes, and the supernatant was transferred into a fresh tube, to remove the cell debris pellet. The protein samples were stored in aliquots at -80°C until use.

The Pierce™ bicinchoninic acid (BCA) assay kit (ThermoFisher Scientific, USA) was used to quantify total protein in samples. The BCA assay method relies on the interaction between the bicinchoninic acid, and the cuprous ion produced during the biuret reaction, which occurs in an alkaline environment. Certain amino acids, such as cysteine, tryptophan, and tyrosine, as well as peptide bonds, can convert cupric ions (Cu²⁺) to cuprous ions (Cu⁺) (Huang *et al.*, 2010). The resulting bicinchoninic acid cuprous complex exhibits a vibrant blue colour that can be measured at a wavelength of 562 nm. The detection range for this assay is 0.2–50 µg/ml. The protein samples were diluted with RIPA buffer (range of 1 in 5 to 1 in 10), and 10 µL of diluted sample were transferred to a 96-well plate, in duplicate, as well as a range of concentration of the Bovine serum albumin (BSA) standards, followed by addition of 200 µL of working reagent (WR) per well. The plate was wrapped with plastic wrap and incubated for 30 minutes at 37°C. The BSA standards had a concentration range of 2000 µg/ml, 1000 µg/ml, 500 µg/ml, 125 µg/ml, and 0 µg/ml. The absorbance was measured at 560nm with the Glo-Max®-Multi+ multi-plate reader (Promega, USA). Protein sample concentrations were calculated from the BSA standard curve plotted on Microsoft Excel software (Microsoft Office Professional Plus 2019, version 1808).

2.14 SDS-PAGE and western blotting.

Protein samples extracted using RIPA cell lysis buffer were then separated using SDS-PAGE (sodium dodecyl sulfate-polyacrylamide gel electrophoresis) by molecular weight, on resolving gel (8% or 15%, Appendix B) and a 5% stacking gel (Appendix B), using the Mini-PROTEAN 3 casting apparatus (Bio-Rad, California, USA). All protein samples were prepared as per Table 2.1 below and denatured at 95°C for 5 minutes. The BenchMark™ Pre-stained 1 Kb Protein Ladder

(ThermoFisher™ Scientific, USA) was loaded into at least one well and 5 µl of 5 × SDS loading dye (Appendix B) was loaded into empty wells. The gel was electrophoresed at 100 volts for 2-2.5 hours in 1 × running buffer (Appendix B).

Table 2.1. Components of protein samples loaded onto SDS-PAGE gels.

Substance	Volume (µl)
Protein sample (µg)	*
100 mM Dithiothreitol (DTT)	1
5 X SDS loading dye	6
RIPA buffer	Up to 20 µl

* Indicates variable volume.

Following electrophoresis, the gel (resolving portion only) was assembled, under 1 x transfer buffer (Appendix B) as shown in Figure 2.1 below and placed within a gel holder cassette to transfer the separated proteins onto a nitrocellulose membrane (Bio-Rad, California, USA). The cassette was inserted into the Mini-PROTEAN 3 casting apparatus (Bio-Rad, California, US), covered with cold 1 x Transfer buffer (Appendix B), and connected to a power pack for transfer to proceed at 100 V for 75 minutes.

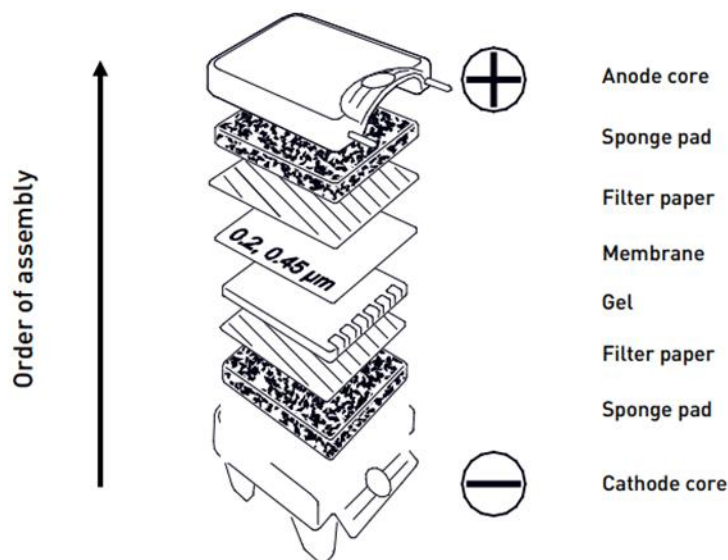


Figure 2.1. Diagram illustrating the “Western Blot Sandwich” cassette orientation for protein transfer (ThermoFischer™, USA).

2.14.1 Antibody incubation and protein detection.

Nitrocellulose membrane containing transferred protein was washed in washing buffer (Appendix B). Before blocking, membranes were stained using Ponceau S solution (Appendix B) to verify successful transfer. The membrane was blocked for 2 hours at RT in a Blocking buffer (Appendix B) with gentle agitation. This was followed by incubation in primary antibody diluted in blocking buffer at 4°C, with gentle agitation, overnight. The primary antibodies used were PARP-1 (F-2): sc-8007 (primary antibody dilution 1: 2000), caspase-3 (31A1067): sc-56053 (primary antibody dilution 1: 1000), and β -Actin (C4): sc-47778 (secondary antibody dilution 1: 10000) (Santa Cruz Biotechnology, USA).

After the overnight incubation, the membrane was washed with TBST buffer (Appendix B) (2 times for 5 minutes followed by 2 times for 10 minutes) with gentle agitation at RT. This was followed by incubation in the appropriate horseradish peroxidase (HRP)-conjugated secondary antibody, namely horse anti-mouse IgG (Cell Signaling Technology, USA) which was diluted in blocking buffer (1: 5000), for 1 hour at room temperature with gentle agitation. The membrane was then washed as before and visualized through enhanced chemiluminescence using the Clarity™ Western ECL substrate as per the manufacturer's instructions (Bio-Rad, California, USA). Membranes were exposed to X-ray film and the resulting chemiluminescent signal was captured by developing and fixing the film. The intensity of the bands was quantified using the ImageJ software (version 1.8.0) (National Institute of Health, Maryland, USA).

2.14.2 Membrane stripping.

The antibodies were stripped from the nitrocellulose membranes for re-probing by immersing them in a pre-heated stripping buffer (Appendix B) at a temperature of 50°C for 30 minutes, with brief agitation every 10 minutes. Following this, the membrane underwent three washes lasting 10 minutes each with PBST buffer (Appendix B). The membrane could then be reused starting

from the blocking stage, as previously described. This procedure was implemented when the membranes were subjected to probing to detect a protein acting as an internal loading.

2.15 Statistical analyses.

Statistical evaluations were conducted by employing student t-tests and one-way analysis of variance (ANOVA) tests, with significance being acknowledged at a threshold of $p < 0.05^*$. The GraphPad Prism software v9 (USA) was used to carry out all statistical analyses. In instances where statistical analyses were not performed, a representative of the outcome was provided. This approach was adopted due to the reproducibility of the general trend observed in the data for each experiment, while the fold changes exhibited variability between experiments for various reasons such as the performance of the kit and/or antibody and so on.

Ethics.

No ethical considerations for the use of animal or human samples were necessary for this investigation. The use of established cell lines in the study was approved by the UCT Faculty of Health Sciences Human Research Ethics Council (Reference: 813/2023).

Chapter 3

Results

3.1 Aqueous extract of *Dodonaea viscosa* exhibits selective cytotoxicity against diffuse large B cell lymphoma cells, relative to non-cancerous lymphoblastoid cells.

The initial step of this investigation was to establish whether aqueous extracts of *Dodonaea viscosa* (DVE) exhibited cytotoxic effects on DLBCL cells, and how these effects compared to their impact on non-malignant lymphoblastoid cells. The use of the aqueous extract was preferred over the methanolic extract to imitate the method employed by South African traditional healers when preparing the *D. viscosa* extract for treating various ailments. The cells were then treated with various doses of DVE (ranging from 0 to 200 µg/ml) for 24 hours (section 2.4), after which their viability was assessed using the WST-1 assay. This assay relies on the cleavage of a tetrazolium salt, which is accomplished by cellular components primarily located at the cell's surface and is heavily dependent on NAD(P)H production by viable cells (Lutter *et al.*, 2017). Consequently, the quantity of formazan dye produced, which can be measured using spectrophotometry, directly corresponds to the number of metabolically active cells.

In this experiment, we evaluated the impact of DVE on two types of DLBCL cell lines, specifically SU-DHL-4 (GCB subtype) (Cellosaurus *et al.*, 2023) and HBL-1 (ABC subtype) (Cellosaurus *et al.*, 2023). The study also included PB-B95-8H, a lymphoblastoid cell line (LCL) that was derived from human peripheral blood lymphocytes and immortalized using the B95-8 strain of EBV so that it could be maintained in culture for extended periods (Leopizzi *et al.*, 2024). The objective of the viability assay was to determine the IC₅₀ value, which represents the concentration of extract needed to inhibit half of the cell viability. This value can then be used to calculate the selectivity index (SI) of DVE, which indicates its cytotoxic selectivity towards cancer cells compared to non-cancerous cells (section 2.6). Generally, compounds with selectivity indices greater than 1

demonstrate higher toxicity toward tumour cells in comparison to normal cells (Krzywik *et al.*, 2020).

Shown in Figure 3.1 below is a representation of multiple repetitions of the assay, revealing a decline in cell viability as the concentration of DVE increases. Notably, the DLBCL cell lines displayed a significantly higher sensitivity to DVE compared to the LCL. The IC₅₀ values for SU-DHL-4 and HBL-1 were approximately 40 µg/ml and 30 µg/ml, respectively, whereas PB-B95-8H had an IC₅₀ of around 90 µg/ml (Figures 3.1 a & b). Using these values, the selectivity indices (IC₅₀ of non-cancerous cell line divided by IC₅₀ of cancer cell line) were determined to be 2.25 for SU-DHL-4 vs. PB-B95-8H and 3 for HBL-1 vs. PB-B95-8H. These selectivity indices indicate that DVE exhibits a preference for eliminating DLBCL cells in comparison to non-cancerous cells.

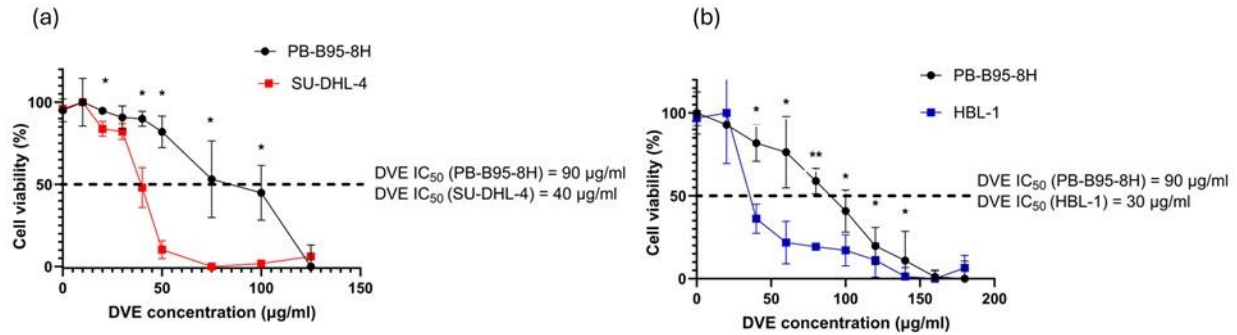


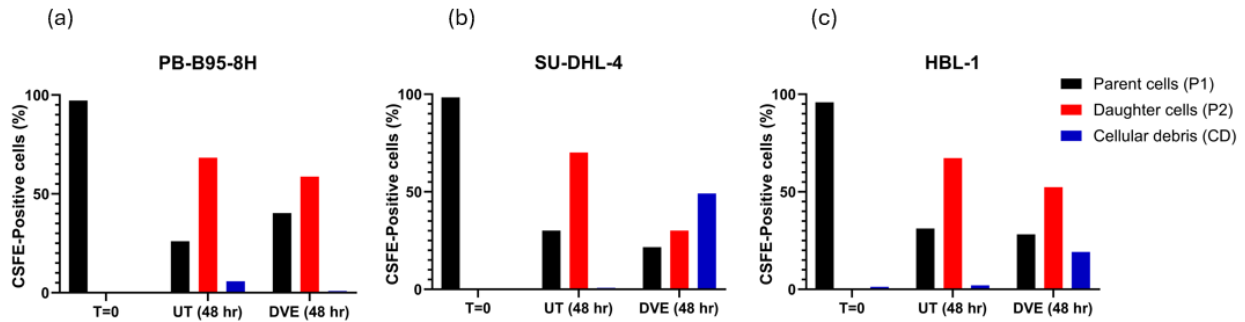
Figure 3.1. Determination of IC₅₀ and SI values for the aqueous extract of *D. viscosa* (DVE) using the WST-1 viability assay. The cell viability of diffuse large B cell lymphoma cell lines (SU-DHL-4 and HBL-1) as well as the non-cancerous cell line PB-B95-8H was assessed after treatment with varying concentrations of DVE (0-200 µg/ml) for 24 hours, using the WST-1 assay. The data represents the mean ± standard deviation (SD) (N=3) for each concentration. Statistical analysis was performed using a 2-way ANOVA and Sidák's multiple comparisons test on GraphPad Prism 9 software. P values are indicated as *p<0.05, **p<0.01. The experiments were performed at least in triplicates.

3.2 The proliferation and viability of DLBCL cells are inhibited by DVE as demonstrated by proliferation-tracking.

A proliferation-tracking assay *was* used to examine the rate of cell division over time in DLBCL cells and non-cancerous LCLs in the presence of DVE. This assay, known as CFSE CellTrace (section 2.7), makes use of a cell-permeable dye called carboxyfluorescein diacetate succinimidyl ester (CFSE). CFSE is added to the cell growth medium at the beginning of the experiment and reacts with the amine groups of proteins within the cells, resulting in a stable and long-lasting form (Tario *et al.*, 2018). When a CFSE-labeled cell undergoes cell division, the fluorescence intensity is halved in the daughter cells. This change in intensity can be tracked using flow cytometry (Figure A1 in Appendix A shows representative Flow cytometry data) and is directly related to the rate of cell proliferation. A representative result of duplicate experiments is displayed in Figure 3.2 below. On the day of cell plating and staining, 97% (average of 96%, 97%, and 98%) of the parental cells (P1 generation for PB-B95-8H, SU-DHL-4, and HBL-1) successfully incorporated the dye, as determined by flow cytometry (Figure 3.2 a; T=0 hr, P1 – black bar). Immediately after staining, the cells were divided into two groups: treated with DVE (40 µg/ml) or untreated with PBS. They were then incubated for 48 hours before being assessed using flow cytometry (section 2.7). For the LCL cells, after 48 hours, approximately 65% of the untreated cells progressed to P2, while 57% of the cells treated with DVE also progressed to P2. This represents a reduction of 0.87-fold between the treated and untreated cells (Figure 3.2 a; T=48 hr, LHS panel, UT and DVE).

Notably, there was no significant disparity in the number of cellular debris (CD) observed in both the treated and untreated cells, for all cell lines. With regards to the SU-DHL-4 cells, after 48 hours, approximately 70% of untreated cells had progressed to P2, while 30% of DVE-treated cells progressed to P2, which represents a reduction of 2.3-fold between treated and untreated. (Figure 3.2 a; T=48 hr, middle panel, UT and DVE, and Figure 3.2b). Notably, within the DVE-treated SU-DHL-4 population, 49% of cell particles, corresponding to cellular debris/death (blue bar), were detected. For the second DLBCL cell line HBL-1, approximately 67% of untreated cells

progressed to P2 after 48 hours of treatment, while 52% of treated cells progressed to P2, which represents a reduction of 0.77-fold between treated and untreated. (Figure 3.2 a; T=48 hr, RHS panel, UT and DVE and Figure 3.2b). Among the DVE-treated HBL-1 population, 19 % of cell particles, corresponding to cellular debris/ death (blue bar), were detected.



	P2 (UT) %	P2 (T) %	Fold decrease	CD (UT) %	CD (T) %
PB-B95-8H	65	57	0.87	3.80	1
SU-DHL-4	70	30	2.3	0.82	49
HBL-1	67	52	0.77	2	19

Figure 3.2. DVE slows down the proliferation of DLBCL cells in comparison to LCLs and induces cell death. DLBCL cell lines SU-DHL-4 and HBL-1 as well as a non-cancerous cell line PB-B95-8H were stained with 0.5 μ M CFSE Cell Trace dye, seeded and treated with either 1x PBS (vehicle control-untreated (UT)) or DVE (40 μ g/ml). After 48 hours of treatment with DVE or vehicle, cells were fixed in 70% methanol and samples were examined using flow cytometry. A T = 0 sample was included to track P1 (parental cell) generation and P2 (daughter cell generation). Analysis was performed using the FlowJo v10.9 software. The experiment was carried out in duplicate.

3.3 DVE inhibits the proliferation of DLBCL cells in a semi-solid medium.

To further investigate the anti-proliferative effects of DVE, cell growth was assessed in a semi-solid matrix. Traditional liquid cell culture media is designed to ensure the continuous proliferation of cancer cells and does not replicate the microenvironment of tumours. In cancer research, a semi-solid matrix is commonly used to mimic the 3D microenvironment found *in vivo*. This allows for the assessment of the ability of cancer cells to form colonies from single cells and propagate. While the agar-based medium is widely used in these assays, it was not suitable for the growth of lymphocyte cell lines. Therefore, the methylcellulose-based semi-solid medium, MethoCult, is used. MethoCult contains specific supplements and growth factors that support the growth of hematopoietic-derived cells (Abuwatfa *et al.*, 2024). In this experiment, cells were seeded in MethoCult with or without the addition of DVE (30 µg/ml and 60 µg/ml), and proliferation was monitored over seven days (section 2.8).

Data was captured on Days 1, 3, 5, and 7. Representative images, captured on Day 1 and Day 7 are shown in Figure 3a below. In culture dishes that did not contain DVE, there is visual evidence of colony formation for all 3 cell lines, on Day 7. In contrast, in the presence of DVE, colony formation appeared to have been significantly inhibited. Using multiple images, the data was quantified using appropriate software (ImageJ, Version 1.8.0), and is shown in Figure 3b. Overall, the impact of DVE on colony formation was significantly more pronounced than in both DLBCL cell lines compared to the non-cancerous lymphoblastoid cell line (PB-B95-8H), from Day 3, through to Day 7, at both concentrations of DVE used. Interestingly, at both DVE concentrations, the percentage of HBL-1 colonies was slightly higher on Day 7, compared to Day 5, indicating an increase in proliferation from Day 5 to Day 7 in this ABC-DLBCL cell line, despite the presence of DVE. The same effect was not observed for SU-DHL-4, the GCB-DLBCL cell line. Overall, the results indicate that DVE preferentially retards the proliferation of SU-DHL-4 and HBL-1 cells compared to PB-B95-8H (Figure 3.3).

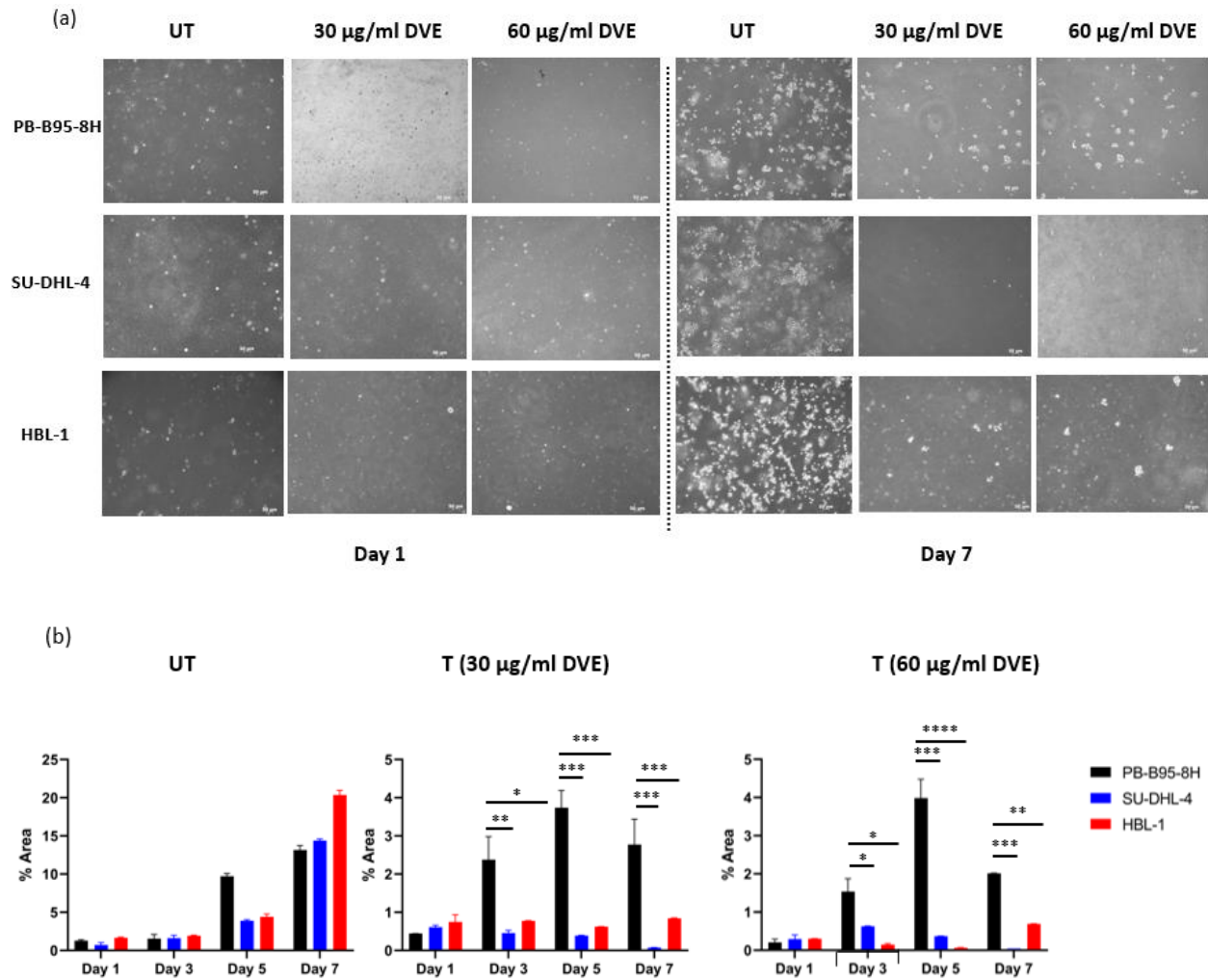


Figure 3.3. DVE inhibits the proliferation of DLBCL cells in a semi-solid medium. (a) Phase contrast images, at Day1 and Day 7, of DLBCL cells HBL-1 and SU-DHL-4, as well as the non-cancerous lymphoblastoid cells PB-B95-8H, cultured in MethoCult semi-solid medium, with (30 $\mu\text{g/ml}$ and 60 $\mu\text{g/ml}$) or without (Untreated -UT) DVE. (b) Evaluation of colony formation using ImageJ (Version 1.8.0). The software calculates the proportion of space (% area) occupied by the colonies in the captured images. Statistical analysis was performed using a 2-way ANOVA and Sidák's multiple comparisons test on GraphPad Prism 9 software. The data represents the mean \pm standard deviation (SD) (N =3). P values are indicated as * $p < 0.05$, ** $p < 0.01$, *** $p < 0.001$, **** $p < 0.0001$. The experiments were conducted at least in triplicate.

3.4 DVE does not modify the cell cycle profile of DLBCL cells and induces cell death.

The impact of DVE on the various phases of the cell cycle was investigated. The phases of the cell cycle include G0/G1, S, G2, and M. The process of mitosis contains several cell cycle checkpoints that play vital roles in maintaining the genome integrity of the cell and ensuring that a cell is only allowed to divide when the conditions are appropriate. In this way, cells harbouring genetic errors, and/or other abnormalities are prevented from propagating (Sherr and Bartek, 2017). When a checkpoint is triggered, for instance, due to DNA damage by a chemotherapeutic drug, the cell cycle is halted, and cells may accumulate within that phase, or undergo apoptosis, depending on the severity of the damage (Panagopoulos and Altmeyer, 2021). Certain anti-cancer drugs specifically target cell cycle mechanisms to induce cell death using various strategies. These strategies include inhibiting the activity of cell cycle regulators and proliferation factors, such as cyclins, cyclin-dependent kinases (CDKs), and cyclin-dependent kinase inhibitors (CDKIs) (Sherr and Bartek, 2017). Another mechanism via which cancer drugs may work is by activating TP53, a major trigger of the apoptotic cell death pathway. Overall, these approaches aim to disrupt the cell cycle and facilitate cell death as a therapeutic strategy against cancer.

In this experiment, following treatment (DVE and control), cells were fixed, and the DNA was stained using propidium iodide, followed by analysis by flow cytometry (section 2.9) (Figure A2 in Appendix A shows representative Flow cytometry data). A representation of the findings from three repeats of the experiment is presented in Figure 3.4 below. For all three cell lines, the untreated cells exhibited a typical cell cycle profile with most cells in the G1 phase of the cell cycle, the second largest cell population being in the G2/M phase, and a small population undergoing DNA replication (S phase) (Figure 3.4a, LHS panels). The sub-G1 population, which is indicative of dead or damaged cells, is consistent throughout all treatments for PB-B95-8H cells (Figure 3.4b, upper panel). In contrast, there is a significant increase in the sub-G1 population in SU-DHL-4 DVE-treated cells by ~10% (~2-fold) in cells treated with 60 µg/ml of DVE (Figure 3.4b, middle panel). For HBL-1 cells, there was a significant increase in the sub-G1 population, by ~6% (~3-fold), at both 30 µg/ml and 60 µg/ml of DVE treatment (Figure 3.4b, lower panel). Overall,

these findings suggest that DVE does not alter the cell cycle profile of DLBCL cells but does induce cell death.

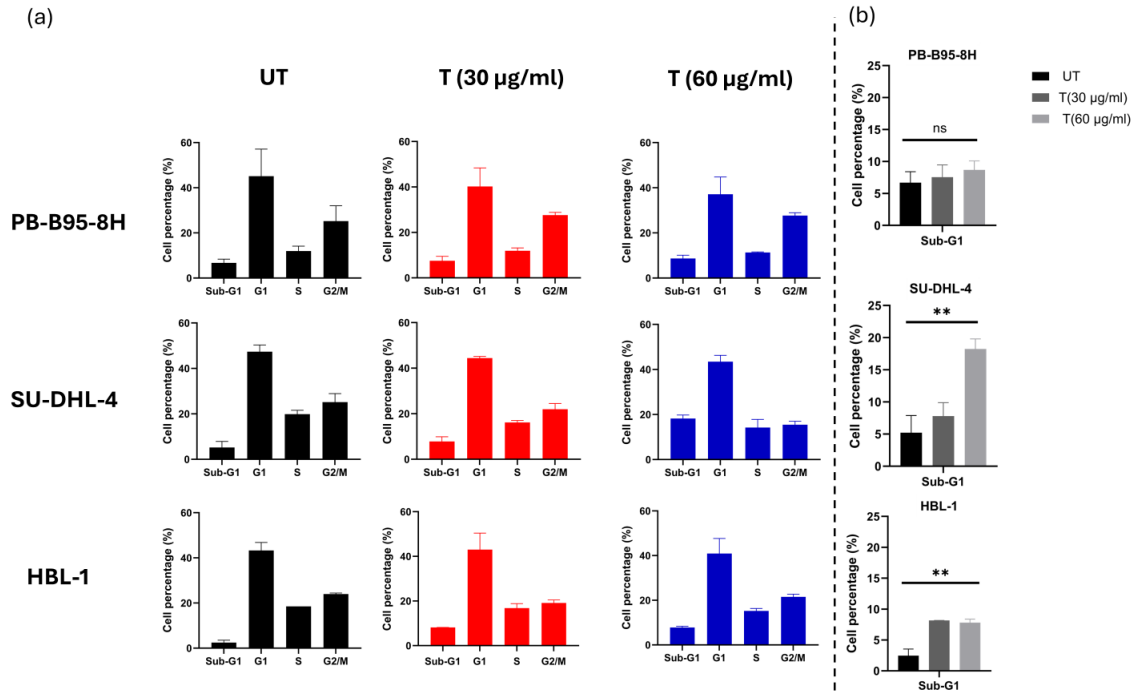
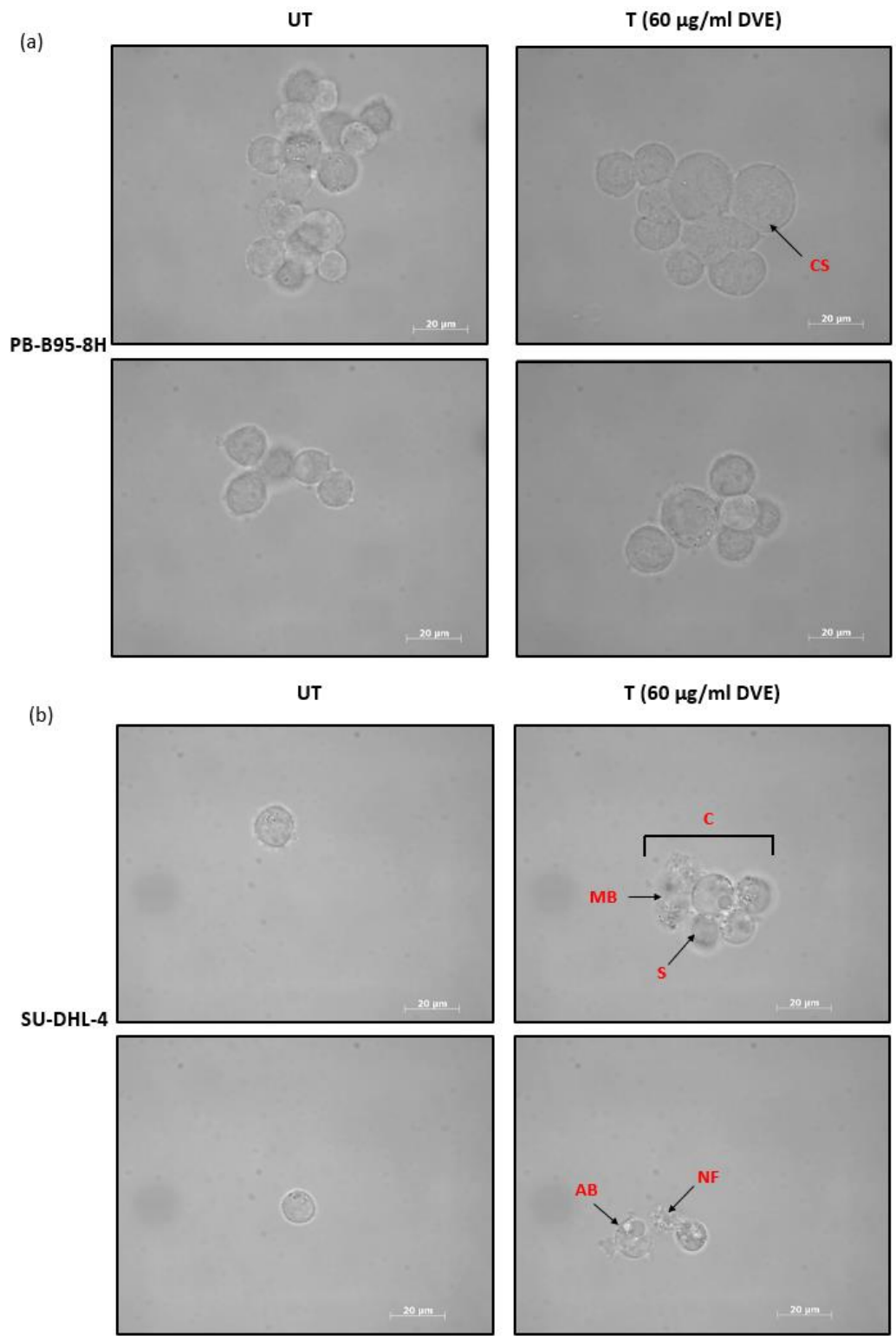


Figure 3.4. DVE does not modify the cell cycle profile of DLBCL cells and induces cell death. (a) DLBCL cell lines SU-DHL-4 and HBL-1, as well as a non-cancerous cell line PB-B95-8H, were treated with DVE (30 and 60 µg/ml) or treated with 1 x PBS (vehicle control- Untreated (UT)) for 24 hours. Post-treatment, the cells were fixed using 70% methanol and stained with FxCycle™ PI/RNase. Subsequently, the samples were analysed using BD Flow Cytometry (FACSCalibur™, Becton Dickinson, USA). (b) Comparison of sub-G1 populations, for each cell line, under each treatment condition. Statistical analysis was performed using a one-way ANOVA test on GraphPad Prism 10 software. The data represents the mean ± standard deviation (SD) (N =3). P values are indicated as *p<0.05, **p<0.01; ns – not significant. The experiments were conducted in at least in triplicates.

3.5 DLBCL cells exposed to DVE display typical apoptotic morphological features.

Having established that DVE induces cell death in the DLBCL cells, the mode of cell death was investigated. Apoptosis, which is a programmed mode of cell death, is a form of “cellular suicide” used by cells to eliminate damaged or abnormal cells. This mechanism is typically inhibited in cancer cells through diverse mechanisms, but most commonly through the overexpression of anti-apoptotic proteins, and the upregulation of pro-apoptotic proteins (Hanahan and Weinberg, 2011).

As a cell undergoes apoptosis, it is characterized by a series of typical morphological features such as cell shrinkage, membrane blebbing, chromatin condensation, nuclear fragmentation, and others (Banfalvi, 2017; Tixeira et al., 2017). These typical features were assessed in cells treated with DVE for 24 hours and compared to untreated cells (section 2.10). The data was captured using phase-contrast microscopy and representative images are shown in Figure 3.5 below. In the non-cancerous LCLs (PB-B95-8H), it appeared that exposure to DVE led to some cell swelling, but most cells displayed the same morphology as seen for cells that received no DVE (Figure 3.5 a). In contrast, both DLBCL cell lines exposed to DVE displayed typical features of apoptosis in most cells (Figure 3.5 b and c). Some of the typical features observed were shrinkage (S), clumping (C), membrane blebbing (MB), nuclear fragmentation (NF), and the appearance of apoptotic bodies (AB). The corresponding controls (cells not exposed to DVE) maintained their regular round shapes.



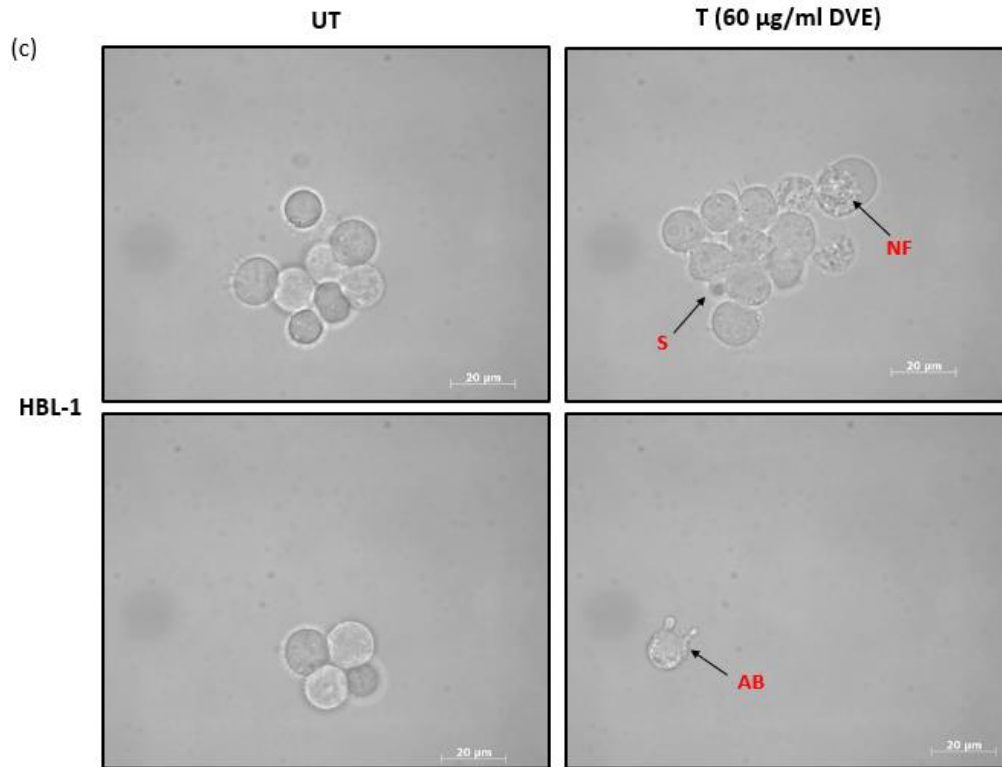


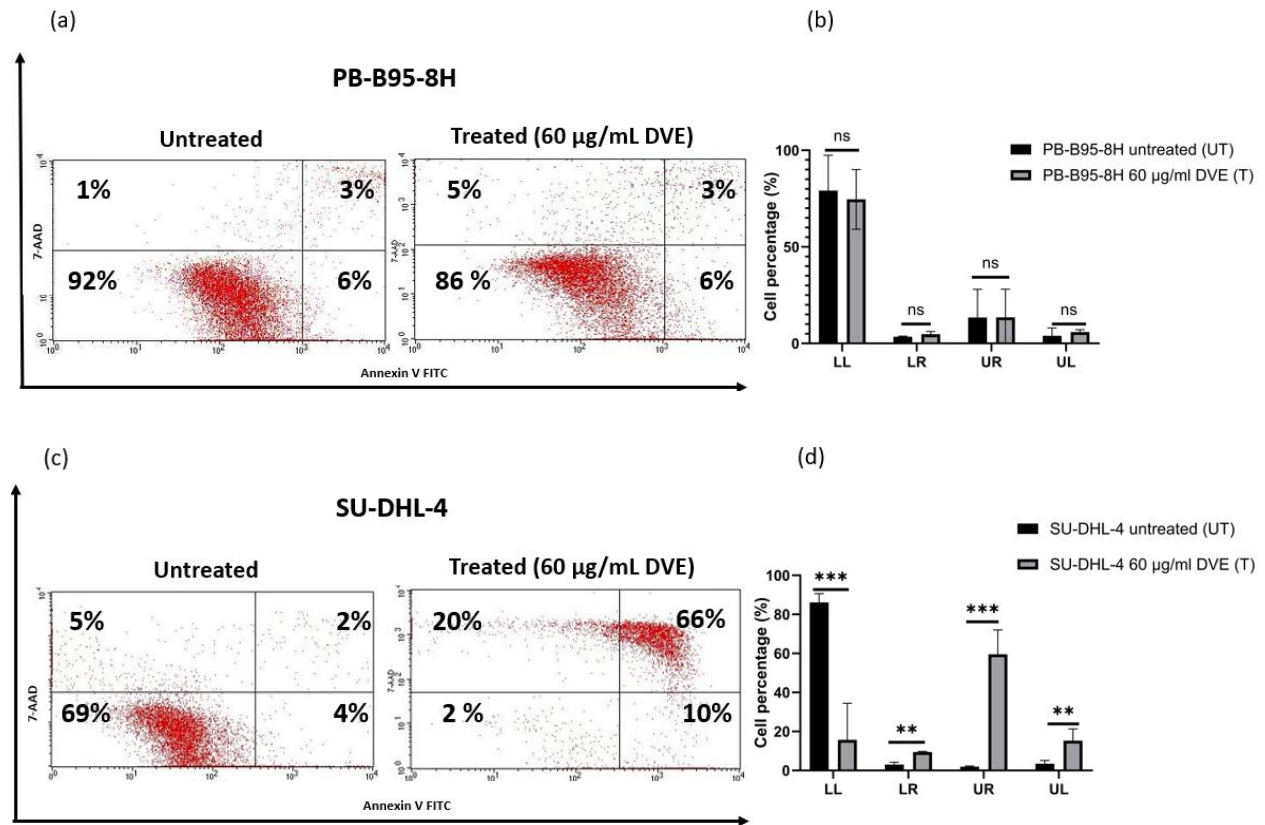
Figure 3.5. Morphological analysis of cells treated with DVE. Cells (PB-B95-8H, SUDHL-4, and HBL-1) were treated with either 1 x PBS (untreated (UT)) or 60 $\mu\text{g}/\text{ml}$ of DVE (treated (T)) for 24 hours. The analysis of cell morphology was performed using phase-contrast microscopy at a magnification of x100. The observed changes included cell swelling (CS), shrinkage (S), clumping (C), membrane blebbing (MB), nuclear fragmentation (NF), and apoptotic bodies (AB). The experiment was performed in triplicate.

3.6 Annexin V assay shows widespread cell death of DVE-treated DLBCL cells, relative to LCLs.

To validate the apoptotic effects of DVE on DLBCL cells, the Annexin V assay was utilized. The use of a cytofluorimetric technique allows for precise quantification of apoptosis by identifying cellular shrinkage, loss of membrane permeability, translocation of phosphatidylserine, and fragmentation of DNA. Additionally, the Annexin V/7-amino-actinomycin D staining method allows for differentiation between early apoptosis, late apoptosis, and non-viable/necrosis (Zimmermann and Meyer, 2011). Early apoptotic cells are identified by the presence of phosphatidylserines on the outer leaflet of the plasma membrane, which is visualized through labeled annexin V staining. Late apoptotic cells and necrotic cells, on the other hand, exhibit loss of cell membrane integrity, becoming permeable to vital dyes such as 7-AAD (DNA intercalator) (Zimmermann and Meyer, 2011). In this investigation, cells positive for 7-AAD were exclusively found in the upper left quadrants (UL) (non-viable/necrotic cells). Cells that were negative for both stains were found in the lower left quadrants (LL) and are viable cells. Cells positive for just Annexin V were in the lower right quadrants (LR) and were in the early stages of apoptosis. Finally, cells positive for both Annexin-V and 7-ADD were seen in the top right quadrants (UR) and were late apoptotic cells.

Cells were exposed to DVE for 24 hours, while controls did not receive DVE (section 2.11), after which they were processed and analysed using a flow cytometer. A typical Annexin V/PI plot is shown in Figure A3 (Appendix A). As shown in Figure 3.6 below, which is representative of at least three repeats of the experiment, there was a negligible and not significant change in the distribution of cells in the various quadrants for the non-cancerous PB-B95-8H cells from untreated to treated (Figure 3.6 a and b). In both treated and untreated PB-B95-8H cells, around 3% were in early apoptosis and 6% were in late apoptosis, while, in the DVE-treated PB-B95-8H, 5% of the cell population was non-viable/necrotic, compared to 1% of the cell population in the untreated cells.

In the GCB-DLBCL cell line SU-DHL-4, there were significant changes for all groups, i.e., viable (LL), early apoptotic (LR), late apoptotic (UR), and non-viable/necrotic cells (UL), upon exposure to DVE. Significant increases by ~2.5-fold, ~33-fold, and ~4-fold for early apoptotic, late apoptotic, and non-viable/necrotic cells respectively (Figure 3.6 c and d). In the ABC-DLBCL cell line HBL-1, there was a significant change observed in the LL quadrant, indicating that the cells were susceptible to DVE, however, in contrast to SU-DHL-4, most affected cells were located in the LR quadrant (~50-fold), which is indicative of cells in the early apoptotic phase (Figure 3.6 e and F).



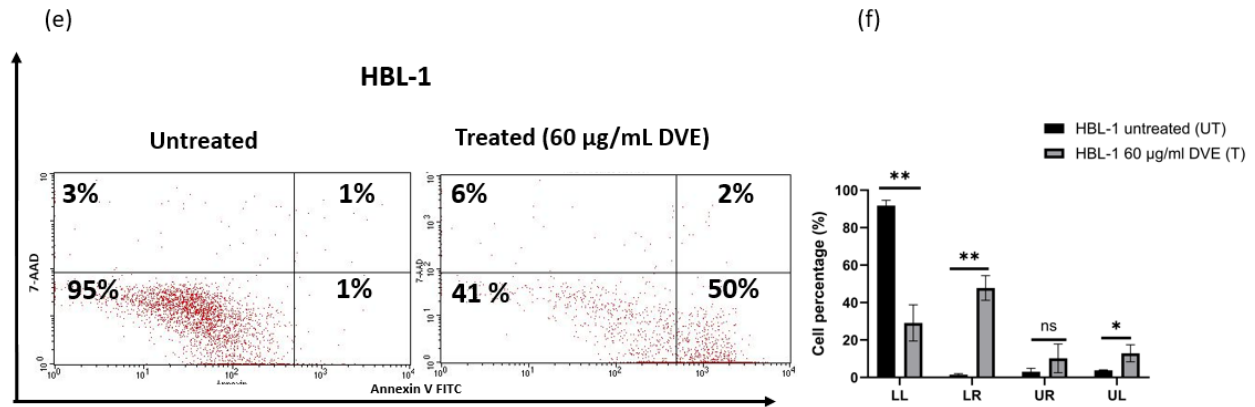


Figure 3.6. DVE induces apoptosis in DLBCL cells. Cells (PB-B95-8H, SUDHL-4, and HBL-1) were treated with either 1 x PBS (untreated (UT)) or 60 µg/ml of DVE (treated (T)) for 24 hours. Following treatment; the cells were stained with 7-Aminoactinomycin D (7-AAD) and Annexin V and fixed with 70% methanol. The samples were analysed using BD Flow Cytometry (FACSCalibur™, Becton Dickinson, USA) within 1 hour of staining (A, C, E) and the data was plotted using GraphPad Prism 10 (B, D, F). The quadrant abbreviations are LL – lower left, LR – lower right, UR – upper right, and UL – upper left. The experiments were conducted in at least triplicates. Statistical analysis was performed using a Two-way ANOVA test on GraphPad Prism 10 software. The data represents the mean ± standard deviation (SD) (N =3). P values are indicated as *p<0.05, **p<0.01, ***p<0.001; ns – not significant.

3.7 DVE potently induces the activity of early-stage executioner caspase-3/7.

Caspases are a class of proteases that contain cysteine aspartyl and are known to have a critical role in apoptosis. During apoptosis, they undergo activation and subsequently cleave a multitude of cellular proteins, which eventually results in the orderly disassembly of the dying cells (Shim *et al.*, 2017). Initiator caspases (2, 8, 9) have long N-terminal prodomains (100-200 amino acids) and are activated through extrinsic and intrinsic apoptosis, while executioner caspases have short N-terminal prodomains (20 amino acids) and are cleaved by initiator caspases to become active and target specific substrates, resulting in cell death (Cade and Clark, 2015). Executioner caspase-3 and caspase-7 are recognized as the primary executioner caspases that participate in the initial stages of apoptosis in viable cells and are accountable for cleaving different cellular substrates, leading to the disintegration of the cell and its ultimate death (Shim *et al.*, 2017).

The Caspase-Glo® 3/7 Assay was used to evaluate the impact of DVE on the initiation of early-stage apoptosis in both DLBCL cells and non-cancerous cells. This assay uses luminescence to measure the activity of caspase-3 and -7 (Shi, 2004). The Caspase-Glo® 3/7 assay kit includes a caspase-3/7 DEVD-aminoluciferin substrate and a thermostable luciferase in a reagent optimized for caspase-3/7 activity, luciferase activity, and cell lysis. By adding the Caspase-Glo 3/7 Reagent in an add-mix-measure format, cell lysis occurs, followed by caspase cleavage of the substrate. This releases free aminoluciferin, which is then consumed by the luciferase, resulting in a luminescent signal. The intensity of the signal corresponds to caspase 3/7 activity (Fink and Cookson,2005).

DLBCL cells (SU-DHL-4 and HBL-1) as well as non-cancerous lymphoblastoid cells (PB-B95-8H) were exposed to DVE for 24 hours while control cells were treated with corresponding amounts of 1 x PBS (section 2.12). As is shown in Figure 3.7 below, there was an unexpected but significant increase in caspase 3/7 activity, of ~2.5-fold, in the PB-B95-8H cells. Similarly, an increase was observed for the HBL-1 cells, albeit to a smaller extent (1.5-fold), and not statistically significant. In the SU-DHL-4 cells, there appears to be a decrease in caspase 3/7 activity (~3.2-fold), but once again, not statistically significant.

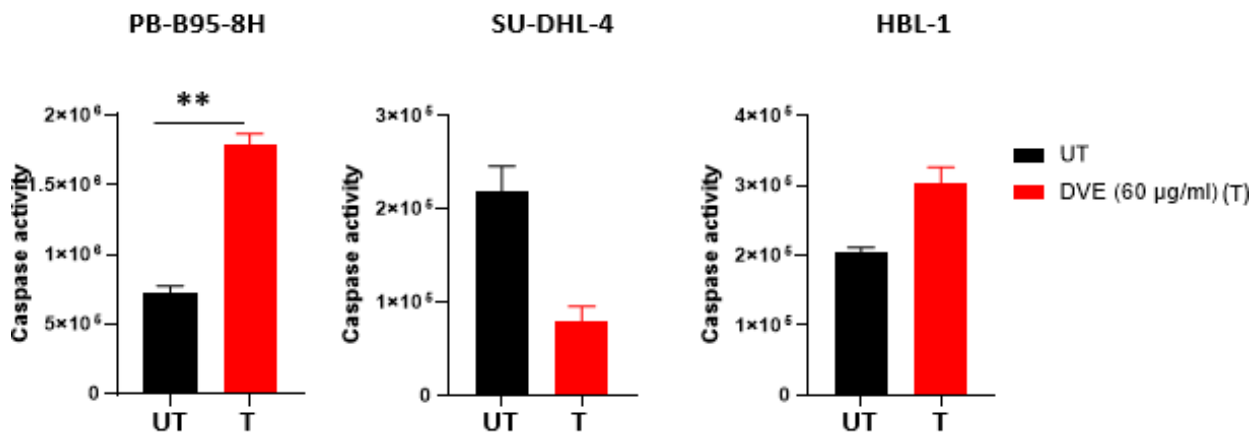


Figure 3.7. DVE potently induces the activity of early-stage executioner caspase-3/7. Cells were treated with 60 µg/ml DVE (treated (T)) or with the vehicle control 1x PBS (untreated (UT)) for 24 hours and caspase 3/7 activity was measured using Caspase-Glo® 3/7 luminescent assay. Caspase activity was significantly enhanced in the PB-B95-8H cells (~2.5-fold; LHS panel). An increase was also observed for DVE-treated HBL-1 (1.5-fold), while a decrease was observed for DVE-treated SU-DHL-4 cells (3.2-fold), both non-statistically significant. Statistical analysis was performed using a One-way ANOVA and Sidák's

multiple comparisons test on GraphPad Prism 9 software. The data represents the mean \pm standard deviation (SD) (N =3). P values are indicated as **p<0.01.

3.8 DVE modulates the expression of apoptotic markers caspase-3 and PARP-1.

The impact of DVE on the expression of two markers of apoptosis, namely executioner caspase-3, and its target poly (ADP-ribose) polymerase (PARP) was investigated using the western blot analysis. Upon induction of apoptosis, caspase-3 (executioner) gets cleaved by caspase-8/9 (initiator) to yield two subunits, namely p11 and p17 (Jan 2019). PARP-1 is a major target of caspases, including caspase-3, and gets cleaved into two main fragments, namely an 89 kDa and a 24 kDa fragment. Therefore, the presence of the cleaved products of caspase-3 and PARP-1 are considered hallmarks of apoptosis. Of note however, is that PARP-1 is also processed during necrosis, but is cleaved differently to apoptosis, whereby, in addition to the 89 kDa band, it also produces smaller products ranging from 74 to 42 kDa (Gobeil *et al.*, 2001).

DLBCL cells (SU-DHL-4 and HBL-1), as well as non-cancerous lymphoblastoid cells (PB-B95-8H), were exposed to 30 and 60 $\mu\text{g/ml}$ DVE for 24 hours while control cells were treated with corresponding amounts of 1 x PBS. Thereafter, total proteins were extracted and subjected to western blot analyses (section 2.14), probing for caspase 3, using an antibody able to detect all three bands, namely the uncleaved 32 kDa procaspase protein, as well as the cleaved products. The uncleaved 32 kDa protein was detectable in all samples (Figure 3.8a). Cleaved caspase-3 products were visible for HBL-1 DVE-treated cells, the 17 kDa band being dominant in the 30 $\mu\text{g/ml}$ DVE-treated sample, and the 11 kDa band being dominant in the 60 $\mu\text{g/ml}$ DVE-treated sample. In contrast, there were no prominent cleaved caspase-3 bands observable within the DVE-treated SU-DHL-4 lanes, however, upon close inspection, the 17 kDa band can be faintly detected in the 30 $\mu\text{g/ml}$ DVE-treated SU-DHL-4 sample (indicated by blue arrow).

The results of our assays thus far indicate that the SU-DHL-4 cell line is more sensitive to DVE, compared to HBL-1 (for instance, in Figures 3.2, 3.4, and 3.6), and we therefore hypothesized that, if SU-DHL-4 was exposed to lower doses of DVE, cleaved caspase-3 products would be more

readily detected. To investigate this, a dose-response assay was performed, whereby SU-DHL-4 cells were treated with a range of DVE (0, 5, 10, 20, 30, and 60 $\mu\text{g}/\text{ml}$) for 24 hours, and the protein samples were subjected to western blot analysis as before. Besides a faint 17 kDa band in some lanes, it did not appear that the cleavage of procaspase-3 occurred when these cells were exposed to DVE (Figure 3.8b). Despite longer exposures, no bands representing the cleaved caspase-3 proteins were observed (data not shown).

The major cleaved product of PARP-1, namely the 89 kDa protein is present in DVE-treated PB-B95-8H, as well as HBL-1 cells, with the band being more prominent in the HBL-1 cells, especially in cells treated with 60 $\mu\text{g}/\text{ml}$ of DVE (Figures 3.8 c and d). The dose-response samples were used to detect cleaved PARP-1 in the SU-DHL-4 cells. The cleaved 89 kDa PARP-1 protein was visible in all DVE-treated samples, with the highest expression observed in the 60 $\mu\text{g}/\text{ml}$ DVE-treated sample (Figure 3.8 e). Interestingly, additional cleaved PARP-1 products were also detected, especially in the 60 $\mu\text{g}/\text{ml}$ DVE-treated sample. For all blots, the β -actin protein was detected to serve as an internal loading control, and images of the blots are depicted directly underneath the relevant experimental blots (Figures 3.8 a, b, c, d, and e).

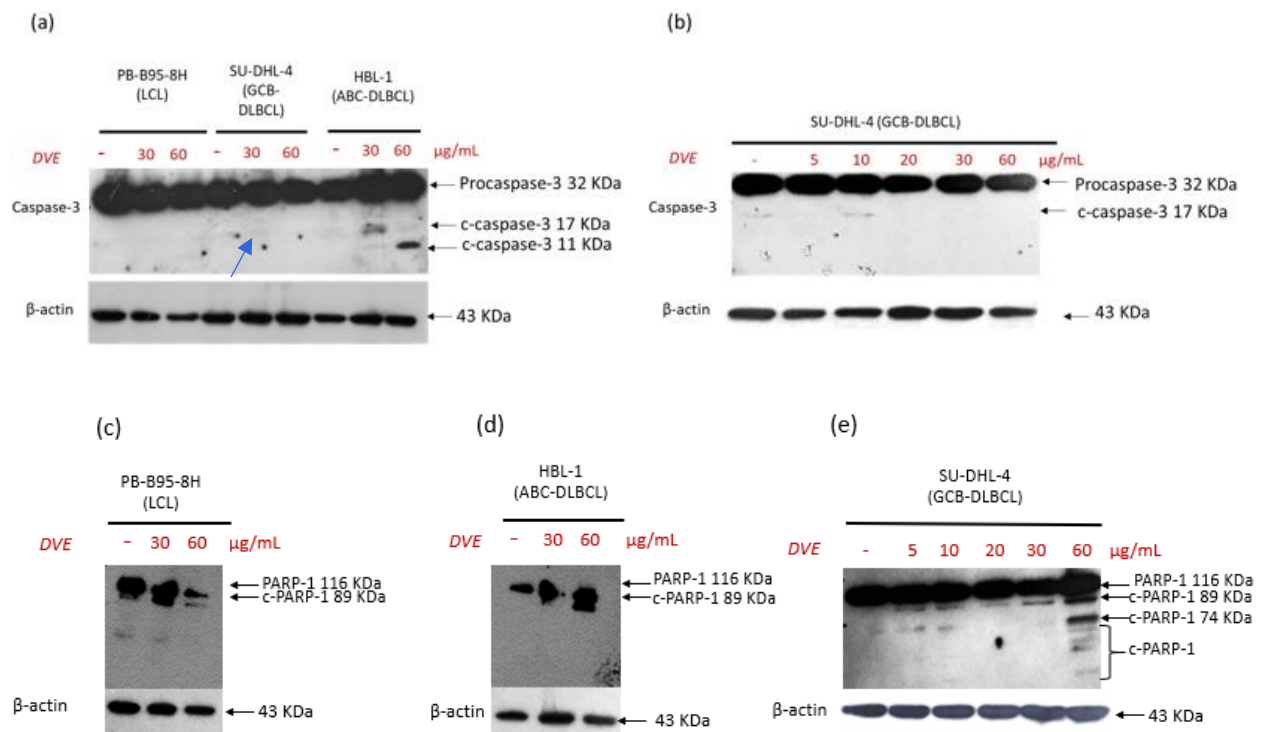


Figure 3.8. DVE modulates the expression of apoptotic markers caspase-3 and PARP-1. Cells were treated with the indicated concentrations of DVE for 24 hours, total protein was extracted and subjected to western blotting using antibodies against full-length and cleaved products of caspase-3 and PARP-1. The loading control was determined using an anti- β -actin antibody. The experiments were conducted in duplicate.

Chapter 4

Discussion

Complementary and alternative medicine (CAM) refers to a broad range of healthcare practices that are not integrated into the primary healthcare system. One of the most prevalent types of alternative medicine is called “traditional medicine” which includes the use of animal, plant, or mineral-based substances to treat a variety of ailments (Jermini *et al.*, 2019). Medicinal plants have a long history of usage in traditional medicine, particularly in South Africa. Approximately 80% of South Africans rely on traditional healers, who mostly use plants to treat various ailments including cancer (Boum *et al.*, 2021). The importance of traditional medicinal plants extends beyond traditional applications since a significant number of approved anti-cancer therapeutic drugs are derived from plants. This illustrates that the study of the medicinal properties of plants is of importance to the pharmaceutical industry (Voicu *et al.*, 2023; Greenwell and Rahman, 2015).

Dodonaea viscosa var. *angustifolia* is a medicinal plant that is widely used by the Rastafarian traditional healers in the Western Cape of South Africa, to treat a variety of ailments. Previous studies have indicated that *D. viscosa* extract displays cytotoxic effects in breast, colon, cervical, ovarian, and colorectal cancer cells, signifying its potential as a source of bioactive compounds for the development of anti-cancer agents (Al-Musawi and Al-Saadi, 2021; Herrera-Calderon *et al.*, 2020; Jayaraman *et al.*, 2021; Mossa and Al Shawi, 2015; Palanisamy *et al.*, 2021; Ramkumar *et al.*, 2021). Our previous study demonstrated that aqueous extracts of *D. viscosa* (DVE) were selectively toxic against Burkitt lymphoma (BL) cells relative to non-cancerous cells (Unpublished data). BL is an aggressive B cell-derived cancer that is overrepresented among HIV-infected individuals.

The current study provides strong evidence to show that DVE is selectively cytotoxic towards Diffuse large B cell lymphoma (DLBCL), a highly aggressive B-cell derived cancer, which is the most prevalent type of non-Hodgkin lymphoma worldwide, but also the most prevalent HIV-associated

lymphoma (Pasqualucci, 2013; Berhan *et al.*, 2022). DLBCL can be broadly categorized into two main subtypes, namely germinal-centre B cell type (GBC) and activated-B cell type (ABC), with the latter having a more aggressive clinical course, and poorer outcome in patients.

Aqueous extracts of DVE demonstrated favourable selectivity indices for both the GCB-DLBCL cell line SU-DHL-4 (SI of 2.25) and the ABC-DLBCL cell line HBL-1 (SI of 3) which indicates good therapeutic potential with potentially minimal side effects. In the current study, the aqueous extract was tested over the methanolic extract to align with how the plant more closely is used by South African traditional healers, which is most often infused in water (as a tea). In future studies, extracts derived from organic solvents will also be investigated since it is well established that the phytochemical composition is different depending on the solvent used. To date, most studies have tested ethanolic extracts of DVE. For instance, Shafek and colleagues demonstrated that an 80% ethanolic extract of *Dodonaea viscosa* achieved higher cytotoxic activity against breast cancer cells compared to the approved drug cisplatin (Shafek *et al.*, 2015). In a previous study, it was reported that *Dodonaea viscosa* compounds, dodoneasides A and B, as well as the CH₂Cl₂ fraction of the extract, exhibited significant antiproliferative activity against the A2780 ovarian cancer cell line, with IC₅₀ values ranging from 0.70 to 6.0 mg/mL (Cao, 2009). The IC₅₀ dosages of both DLBCL cell lines (SU-DHL-4 and HBL-1) are significantly lower than the previously reported IC₅₀ doses of DVE for other malignancies. It is worth mentioning, however, that the *D. viscosa* plants originated from different geographical areas, which may lead to variations in the relative amounts of phytochemicals, aside from the fact that the *D. viscosa* extracts were prepared differently.

Proliferation is a key characteristic of cancer, whereby cancer cells grow uncontrollably and excessively (Hanahan, 2022). Within DLBCL, the survival and growth of the malignant B-cells are supported by a signalling pathway called B-cell receptor (BCR) signalling (Young *et al.*, 2015). The activation of this pathway can occur due to activating mutations within the BCR complex or downstream signalling components. Additionally, even in the absence of external signals, the BCR pathway can still be activated through a phenomenon known as ligand independent tonic BCR signalling (Young *et al.*, 2015). Previous studies have identified two kinases, SYK and BTK, which are associated with the BCR complex and have emerged as potential therapeutic targets for

DLBCL (Profitós-Pelejà *et al.*, 2022; Wang *et al.*, 2021). Thus, targeting the BCR signalling pathway holds significant potential for the treatment of DLBCL.

DVE preferentially retards the proliferation of the DLBCL cells (SU-DHL-4 and HBL-1) relative to the proliferation of the non-cancerous LCL cells (PB-B95-8H). This was demonstrated using an assay that tracks cell proliferation over time, as well as a colony-forming assay. Additionally, DVE induced cell death in the DLBCL cells. Our findings indicated that, at the same concentration of DVE, SU-DHL-4 cells were more sensitive than HBL-1 in both the proliferation tracking assay (2.3-fold reduction in cell progression to P2 in SU-DHL-4 cells, while HBL-1 cells exhibited a 0.78-fold reduction in cell progression to P2) as well as in the colony forming assay, where less area was covered by SU-DHL-4 cells, compared to HBL-1 cells, in medium containing DVE, at days 5 and 7. Interestingly, in the HBL-1 cell line, the percentage of colonies was slightly higher on Day 7 compared to Day 5, indicating that the cells may have started recovering from Day 5, or that a small percentage of resistant HBL-1 cells may have taken over the population and started expanding. The same was not observed for the SU-DHL-4 cell line. It is quite well documented that ABC-DLBCL is a more aggressive disease than GCB-DLBCL, with a higher proliferation index, and that ABC-DLBCL is associated with poorer outcomes when treated with standard therapy, compared to GCB-DLBCL (Cheng *et al.*, 2022). Our data therefore confirms what is reported in the literature.

Cell cycle profiling in cancer involves analyzing the effects of factors on the ability of cells to progress through the various phases of the cell cycle, namely G1, S, G2 and M. A block in a specific phase of the cell cycle could indicate inhibition of cell cycle regulators such as cyclins and cyclin-dependent kinases. The result of the cell cycle profiling suggests that DVE does not significantly alter the cell cycle profile of DLBCL cells, but rather it induces cell death, as evidenced by the presence of a sub-G1 peak. As was observed in the assays measuring proliferation, the SU-DHL-4 cells were found to be more sensitive to DVE, compared to the HBL-1 cells. For instance, at 60 µg/ml of DVE, 15% of the SU-DHL-4 population had cleaved DNA, represented by the sub-G1 peak, compared to only 5% for HBL-1. Similar observations were also made in a comprehensive study that evaluated a bioactive compound extracted from seaweed, fucoidan. The results

exhibited a dose- and time-dependent inhibition of DLBCL cell growth like the observation made in our study (Yang *et al.*, 2015). This inhibition was accompanied by sub-G1 cell cycle arrest, a phenomenon associated with the prevention of cell proliferation as well as sub-G0 cell cycle arrest associated with cell death. Additionally, fucoidan downregulated the expression of cyclin D1, Cdk4, and Cdk6, which are key regulators of the cell cycle (Yang *et al.*, 2015).

It should be mentioned that there was no notable increase in the non-cancerous lymphoblastoid (PB-B95-8H) cell sub-G1 population across treatments (untreated (UT) as well as 30 and 60 µg/ml DVE). The noticeably high percentages of the sub-G1 cell population of PB-B95-8H cells may be due to their non-cancerous nature, making them more fragile than cancer cells. It could be that during the preparation of the cells for flow cytometry, they were damaged. Another possibility is that a small population of cells is constantly undergoing apoptosis, which is a feature of this cell line and can be observed under the microscope during routine culturing.

Morphological analyses revealed that DLBCL cell lines developed typical features of the programmed cell death mechanism of apoptosis, upon exposure to DVE. These features included cell shrinkage, clumping, membrane blebbing, nuclear fragmentation, and the appearance of apoptotic bodies. The same was not observed for the non-cancerous LCLs. Apoptosis is the desirable mode of cell death by chemotherapeutic agents as it does not induce a severe inflammatory response. The two main pathways inducing apoptosis are the intrinsic (mediated by the mitochondria) and extrinsic (mediated by trans-membrane receptors) pathways, with both ultimately culminating towards the activation of initiator and executioner caspases (Beigl *et al.*, 2023; O'Connor *et al.*, 2023; Liao, 2021). Although the DVE-treated PB-B95-8H cells did not display features of apoptosis, some cells did appear to swell, which is not a typical feature of apoptosis, but rather an early feature of necrosis. Necrosis is uncontrolled cell death, and not desirable, due to the uncontrolled and sudden release of inflammatory factors, causing a domino effect of cell damage. However, the doses of DVE used in the study appear to be below the threshold needed to induce advanced necrosis in the PB-B95-8H cells.

The morphological analysis results were further validated with Annexin V assays, for assessment of early and late apoptotic populations, as well as populations that have reached an advanced

stage of cell death (which could include necrosis). The distribution of PB-B95-8H cells in different categories (quadrants) did not show a significant change between the untreated and DVE-treated cells. In the GCB-DLBCL cell line (SU-DHL-4), all three categories - early apoptosis, late apoptosis, and non-viable/necrotic cells - showed an increase upon exposure to DVE. The most significant increase was observed in the percentage of late apoptotic cells, which increased from 2% to 66% of the total cell population. Additionally, the percentage of non-viable/necrotic cells also noticeably increased from 5% to 20% of the total cell population. In the ABC-DLBCL cell line, a major increase was observed in the percentage of early apoptotic cells -from 1% to 50%. There was a less pronounced increase in the percentage of non-viable/necrotic cells, which increased from 3% to 6%. This contrasts with the GCB-DLBCL cell line, where the major increase was observed in late apoptotic cells suggesting that the GCB-DLBCL cell line (SU-DHL-4) is more sensitive to treatment with DVE relative to the ABC-DLBCL cell line. Once again, a distinct difference in response can be observed between the two cell lines, with the GCB-DLBCL cell line being more sensitive than the ABC-DLBCL cell line, at the same concentration of DVE. Thus, while using a variety of different assays, the same trend was consistently observed and confirmed.

The Annexin V assay result was further supported by the caspase 3/7 activity assay along with the western blot analyses. The caspase-3/7 activity was significantly increased in the non-cancerous lymphoblastoid cells (PB-B95-8H) treated with DVE relative to the untreated cells. The changes in caspase 3/7 activity in HBL-1 and SU-DHL-4 cells were not statistically significant, indicating that the observed changes were variable and inconsistent. The caspase 3/7 activity assay measures the early stage of apoptosis, likely before any obvious changes in cell morphology. This may explain the result observed in the non-cancerous lymphoblastoid cells, which is, a significant increase in caspase 3/7 activity in DVE-treated cells – we hypothesize that DVE induces stress in these cells and primes them for apoptosis by activating the caspases, but other combinatorial factors required for progression in advanced stage apoptosis are not induced, and thus the cells do not proceed into apoptosis. In the DLBCL cells, more advanced stages of apoptosis have been attained, where caspase 3/7 have themselves begun to be degraded/inactivated. This hypothesis can be supported by the western blot result, where

copious amounts of cleaved PARP-1, which gets processed by caspase-3, can be seen in the DVE-treated DLBCL cells.

Unexpectedly, no clear bands indicating the presence of cleaved caspase-3 could be detected in the SU-DHL-4 cells treated with DVE, even when exposed to lower concentrations of DVE. This suggests that, in the SU-DHL-4 cells, caspase-3 may not be the protein of choice in driving apoptosis. Caspase-3, while being the dominant executioner caspase, is not the only one, with caspase-6 and 7 able to perform the same function (McIlwain *et al.*, 2013). Due to time constraints, this could not be verified but is planned as a future experiment.

Another interesting finding was the presence of the 74 KDa PARP-1 fragment as well as other smaller cleaved products of PARP-1. The detection of the 74 KDa PARP-1 fragment has been previously reported to be a feature of necrotic cells (Gobell *et al.*, 2001). This, together with the Annexin V result showing an increase in non-viable/necrotic cells, suggests that DVE may be inducing both necrosis and apoptosis in the SU-DHL-4 cells. Future studies are being planned to verify this by using western blotting to detect specific and validated markers of necrosis, such as RIPK1 and RIPK2, as well as others (Wu *et al.*, 2020).

Conclusion

In summary, these findings suggest that DVE induces selective cytotoxicity against DLBCL cells (SU-DHL-4 and HBL-1), while the non-cancerous cells remain largely unaffected. In addition, our data show that the ABC-DLBCL cell line is less sensitive to DVE, compared to the GCB-DLBCL cell line. This therefore suggests that a dose-adjusted approach should be taken during treatment, depending on the subtype. Similarly, DVE more potently affected the colony formation of DLBCL cells as observed over a 7-day period. While cell cycle phases remained unaffected, DVE induced cell death as evidenced by a sub-G1 peak in DLBCL cell populations. Typical morphological features of apoptosis were identified in the DVE-treated DLBCL cells, which was corroborated with Annexin V assays, caspase-3/7 activity assays, as well as expressions of cleaved caspase-3 and cleaved PARP-1. The results also revealed different modes of cell death between the two subtypes of DLBCL, which requires further investigation.

Future studies will focus on further characterizing the mode, as well as the mechanism of cell death induced by DVE in DLBCL. Moreover, efforts are being made to identify potential bioactive compounds in DVE by fractionation assays. Currently, at least 4 flavonoids have been isolated from DVE, and their cytotoxicity will be assessed. Additionally, pre-clinical assays, using DLBCL xenograft mouse models are being developed to test the effect of DVE on the progression of tumour growth *in vivo*.

The selective cytotoxicity of the DVE against DLBCL cells, while sparing non-cancerous cells, underscores its potential as a promising source of anticancer bio-active compounds for therapy. This comprehensive investigation of *Dodonaea viscosa* cytotoxic effects on DLBCL cells fills a crucial research gap and sets the stage for further exploration of novel phytochemicals with potential anticancer properties.

The study demonstrates that our natural flora holds medicinal potential and highlights the benefits of exploring this resource. However, it is crucial that these investigations be conducted in a considered and sustainable manner, being mindful of the communities who make use of these traditional remedies. Engaging in efforts to document, protect, and commercialize these plants can improve the economic status of these communities and help conserve important plant species for healthcare, new drug development, and sustainable management of biomes. By integrating traditional healing methods with modern scientific research, and identifying plant species with medicinal properties, we can fully unlock the benefits of natural flora for human health and environmental protection.

References

1. Abdullahi, A.A., 2011. Trends and challenges of traditional medicine in Africa. *African journal of traditional, complementary, and alternative medicines*, 8(5S).
2. Abramson, J.S., 2019. Hitting back at lymphoma: How do modern diagnostics identify high-risk diffuse large B-cell lymphoma subsets and alter treatment? *Cancer*, 125(18), pp.3111-3120.
3. Adan, A., Kiraz, Y. and Baran, Y., 2016. Cell proliferation and cytotoxicity assays. *Current pharmaceutical biotechnology*, 17(14), pp.1213-1221.
4. Alaggio, R., Amador, C., Anagnostopoulos, I., Attygalle, A.D., Araujo, I.B.D.O., Berti, E., Bhagat, G., Borges, A.M., Boyer, D., Calaminici, M. and Chadburn, A., 2022. The 5th edition of the World Health Organization classification of haematolymphoid tumours: lymphoid neoplasms. *Leukemia*, 36(7), pp.1720-1748.
5. Alanazi, A.Z., Al-Rejaie, S.S., Ahmed, M.M., Alhazzani, K., Alhosaini, K., Sobeai, H.M.A., Alsanea, S., Alam, P., Almarfadi, O.M., Alqahtani, A.S. and Alhamed, A.S., 2023. Protective role of *Dodonaea viscosa* extracts against streptozotocin-induced hepatotoxicity and nephrotoxicity in rats. *Saudi Pharmaceutical Journal*, 31(8), p.101669.
6. Alasmari, A., 2022. Hepatoprotective activity of *Dodonaea viscosa* leaf extract nanoparticles against N-nitrosodiethylamine induced tumour initiation in rat liver: Modulation of apoptosis and signaling pathways. *Journal of Environmental Biology*, 43(2), pp.177-187.
7. Al Bimani, B.M.H. and Hossain, M.A., 2020. A new antimicrobial compound from the leaves of *Dodonaea viscosa* for infectious diseases. *Bioactive Materials*, 5(3), pp.602-610.
8. Alghamdi, M.D., Nazreen, S., Ali, N.M. and Amna, T., 2022. ZnO nanocomposites of *juniperus procera* and *dodonaea viscosa* extract as antiproliferative and antimicrobial agents. *Nanomaterials*, 12(4), p.664.
9. Aliyu, B.S., 2006. Some ethno medicinal plants of the Savannah regions of West Africa: description and phytochemicals. *Triumph publishing company*, 1, pp.135-152.

10. Almatroodi, S.A., Alsahli, M.A., Almatroudi, A., Verma, A.K., Aloliqi, A., Allemailem, K.S., Khan, A.A. and Rahmani, A.H., 2021. Potential therapeutic targets of quercetin, a plant flavonol, and its role in the therapy of various types of cancer through the modulation of various cell signaling pathways. *Molecules*, 26(5), p.1315.
11. Al-Musawi, Z.F. and Al-Saadi, N.H., 2021. antitumour activities of biosynthesized silver nanoparticles using *Dodonaea viscosa* (L.) leaves extract. *Basrah Journal of Agricultural Sciences*, 34(2), pp.42-59.
12. Amanda, N., Henning., Myagmarjav, Budeebazar., Delgerbat, Boldbaatar., Dahgwahdorj, Yagaanbuyant., Davaadorj, Duger., Khishigjargal, Batsukh., Huizhi, Zhou., Ryan, Baumann., Robert, D., Allison., Harvey, J., Alter., Naranjargal, Dashdorj., Valeria, De, Giorgi., 2022. Peripheral B cells from patients with hepatitis C virus-associated lymphoma exhibit clonal expansion and an anergic-like transcriptional profile. *iScience*, Available from: 10.1016/j.isci.2022.105801.
13. Anandan, M., Poorani, G., Boomi, P., Varunkumar, K., Anand, K., Chuturgoon, A.A., Saravanan, M. and Prabu, H.G., 2019. Green synthesis of anisotropic silver nanoparticles from the aqueous leaf extract of *Dodonaea viscosa* with their antibacterial and anticancer activities. *Process Biochemistry*, 80, pp.80-88.
14. Andreas, Schicho., Werner, Habicher., Christina, Wendl., Christian, Stroszczyński., Quirin, David, Strotzer., Marco, Dollinger., Andreas, G., Schreyer., Stephan, Schleder., 2022. Clinical Value of Diffusion-Weighted Whole-Body Imaging with Background Body Signal Suppression (DWIBS) for Staging of Patients with Suspected Head and Neck Cancer. *Tomography*, doi: 10.3390/tomography8050210
15. Ansell, S.M., 2015, November. Hodgkin lymphoma: diagnosis and treatment. In *Mayo Clinic Proceedings* (Vol. 90, No. 11, pp. 1574-1583). Elsevier.
16. Arlt, D., Huber, W., Liebel, U., Schmidt, C., Majety, M., Sauermann, M., Rosenfelder, H., Bechtel, S., Mehrle, A., Bannasch, D. and Schupp, I., 2005. Functional profiling: from microarrays via cell-based assays to novel tumour relevant modulators of the cell cycle. *Cancer Research*, 65(17), pp.7733-7742.

17. Arun, M. and Asha, V.V., 2008. Gastroprotective effect of *Dodonaea viscosa* on various experimental ulcer models. *Journal of ethnopharmacology*, 118(3), pp.460-465.
18. Ashkenazi, A. and Salvesen, G., 2014. Regulated cell death: signaling and mechanisms. *Annual review of cell and developmental biology*, 30, pp.337-356.
19. Aslam, M.S., Naveed, S., Ahmed, A., Abbas, Z., Gull, I. and Athar, M.A., 2014. Side effects of chemotherapy in cancer patients and evaluation of patients opinion about starvation based differential chemotherapy. *Journal of Cancer Therapy*, 2014. Abbas, Z. and Rehman, S., 2018. An overview of cancer treatment modalities. *Neoplasms*, 1, pp.139-57.
20. Aslantürk, Ö.S., 2018. In vitro cytotoxicity and cell viability assays: principles, advantages, and disadvantages. *Genotoxicity-A predictable risk to our actual world*, 2, pp.64-80.
21. Aydın, A., Aktay, G. and Yesilada, E., 2016. A guidance manual for the toxicity assessment of traditional herbal medicines. *Natural Product Communications*, 11(11), p.1934578X1601101131.
22. Bachanova, V., Perales, M.A. and Abramson, J.S., 2020. Modern management of relapsed and refractory aggressive B-cell lymphoma: a perspective on the current treatment landscape and patient selection for CAR T-cell therapy. *Blood Reviews*, 40, p.100640.
23. Bakshi, S.S., McMahon, S., George, A., Yumkella, F., Bangura, P., Kabano, A. and Diaz, T., 2013. The role of traditional treatment on health care seeking by caregivers for sick children in Sierra Leone: results of a baseline survey. *Acta tropica*, 127(1), pp.46-52.
24. Barrans, S., Crouch, S., Smith, A., Turner, K., Owen, R., Patmore, R., Roman, E. and Jack, A., 2010. Rearrangement of MYC is associated with poor prognosis in patients with diffuse large B-cell lymphoma treated in the era of rituximab. *Journal of clinical oncology*, 28(20), pp.3360-3365.
25. Barajas Jr, R.F., Politi, L.S., Anzalone, N., Schöder, H., Fox, C.P., Boxerman, J.L., Kaufmann, T.J., Quarles, C.C., Ellingson, B.M., Auer, D. and Andronesi, O.C., 2021. Consensus recommendations for MRI and PET imaging of primary central nervous system lymphoma: guideline statement from the International Primary CNS Lymphoma Collaborative Group (IPCG). *Neuro-oncology*, 23(7), pp.1056-1071.

26. Barreca, M., Stathis, A., Barraja, P. and Bertoni, F., 2020. An overview on anti-tubulin agents for the treatment of lymphoma patients. *Pharmacology & therapeutics*, 211, p.107552.
27. Begum, H., Murugesan, P. and Tangutur, A.D., 2022. Western blotting: a powerful staple in scientific and biomedical research. *Biotechniques*, 73(1), pp.58-69.
28. Beigl, T.B., Paul, A., Weller, S., Schäfer, B., Aulitzky, W.E., Kopp, H.G., Fellmeth, T., Pluhackova, K., Rehm, M. and Essmann, F., 2023. Critical interactions and tumour-specific mutations of Bcl-2 transmembrane domains revealed by a novel split luciferase assay. *Cancer Research*, 83(7_Supplement), pp.2524-2524.
29. Berhan, A., Bayleyegn, B. and Getaneh, Z., 2022. HIV/AIDS Associated Lymphoma. *Blood and Lymphatic Cancer: Targets and Therapy*, pp.31-45.
30. Bertoli, C., Skotheim, J.M. and De Bruin, R.A., 2013. Control of cell cycle transcription during G1 and S phases. *Nature reviews Molecular cell biology*, 14(8), pp.518-528.
31. Bhambhani, S., Kondhare, K.R. and Giri, A.P., 2021. Diversity in chemical structures and biological properties of plant alkaloids. *Molecules*, 26(11), p.3374.
32. Bhosale, P.B., Ha, S.E., Vetrivel, P., Kim, H.H., Kim, S.M. and Kim, G.S., 2020. Functions of polyphenols and its anticancer properties in biomedical research: a narrative review. *Translational Cancer Research*, 9(12), p.7619.
33. Black, G.B., Boswell, L., Harris, J. and Whitaker, K.L., 2023. What causes delays in diagnosing blood cancers? A rapid review of the evidence. *Primary health care research & development*, 24, p.e26.
34. Board, P.A.T.E., 2023. Non-Hodgkin Lymphoma Treatment (PDQ®). In PDQ Cancer Information Summaries [Internet]. National Cancer Institute (US).
35. Bobillo, S., Joffe, E., Sermer, D., Mondello, P., Ghione, P., Caron, P.C., Hamilton, A., Hamlin, P.A., Horwitz, S.M., Kumar, A. and Matasar, M.J., 2021. Prophylaxis with intrathecal or high-dose methotrexate in diffuse large B-cell lymphoma and high risk of CNS relapse. *Blood cancer journal*, 11(6), p.113.
36. Bogusz, A.M., Kovach, A.E., Le, L.P., Feng, D., Baxter, R.H. and Sohani, A.R., 2017. Diffuse large B-cell lymphoma with concurrent high MYC and BCL2 expression shows evidence of

- active B-cell receptor signaling by quantitative immunofluorescence. *PLoS One*, 12(2), p.e0172364.
37. Boum, Y., Kwedi-Nolna, S., Haberer, J.E. and Leke, R.R., 2021. Traditional healers to improve access to quality health care in Africa. *The Lancet Global Health*, 9(11), pp.e1487-e1488.
38. Brady, A.J., Kearney, P. and Tunney, M.M., 2007. Comparative evaluation of 2, 3-bis [2-methoxy-4-nitro-5-sulfophenyl]-2H-tetrazolium-5-carboxanilide (XTT) and 2-(2-methoxy-4-nitrophenyl)-3-(4-nitrophenyl)-5-(2, 4-disulfophenyl)-2H-tetrazolium, monosodium salt (WST-8) rapid colorimetric assays for antimicrobial susceptibility testing of staphylococci and ESBL-producing clinical isolates. *Journal of microbiological methods*, 71(3), pp.305-311.
39. Bray, F., Laversanne, M., Weiderpass, E. and Soerjomataram, I., 2021. The ever-increasing importance of cancer as a leading cause of premature death worldwide. *Cancer*.
40. Buwa-Komoren, L.V., Mayekiso, B., Mhinana, Z. and Adeniran, A.L., 2019. An ethnobotanical and ethnomedicinal survey of traditionally used medicinal plants in Seymour, South Africa: An attempt toward digitization and preservation of ethnic knowledge. *Pharmacognosy Magazine*, 15(60), pp.115-123.
41. Calitz, C., Gouws, C., Viljoen, J., Steenekamp, J., Wiesner, L., Abay, E. and Hamman, J., 2015. Herb-drug pharmacokinetic interactions: transport and metabolism of indinavir in the presence of selected herbal products. *Molecules*, 20(12), pp.22113-22127.
42. Camille, Golfier., Gilles, Salles. (2020). Antibody Therapy Maintenance in Follicular Lymphoma. *Hematology-oncology Clinics of North America*, Available from: 10.1016/J.HOC.2020.02.005
43. Cancer stat facts: bladder cancer. National Cancer Institute / Surveillance, Epidemiology, and End Results Program. Accessed February 7, 2022. <https://seer.cancer.gov/statfacts/html/urinb.html>
44. Cao, S., Brodie, P., Callmander, M., Randrianaivo, R., Razafitsalama, J., Rakotobe, E., Rasamison, V.E., TenDyke, K., Shen, Y., Suh, E.M. and Kingston, D.G., 2009.

- Antiproliferative triterpenoid saponins of *Dodonaea viscosa* from the Madagascar dry forest. *Journal of natural products*, 72(9), pp.1705-1707.
45. Carbone, A., Vaccher, E. and Ghoghini, A., 2021. Hematological cancers in individuals infected by HIV. *Blood*.
46. Caron, A.J., 2019. Non-Hodgkin Lymphoma. *Hematology-oncology Clinics of North America*, 33(4) doi: 10.1016/S0889-8588(19)30068-1
47. Cellosaurus., 2023. Cellosaurus SU-DHL-4 (CVCL_0539). Available: https://www.cellosaurus.org/CVCL_0539. Accessed: 22 January 2023.
48. Chao, C., Silverberg, M.J., Martínez-Maza, O., Chi, M., Abrams, D.I., Haque, R., Zha, H.D., McGuire, M., Xu, L. and Said, J., 2012. Epstein-Barr virus infection and expression of B-cell oncogenic markers in HIV-related diffuse large B-cell Lymphoma. *Clinical Cancer Research*, 18(17), pp.4702-4712.
49. Chapuy, B., Cheng, H., Watahiki, A., Ducar, M.D., Tan, Y., Chen, L., Roemer, M.G., Ouyang, J., Christie, A.L., Zhang, L. and Gusenleitner, D., 2016. Diffuse large B-cell lymphoma patient-derived xenograft models capture the molecular and biological heterogeneity of the disease. *Blood, The Journal of the American Society of Hematology*, 127(18), pp.2203-2213.
50. Che, E., Gao, Y., Wan, L., Zhang, Y., Han, N., Bai, J., Li, J., Sha, Z. and Wang, S., 2015. Paclitaxel/gelatin coated magnetic mesoporous silica nanoparticles: Preparation and antitumour efficacy in vivo. *Microporous and Mesoporous Materials*, 204, pp.226-234.
51. Chen, Y., Luo, L., Chen, L., Zheng, X., Yang, X., Zheng, Z., Zheng, J., Liu, T., Yang, T. and Hu, J., 2023. Clinical characteristics and prognosis of patients with co-existing follicular lymphoma and diffuse large B-cell lymphoma components in rituximab era. *Journal of Cancer Research and Clinical Oncology*, 149(6), pp.2311-2318.
52. Cheng, C.L., Yeh, P.T., Fang, W.Q., Ma, W.L., Hou, H.A., Tsai, C.H., Lin, C.P. and Tien, H.F., 2023. Long-term outcomes of combined intravitreal methotrexate and systemic high-dose methotrexate therapy in vitreoretinal lymphoma. *Cancer Medicine*, 12(7), pp.8102-8111.

53. Cheng, J., Smyers, M., Trotta, M., Carleton, N.M., Maurer, L.M., Lucas, P.C. and McAllister-Lucas, L.M., 2022. Abstract A18: GRK2, an inhibitor of MALT1-dependent oncogenic signaling, is downregulated by microRNA in ABC-DLBCL. *Blood Cancer Discovery*, 3(5_Supplement), pp. A18-A18.
54. Chihara, D. and Dunleavy, K., 2021. Primary central nervous system lymphoma: evolving biologic insights and recent therapeutic advances. *Clinical Lymphoma Myeloma and Leukemia*, 21(2), pp.73-79.
55. Choi, W.W., Weisenburger, D.D., Greiner, T.C., Piris, M.A., Banham, A.H., Delabie, J., Braziel, R.M., Geng, H., Iqbal, J., Lenz, G. and Vose, J.M., 2009. A new immunostain algorithm classifies diffuse large B-cell lymphoma into molecular subtypes with high accuracy. *Clinical cancer research*, 15(17), pp.5494-5502.
56. Choudhury, J.D., Kumar, S., Mayank, V., Mehta, J. and Bardalai, D., 2012. A review on apoptosis and its different pathway. *International Journal of Biological and Pharmaceutical Research*, 3(7), pp.848-861.
57. Coiffier, B., Thieblemont, C., Van Den Neste, E., Lepeu, G., Plantier, I., Castaigne, S., Lefort, S., Marit, G., Macro, M., Sebban, C. and Belhadj, K., 2010. Long-term outcome of patients in the LNH-98.5 trial, the first randomized study comparing rituximab-CHOP to standard CHOP chemotherapy in DLBCL patients: a study by the Groupe d'Etudes des Lymphomes de l'Adulte. *Blood, The Journal of the American Society of Hematology*, 116(12), pp.2040-2045.
58. Cooper, G.M., 2000. *The cell: a molecular approach* 2nd Edition.
59. Corley, D.A., Sedki, M., Ritzwoller, D.P., Greenlee, R.T., Neslund-Dudas, C., Rendle, K.A., Honda, S.A., Schottinger, J.E., Udaltsova, N., Vachani, A. and Kobrin, S., 2021. Cancer screening during the coronavirus disease-2019 pandemic: a perspective from the National Cancer Institute's PROSPR Consortium. *Gastroenterology*, 160(4), pp.999-1002.
60. Cornberg, M., Protzer, U., Dollinger, M.M., Petersen, J., Wedemeyer, H., Berg, T., Jilg, W., Erhardt, A., Wirth, S., Schirmacher, P. and Fleig, W.E., 2007. Prophylaxis, diagnosis and therapy of hepatitis B virus (HBV) infection: the German guidelines for the management of HBV infection. *Zeitschrift für Gastroenterologie*, 45(12), pp.1281-1328.

61. Crane, A.M., and Bhattacharya, S.K., 2013. The use of bromodeoxyuridine incorporation assays to assess corneal stem cell proliferation. In *Corneal Regenerative Medicine* (pp. 65-70). Humana Press, Totowa, NJ.
62. Dagogo-Jack, I. and Shaw, A.T., 2018. Tumour heterogeneity and resistance to cancer therapies. *Nature reviews Clinical oncology*, 15(2), pp.81-94.
63. Daliparty, V.M., Amoozgar, B., Mamidanna, S., Kaushal, V., Baloch, Z.A. and Rehman, F., 2021. Presentation of Diffuse Large B-Cell Lymphoma with Shoulder Pain: A Case Report. *The American Journal of Case Reports*, 22, pp.e927828-1.
64. Delaney, G., Jacob, S., Featherstone, C. and Barton, M., 2005. The role of radiotherapy in cancer treatment: estimating optimal utilization from a review of evidence-based clinical guidelines. *Cancer: Interdisciplinary International Journal of the American Cancer Society*, 104(6), pp.1129-1137.
65. De Martel, C., Ferlay, J., Franceschi, S., Vignat, J., Bray, F., Forman, D. and Plummer, M., 2012. Global burden of cancers attributable to infections in 2008: a review and synthetic analysis. *The lancet oncology*, 13(6), pp.607-615.
66. Dhokotera, T., Bohlius, J., Spoerri, A., Egger, M., Ncayiyana, J., Olago, V., Singh, E. and Sengayi, M., 2019. The burden of cancers associated with HIV in the South African public health sector, 2004–2014: a record linkage study. *Infectious agents and cancer*, 14(1), pp.1-12.
67. Díaz, M., Díaz, C.E., Alvares, R.G., González, A., Castillo, L., González-Coloma, A., Seoane, G. and Rossini, C., 2015. Differential anti-insect activity of natural products isolated from *Dodonaea viscosa* Jacq.(Sapindaceae). *Journal of Plant Protection Research*, 55(2).
68. Dinmohamed, A.G., Visser, O., Verhoeven, R.H., Louwman, M.W., van Nederveen, F.H., Willems, S.M., Merks, M.A., Lemmens, V.E., Nagtegaal, I.D. and Siesling, S., 2020. Fewer cancer diagnoses during the COVID-19 epidemic in the Netherlands. *The Lancet Oncology*, 21(6), pp.750-751.
69. Dolcetti, R., Gloghini, A., Caruso, A. and Carbone, A., 2016. A lymphomagenic role for HIV beyond immune suppression?. *Blood, The Journal of the American Society of Hematology*, 127(11), pp.1403-1409.

70. dos Santos Guilherme, R., Caputto, LZ, Fonseca, ALA, Pereira, J. and Fonseca, FLA, 2008. Complementary laboratory tests indicated to support the diagnosis of Diffuse Large B Cell Lymphoma (LDGCB). *Brazilian Archives of Health Sciences* , 33 (3).
71. El-Baba, C., Baassiri, A., Kiriako, G., Dia, B., Fadlallah, S., Moodad, S. and Darwiche, N., 2021. Terpenoids' anti-cancer effects: Focus on autophagy. *Apoptosis*, 26(9-10), pp.491-511.
72. Eloff, J.N., 1998. Antibacterial and Phytochemical screening of antimicrobial components from plants. *Ethnopharmacology*, 60, pp.18-24.
73. EU Directive., 2004. 2004/24/ EC of the European Parliament and of the Council of 31 March 2004, amending, as regards traditional herbal medicinal products. *Directive 2001/83/EC on the Community code relating to medicinal products for human use*.
74. Eyre, T.A., Savage, K.J., Cheah, C.Y., El-Galaly, T.C., Lewis, K.L., McKay, P., Wilson, M.R., Evens, A.M., Bobillo, S., Villa, D. and Maurer, M.J., 2022. CNS prophylaxis for diffuse large B-cell lymphoma. *The Lancet Oncology*, 23(9), pp. e416-e426.
75. Fatima, S., Kumari, A. and Dwivedi, V.P., 2021. Advances in adjunct therapy against tuberculosis: Deciphering the emerging role of phytochemicals. *MedComm*.
76. Fayad, Luis, Fritz Offner, Mitchell R. Smith, Gregor Verhoef, Peter Johnson, Jonathan L. Kaufman, Ama Rohatiner et al. "Safety and clinical activity of a combination therapy comprising two antibody-based targeting agents for the treatment of non-Hodgkin lymphoma: results of a phase I/II study evaluating the immunoconjugate inotuzumab ozogamicin with rituximab." *Journal of Clinical Oncology* 31, no. 5 (2013): 573.
77. Fennell, C.W., Lindsey, K.L., McGaw, L.J., Sparg, S.G., Stafford, G.I., Elgorashi, E.E., Grace, O.M. and Van Staden, J., 2004. Assessing African medicinal plants for efficacy and safety: pharmacological screening and toxicology. *Journal of ethnopharmacology*, 94(2-3), pp.205-217.
78. Ferlay, J., Colombet, M., Soerjomataram, I., Parkin, D.M., Piñeros, M., Znaor, A. and Bray, F., 2021. Cancer statistics for the year 2020: An overview. *International Journal of Cancer*.

79. Ferlay, J.S.E.M., Soerjomataram, I., Ervik, M., Dikshit, R., Eser, S., Mathers, C., Rebelo, M., Parkin, D.M., Forman, D. and Bray, F., 2013. GLOBOCAN 2012 v1. 0. *Cancer incidence and mortality worldwide: IARC CancerBase, 11*.
80. Finestone, E. and Wishnia, J., 2022. Estimating the burden of cancer in South Africa. *SA Journal of Oncology, 6(0)*, p.220.
81. Fink, S.L. and Cookson, B.T., 2005. Apoptosis, pyroptosis, and necrosis: mechanistic description of dead and dying eukaryotic cells. *Infection and immunity, 73(4)*, pp.1907-1916.
82. Fischer, L., Jiang, L., Bittenbring, J.T., Huebel, K., Schmidt, C., Duell, J., Metzner, B., Krauter, J., Glass, B., Huettmann, A. and Schaefer-Eckart, K., 2023. The addition of rituximab to chemotherapy improves overall survival in mantle cell lymphoma—a pooled trials analysis. *Annals of Hematology*, pp.1-11.
83. Freshney, R.I., 2015. *Culture of animal cells: a manual of basic technique and specialized applications*. John Wiley & Sons.
84. Fujikawa, D., Nakamura, T., Yoshioka, D., Li, Z., Moriizumi, H., Taguchi, M., Tokai-Nishizumi, N., Kozuka-Hata, H., Oyama, M. and Takekawa, M., 2023. Stress granule formation inhibits stress-induced apoptosis by selectively sequestering executioner caspases. *Current Biology, 33(10)*, pp.1967-1981.
85. Gali-Muhtasib, H., Hmadi, R., Kareh, M., Tohme, R. and Darwiche, N., 2015. Cell death mechanisms of plant-derived anticancer drugs: beyond apoptosis. *Apoptosis, 20(12)*, pp.1531-1562.
86. Garcia-Oliveira, P., Otero, P., Pereira, A.G., Chamorro, F., Carpena, M., Echave, J., Fraga-Corral, M., Simal-Gandara, J. and Prieto, M.A., 2021. Status and challenges of plant-anticancer compounds in cancer treatment. *Pharmaceuticals, 14(2)*, p.157.
87. Gessese, T., Asrie, F. and Mulatie, Z., 2023. Human Immunodeficiency Virus Related Non-Hodgkin's Lymphoma. *Blood and Lymphatic Cancer: Targets and Therapy*, pp.13-24.
88. Getie, M., Gebre-Mariam, T., Rietz, R., Höhne, C., Huschka, C., Schmidtke, M., Abate, A. and Neubert, R.H.H., 2003. Evaluation of the anti-microbial and anti-inflammatory

activities of the medicinal plants *Dodonaea viscosa*, *Rumex nervosus* and *Rumex abyssinicus*. *Fitoterapia*, 74(1-2), pp.139-143.

89. GLOBOCAN., 2020. *Estimated age-standardized incidence rates (World) in 2020, all cancers, both sexes, all ages*. Available at: <https://www.uicc.org/news/globocan-2020-new-global-cancer-data>. [Accessed: 4 February 2022].
90. Gondwe, Y., Kudowa, E., Tomoka, T., Kasonkanji, E.D., Kaimila, B., Zuze, T., Mumba, N., Kimani, S., Mulenga, M., Chimzimu, F. and Kampani, C., 2022. Comparison of baseline lymphoma and HIV characteristics in Malawi before and after implementation of universal antiretroviral therapy. *Plos one*, 17(9), p.e0273408.
91. Gouveia, G.R., Siqueira, S.A.C. and Pereira, J., 2012. Pathophysiology and molecular aspects of diffuse large B-cell lymphoma. *Revista Brasileira de Hematologia e Hemoterapia*, 34, pp.447-451.
92. Goy, A., Forero, A., Wagner-Johnston, N., Christopher Ehmann, W., Tsai, M., Hatake, K., Ananthakrishnan, R., Volkert, A., Vandendries, E. and Ogura, M., 2016. A phase 2 study of inotuzumab ozogamicin in patients with indolent B-cell non-Hodgkin lymphoma refractory to rituximab alone, rituximab and chemotherapy, or radioimmunotherapy. *British journal of haematology*, 174(4), pp.571-581.
93. Green, K., Munakomi, S. and Hogg, J.P., 2023. Central nervous system lymphoma. In *StatPearls [internet]*. StatPearls Publishing.
94. Greenwell, M. and Rahman, P.K.S.M., 2015. Medicinal plants: their use in anticancer treatment. *International journal of pharmaceutical sciences and research*, 6(10), p.4103.
95. Gress, D.M., Edge, S.B., Greene, F.L., Washington, M.K., Asare, E.A., Brierley, J.D., Byrd, D.R., Compton, C.C., Jessup, J.M., Winchester, D.P. and Amin, M.B., 2017. Principles of cancer staging. *AJCC cancer staging manual*, 8, pp.3-30.
96. Gupta, V., Singh, V., Bajwa, R., Meghal, T., Sen, S., Greenberg, D., Anne, M. and Levitt, M.J., 2022. Site-specific survival of extra nodal diffuse large B-cell lymphoma and comparison with gastrointestinal diffuse large B-cell lymphoma. *Journal of Hematology*, 11(2), p.45.

97. Guzman, C., Bagga, M., Kaur, A., Westermarck, J. and Abankwa, D., 2014. ColonyArea: an ImageJ plugin to automatically quantify colony formation in clonogenic assays. *PLoS one*, 9(3), p.e92444.
98. Habbu, P.V., Joshi, H. and Patil, B.S., 2007. Ph. cog Rev.: Review Article potential wound healers from plant origin. *Pharmacognosy reviews*, 1(2), pp.14-28.
99. Habeeb, Z.F., 2021. Biosynthesis, Characterization, Antioxidant Activity, and Clinical Application of Silver Nanoparticles Synthesized from Dodonaea Viscosa Leaves Extract. *University of Kerbala*.
100. Haidinger, R. and Bauerfeind, I., 2019. Long-term side effects of adjuvant therapy in primary breast cancer patients: results of a web-based survey. *Breast Care*, 14(2), pp.111-116.
101. Hainaut, P. and Plymoth, A., 2013. Targeting the hallmarks of cancer: towards a rational approach to next-generation cancer therapy. *Current opinion in oncology*, 25(1), pp.50-51.
102. Han, X., Jemal, A., Hulland, E., Simard, E.P., Nastoupil, L., Ward, E. and Flowers, C.R., 2017. HIV infection and survival of lymphoma patients in the era of highly active antiretroviral therapy. *Cancer Epidemiology, Biomarkers & Prevention*, 26(3), pp.303-311.
- Hanahan, D., 2022. Hallmarks of Cancer: New Dimensions. *Cancer Discovery*, 12(1), pp.31-46.
103. Hanahan, D., 2022. Hallmarks of Cancer: New Dimensions. *Cancer Discovery*, 12(1), pp.31-46.
104. Hanahan, D. and Weinberg, R.A., 2011. Hallmarks of cancer: the next generation. *Cell*, 144(5), pp.646-674.
105. Hanahan, D. and Weinberg, R.A., 2016. Biological hallmarks of cancer. *Holland-Frei Cancer Medicine*, pp.1-10.
106. Hans, C.P., Weisenburger, D.D., Greiner, T.C., Gascoyne, R.D., Delabie, J., Ott, G., Muller-Hermelink, H.K., Campo, E., Braziel, R.M., Jaffe, E.S. and Pan, Z., 2004. Confirmation of the molecular classification of diffuse large B-cell lymphoma by immunohistochemistry using a tissue microarray. *Blood*, 103(1), pp.275-282.

107. Havas, A.P., 2016. *Defining mechanisms of sensitivity and resistance to histone deacetylase inhibitors to develop effective therapeutic strategies for the treatment of aggressive diffuse large B-cell lymphoma* (Doctoral dissertation, The University of Arizona).
108. Hendriks, R.W., Yuvaraj, S. and Kil, L.P., 2014. Targeting Bruton's tyrosine kinase in B cell malignancies. *Nature Reviews Cancer*, 14(4), pp.219-232.
109. Herrera-Calderon, O., Herrera-Ramírez, A., Cardona-G, W., Melgar-Merino, E.J., Chávez, H., Pari-Olarte, J.B., Loyola-Gonzales, E., Kong-Chirinos, J.F., Almeida-Galindo, J.S., Peña-Rojas, G. and Andía-Ayme, V., 2023. *Dodonaea viscosa* Jacq. induces cytotoxicity, antiproliferative activity, and cell death in colorectal cancer cells via regulation of caspase 3 and p53. *Frontiers in Pharmacology*, 14.
110. Heyman, B. and Yang, Y., 2018. New developments in immunotherapy for lymphoma. *Cancer biology & medicine*, 15(3), p.189.
111. Hleihel, R., Skayneh, H., de Thé, H., Hermine, O. and Bazarbachi, A., 2023. Primary cells from patients with adult T cell leukemia/lymphoma depend on HTLV-1 Tax expression for NF- κ B activation and survival. *Blood Cancer Journal*, 13(1), p.67.
112. Hosseinzadeh, E., Banaee, N. and Ali Nedaie, H., 2017. Cancer and treatment modalities. *Current Cancer Therapy Reviews*, 13(1), pp.17-27.
113. Hsin-Ju, Tsai., Ming, Ju, Wu., Cheng-Hsu, Chen., Sheng-Shun, Yang., Yi-Hsiang, Huang., Yanling, Chang., Horng-Rong, Chang., Teng-Yu, Lee., 2023. Risk Stratification for Hepatitis B Virus Reactivation in Kidney Transplant Recipients with Resolved HBV Infection. *Transplant International*, Available from: 10.3389/ti.2023.11122
114. Huang, M.S. and Weinstein, H.J., 2022. Non-Hodgkin lymphoma. In *Lanzkowsky's Manual of Pediatric Haematology and Oncology* (pp. 473-483). Academic Press.
115. Jan, R., 2019. Understanding apoptosis and apoptotic pathways targeted cancer therapeutics. *Advanced pharmaceutical bulletin*, 9(2), p.205.
116. Jermini, M., Dubois, J., Rodondi, P.Y., Zaman, K., Buclin, T., Csajka, C., Orcurto, A. and E. Rothuizen, L., 2019. Complementary medicine use during cancer treatment and

potential herb-drug interactions from a cross-sectional study in an academic centre. *Scientific reports*, 9(1), p.5078.

117. Jiang, Y., Chen, M., Nie, H. and Yuan, Y., 2019. PD-1 and PD-L1 in cancer immunotherapy: clinical implications and future considerations. *Human vaccines & immunotherapeutics*, 15(5), pp.1111-1122.
118. Jin, W. and Wang, X., 2022. PLAGL2 promotes the proliferation and migration of diffuse large B-cell lymphoma cells via Wnt/ β -catenin pathway. *Annals of Clinical & Laboratory Science*, 52(3), pp.359-366.
119. Kajstura, M., Halicka, H.D., Pryjma, J. and Darzynkiewicz, Z., 2007. Discontinuous fragmentation of nuclear DNA during apoptosis revealed by discrete “sub-G1” peaks on DNA content histograms. *Cytometry Part A: the journal of the International Society for Analytical Cytology*, 71(3), pp.125-131.
120. Kancherla, R.R., Nair, J.S., Ahmed, T., Durrani, H., Seiter, K., Mannancheril, A. and Tse-Dinh, Y.C., 2001. Evaluation of topotecan and etoposide for non-hodgkin lymphoma: Correlation of topoisomerase–DNA complex formation with clinical response. *Cancer*, 91(3), pp.463-471.
121. Kaymaz, Y., Oduor, C.I., Aydemir, O., Luftig, M.A., Otieno, J.A., Ong’echa, J.M., Bailey, J.A. and Moormann, A.M., 2020. Epstein-Barr virus genomes reveal population structure and type 1 association with endemic Burkitt lymphoma. *Journal of Virology*, 94(17), pp.10-1128.
122. Kerr, P.G., 2013. Plants and Tuberculosis: Phytochemicals Potentially Useful in the Treatment of Tuberculosis. In *Fighting Multidrug Resistance with Herbal Extracts, Essential Oils and Their Components* (pp. 45-64). Academic Press
123. Khan, A.Z., Mohammad, A., Iqbal, Z., Anis, I., Shah, M.R., Nadeem, S., Rabnawaz, M., Shahidullah, A., Khan, H. and Khan, I., 2013. Molecular docking of viscosine as a new lipoxygenase inhibitor isolated from *Dodonaea viscosa*. *Bangladesh Journal of Pharmacology*, 8(1), pp.36-39.
124. Khan, M.F., Alqahtani, A.S., Almarfadi, O.M., Ullah, R., Nasr, F.A., Noman, O.M., Siddiqui, N.A., Shahat, A.A. and Ahamad, S.R., 2021. The reproductive toxicity associated

- with *Dodonaea viscosa*, a folk medicinal plant in Saudi Arabia. *Evidence-Based Complementary and Alternative Medicine*, 2021, pp.1-9.
125. Khurram, M., Khan, M.A., Hameed, A., Abbas, N., Qayum, A. and Inayat, H., 2009. Antibacterial activities of *Dodonaea viscosa* using contact bioautography technique. *Molecules*, 14(3), pp.1332-1341.
126. Kim, J., Kim, J.N., Park, I., Sivtseva, S., Okhlopkova, Z., Zulfugarov, I.S. and Kim, S.W., 2020. *Dracocephalum palmatum* Stephan extract induces caspase-and mitochondria-dependent apoptosis via Myc inhibition in diffuse large B cell lymphoma. *Oncology Reports*, 44(6), pp.2746-2756.
127. Kimani, S.M., Painschab, M.S., Horner, M.J., Muchengeti, M., Fedoriw, Y., Shiels, M.S. and Gopal, S., 2020. Epidemiology of haematological malignancies in people living with HIV. *The Lancet HIV*, 7(9), pp.e641-e651.
128. Kiruba Daniel, S.C.G., Vinothini, G., Subramanian, N., Nehru, K. and Sivakumar, M., 2013. Biosynthesis of Cu, ZVI, and Ag nanoparticles using *Dodonaea viscosa* extract for antibacterial activity against human pathogens. *Journal of nanoparticle research*, 15, pp.1-10.
129. Kiruba Daniel, S.C.G., Vinothini, G., Subramanian, N., Nehru, K. and Sivakumar, M., 2013. Biosynthesis of Cu, ZVI, and Ag nanoparticles using *Dodonaea viscosa* extract for antibacterial activity against human pathogens. *Journal of nanoparticle research*, 15, pp.1-10.
130. Kishan Prasad, H.L., Jayaprakash Shetty, K., Mathias, L., Sunil Kumar, Y., Permi, H.S. and Rao, C., 2013. Primary bone lymphoma of humerus diagnosed by FNAC-a rare case report. *Indian journal of surgical oncology*, 4(3), pp.316-319.
131. Koduru, S., Grierson, D.S., and Afolayan, A.J., 2007. Ethnobotanical information of medicinal plants used for treatment of cancer in the Eastern Cape Province, South Africa. *Current Science*, pp.906-908.
132. Koleva, V., Koynova, T., Kuleva, I. and Dragoeva, A., 2023. A simple tool to assess the effect of water-soluble soil pollutants on enzyme activity in human whole blood samples using WST-1 assay. *Revista internacional de contaminación ambiental*, 39.

133. Korkolopoulou, P., Vassilakopoulos, T., Milionis, V. and Ioannou, M., 2016. Recent advances in aggressive large B-cell lymphomas: a comprehensive review. *Advances in Anatomic Pathology*, 23(4), pp.202-243.
134. Kramer, M.H., Hermans, J., Parker, J., Krol, A.D., Kluin-Nelemans, J.C., Haak, H.L., Van Groningen, K., Van Krieken, J.H., De Jong, D. and Kluin, P.M., 1996. Clinical significance of bcl2 and p53 protein expression in diffuse large B-cell lymphoma: a population-based study. *Journal of Clinical Oncology*, 14(7), pp.2131-2138.
135. Krishnan, A. and Zaia, J.A., 2014. HIV-associated non-Hodgkin lymphoma: viral origins and therapeutic options. Hematology 2014, the American Society of Hematology Education Program Book, 2014(1), pp.584-589.
136. Kronstein-Wiedemann, R. and Tonn, T., 2019. Colony formation: an assay of hematopoietic progenitor cells. *Stem Cell Mobilization: Methods and Protocols*, pp.29-40.
137. Krupanidhi, A.M., Dabadi, P., Kulkarni, J., Ekbote, D. and Davan, P., 2018. Anti-neoplastic activities of targeted bio-moieties of Dodonaea Viscosa. *World Journal of Pharmaceutical Sciences*, pp.5-13.
138. Kumar, R.V., Reddy, G.V.R., Sathyanarayana, J., Bikshapathi, T. and Reddy, M.K., 2013. Effect of Melia azedarach and Dodonaea viscosa aqueous leaf extracts on fertility in male albino rats. *Indian Journal of Pharmaceutical and Biological Research*, 1(04), pp.7-12.
139. Kutikov, A., Weinberg, D.S., Edelman, M.J., Horwitz, E.M., Uzzo, R.G. and Fisher, R.I., 2020. A war on two fronts: cancer care in the time of COVID-19. *Annals of internal medicine*, 172(11), pp.756-758
140. Labi, V. and Erlacher, M., 2015. How cell death shapes cancer. *Cell death & disease*, 6(3), pp.e1675-e1675.
141. Lan, T.Y., Lin, Y.C., Tseng, T.C., Yang, H.C., Kao, J.H., Cheng, C.F., Lee, T.J., Huang, S.C., Lu, C.H., Li, K.J. and Hsieh, S.C., 2023. Risk of Hepatitis B Virus (HBV) reactivation in HBsAg-negative, anti-HBc-negative patients receiving rituximab for autoimmune diseases in HBV endemic areas. *Gut and Liver*, 17(2), p.288.

142. Lawal, D. and Yunusa, I., 2013. *Dodonaea Viscosa* Linn: its medicinal, pharmacological and phytochemical properties. *International Journal of Innovation and Applied Studies*, 2(4), pp.476-482.
143. Li, S., Young, K.H. and Medeiros, L.J., 2018. Diffuse large B-cell lymphoma. *Pathology*, 50(1), pp.74-87.
144. Liang, J.L., Luo, G.F., Chen, W.H. and Zhang, X.Z., 2021. Recent Advances in Engineered Materials for Immunotherapy-Involved Combination Cancer Therapy. *Advanced Materials*, 33(31), p.2007630.
145. Liao, D. ed., 2021. *Mechanisms of Cell Death and Opportunities for Therapeutic Development*. Academic Press.
146. Liu, C.M., Ma, J.Q. and Sun, Y.Z., 2012. Puerarin protects the rat liver against oxidative stress-mediated DNA damage and apoptosis induced by lead. *Experimental and Toxicologic Pathology*, 64(6), pp.575-582.
147. Liu, Y. and Barta, S.K., 2019. Diffuse large B-cell lymphoma: 2019 update on diagnosis, risk stratification, and treatment. *American journal of hematology*, 94(5), pp.604-616.
148. Los, M., Mozoluk, M., Ferrari, D., Stepczynska, A., Stroh, C., Renz, A., Herceg, Z., Wang, Z.Q. and Schulze-Osthoff, K., 2002. Activation and caspase-mediated inhibition of PARP: a molecular switch between fibroblast necrosis and apoptosis in death receptor signaling. *Molecular biology of the cell*, 13(3), pp.978-988.
149. Lutter, A.H., Scholka, J., Richter, H. and Anderer, U., 2017. Applying XTT, WST-1, and WST-8 to human chondrocytes: A comparison of membrane-impermeable tetrazolium salts in 2D and 3D cultures. *Clinical hemorheology and microcirculation*, 67(3-4), pp.327-342.
150. Majeed, Z.H., Hasan, S.A., Ismail, R.M., 2022. Evaluate the benefit effects of *Dodonaea viscosa* in kidney of infected rats with *Staphylococcus aureus*. *Journal of Pharmaceutical Negative Results*.
151. Malik, M.N., Haq, I.U., Fatima, H., Ahmad, M., Naz, I., Mirza, B. and Kanwal, N., 2022. Bioprospecting *Dodonaea viscosa* Jacq.; a traditional medicinal plant for

- antioxidant, cytotoxic, antidiabetic and antimicrobial potential. *Arabian Journal of Chemistry*, 15(3), p.103688.
152. Mammadova, J., Fatirخورani, R., Liu, S., Chen, K. and Wang, Z., 2023. Necrosome translocates to lysosome to induce lysosome membrane permeabilization and subsequent necroptotic cell death. *Cancer Research*, 83(7_Supplement), pp.2529-2529.
 153. Mandal, S.C., Chakraborty, R. and Sen, S. eds., 2021. *Evidence Based Validation of Traditional Medicines: A Comprehensive Approach*. Springer Singapore.
 154. Mander, M., Ntuli, L., Diederichs, N. and Mavundla, K., 2007. Economics of the traditional medicine trade in South Africa care delivery. *South African health review*, 2007(1), pp.189-196.
 155. Mark, A., Gromski., Jennifer, L., Peng., Jiehao, Zhou., Howard, C., Masuoka., Attaya, Suvannasankha., Attaya, Suvannasankha., Suthat, Liangpunsakul., Suthat, Liangpunsakul., 2016. Multifocal Gastric Ulcers Caused by Diffuse Large B Cell Lymphoma in a Patient with Significant Weight Loss. *Journal of investigative medicine high impact case reports*, Available from: 10.1177/2324709616683721
 156. McIlwain, D.R., Berger, T., and Mak, T.W., 2013. Caspase functions in cell death and disease. *Cold Spring Harbor perspectives in biology*, 5(4), p.a008656.
 157. Meenu, J.A.N.G.R.A., Sunil, S.H.A.R.M.A. and Manoj, K.U.M.A.R., 2011. Evaluation of antihyperglycemic activity of *Dodonaea viscosa* leaves in normal and STZ-diabetic rats. *Int J Pharm Pharm Sci*, 3(1), pp.69-74.
 158. Miao, Y., Medeiros, L.J., Li, Y., Li, J. and Young, K.H., 2019. Genetic alterations and their clinical implications in DLBCL. *Nature reviews Clinical oncology*, 16(10), pp.634-652.
 159. Moahi, K., Ralefala, T., Nkele, I., Triedman, S., Sohani, A., Musimar, Z., Efstathiou, J., Armand, P., Lockman, S. and Dryden-Peterson, S., 2022. HIV and Hodgkin Lymphoma survival: A prospective study in Botswana. *JCO Global Oncology*, 8, p.e2100163.
 160. Monti, S., Savage, K.J., Kutok, J.L., Feuerhake, F., Kurtin, P., Mihm, M., Wu, B., Pasqualucci, L., Neuberg, D., Aguiar, R.C. and Cin, P.D., 2005. Molecular profiling of diffuse large B-cell lymphoma identifies robust subtypes including one characterized by host inflammatory response. *Blood*, 105(5), pp.1851-1861.

161. Morrison, V.A., Bell, J.A., Hamilton, L., Ogbonnaya, A., Shih, H.C., Hennenfent, K., Eaddy, M., Shou, Y. and Galaznik, A., 2018. Economic burden of patients with diffuse large B-cell and follicular lymphoma treated in the USA. *Future Oncology*, 14(25), pp.2627-2642.
162. Mossa, G.D. and Al-Shawi, A.A., 2015. Induction of apoptosis through S-phase in human breast cancer MDA-MB231 cells by ethanolic extract of *Dodonaea viscosa* L.-an Iraqi medicine plant. *Journal of Basrah Research (Sciences)*, 41(1).
163. Mowla, S. and Ahmed, R., 2022. HIV infection and the risk of cancer: tumourigenicity of HIV-1 auxiliary proteins. *Future Virology*, 17(10), pp.707-710.
164. Mughal, T.I., Mughal, T., Goldman, J., Goldman, J.M., Mughal, S.T. and Mughal, S., 2013. *Understanding leukemias, lymphomas and myelomas*. CRC Press.
165. Mundi, P.S., Sachdev, J., McCourt, C. and Kalinsky, K., 2016. AKT in cancer: new molecular insights and advances in drug development. *British journal of clinical pharmacology*, 82(4), pp.943-956.
166. Muthukumran, P., Begumand, V.H. and Kalaiarasan, P., 2011. Anti-diabetic activity of *Dodonaea viscosa* (L) leaf extracts. *International Journal of PharmTech Research*, 3(1), pp.136-139.
167. Naicker, S.D. and Patel, M., 2013. *Dodonaea viscosa* var. *angustifolia* inhibits germ tube and biofilm formation by *C. albicans*. *Evidence-Based Complementary and Alternative Medicine*, 2013.
168. Naidoo, R., Patel, M., Gulube, Z. and Fenyvesi, I., 2012. Inhibitory activity of *Dodonaea viscosa* var. *angustifolia* extract against *Streptococcus mutans* and its biofilm. *Journal of ethnopharmacology*, 144(1), pp.171-174.
169. Nayak, P.B., Desai, D., Pandit, S. and Rai, N., 2013. Centroblastic variant of diffuse large B-cell lymphoma: Case report and review of literature. *Journal of Oral and Maxillofacial Pathology: JOMFP*, 17(2), p.261.
170. Nayeem, N., Asdaq, S.M.B., Alamri, A.S., Alsanie, W.F., Alhomrani, M., Mohzari, Y., Alrashed, A.A., Alotaibi, N., Alharbi, M.A., Aldhawyan, N.N. and Asad, M., 2021. Wound

- healing potential of *Dodonaea viscosa* extract formulation in experimental animals. *Journal of King Saud University-Science*, 33(5), p.101476.
171. N Nwodo, J., Ibezim, A., Simoben, C.V. and Ntie-Kang, F., 2016. Exploring cancer therapeutics with natural products from African medicinal plants, part II: alkaloids, terpenoids and flavonoids. *Anti-Cancer Agents in Medicinal Chemistry (Formerly Current Medicinal Chemistry-Anti-Cancer Agents)*, 16(1), pp.108-127.
 172. Novak, E.M. and Rego, E.M. eds., 2012. *Physiopathogenesis of hematological cancer*. Bentham Science Publishers.
 173. Nowakowski, G.S., Chiappella, A., Witzig, T.E., Spina, M., Gascoyne, R.D., Zhang, L., Flament, J., Repici, J. and Vitolo, U., 2016. ROBUST: Lenalidomide-R-CHOP versus placebo-R-CHOP in previously untreated ABC-type diffuse large B-cell lymphoma. *Future oncology*, 12(13), pp.1553-1563.
 174. O'Connor, O.A., Ansell, S.M. and Seymour, J.F. eds., 2023. *Precision Cancer Therapies, Volume 1: Targeting Oncogenic Drivers and Signaling Pathways in Lymphoid Malignancies: From Concept to Practice*. John Wiley & Sons.
 175. Obalum, D.C. and Ogo, C.N., 2011. Usage of Complementary and Alternative Medicine (CAM) among osteoarthritis patients attending an urban multi-specialist hospital in Lagos, Nigeria. *The Nigerian postgraduate medical journal*, 18(1), pp.44-47.
 176. Ortega, A., García, P.E., Cárdenas, J., Mancera, C., Marquina, S., del Carmen Garduno, M.L. and Maldonado, E., 2001. Methyl dodonates, a new type of diterpenes with a modified clerodane skeleton from *Dodonaea viscosa*. *Tetrahedron*, 57(15), pp.2981-2989.
 177. Oyebode, O., Kandala, N.B., Chilton, P.J. and Lilford, R.J., 2016. Use of traditional medicine in middle-income countries: a WHO-SAGE study. *Health policy and planning*, 31(8), pp.984-991.
 178. O'Shaughnessy, J., McIntyre, K., Wilks, S., Ma, L., Block, M., Andorsky, D., Danso, M., Locke, T., Scales, A. and Wang, Y., 2021. Efficacy and safety of weekly paclitaxel with or without oral alisertib in patients with metastatic breast cancer: a randomized clinical trial. *JAMA network open*, 4(4), pp.e214103-e214103.

179. Palanisamy, C.P., Cui, B., Zhang, H., Panagal, M., Paramasivam, S., Chinnaiyan, U., Jeyaraman, S., Murugesan, K., Rostagno, M., Sekar, V. and Natarajan, S.P., 2021. Anti-ovarian cancer potential of phytocompound and extract from South African medicinal plants and their role in the development of chemotherapeutic agents. *American journal of cancer research*, 11(5), p.1828.
180. Palucka, K. and Banchereau, J., 2012. Cancer immunotherapy via dendritic cells. *Nature Reviews Cancer*, 12(4), pp.265-277.
181. Pasqualucci, L. and Dalla-Favera, R., 2018. Genetics of diffuse large B-cell lymphoma. *Blood, The Journal of the American Society of Hematology*, 131(21), pp.2307-2319.
182. Patel, A. and West, H.J., 2020. What Does My Stage of Cancer Mean? *JAMA Oncology Patient Page*, 6(8), pp.1308.
183. Patel, M., Philip, V., Omar, T., Turton, D., Candy, G., Lakha, A. and Pather, S., 2015. The impact of human immunodeficiency virus infection (HIV) on lymphoma in South Africa. *Journal of Cancer Therapy*, 6(06), p.527.
184. Patel, M., Srivastava, V. and Ahmad, A., 2020. *Dodonaea viscosa* var *angustifolia* derived 5, 6, 8-trihydroxy-7, 4' dimethoxy flavone inhibits ergosterol synthesis and the production of hyphae and biofilm in *Candida albicans*. *Journal of ethnopharmacology*, 259, p.112965.
185. Patel, M. and Coogan, M.M., 2008. Antifungal activity of the plant *Dodonaea viscosa* var. *angustifolia* on *Candida albicans* from HIV-infected patients. *Journal of Ethnopharmacology*, 118(1), pp.173-176.
186. Peltzer, K., Friend-du Preez, N., Ramlagan, S., Fomundam, H. and Anderson, J., 2010. Traditional complementary and alternative medicine and antiretroviral treatment adherence among HIV patients in Kwazulu-Natal, South Africa. *African Journal of Traditional, Complementary and Alternative Medicines*, 7(2).
187. Peña, M., Montané, C., Paviglianiti, A., Hurtado, L., González, S., Carro, I., Maluquer, C., Domingo-Domenech, E., Gonzalez-Barca, E., Sureda, A. and Mussetti, A.,

2023. Outcomes of allogeneic hematopoietic cell transplantation after bispecific antibodies in non-Hodgkin lymphomas. *Bone Marrow Transplantation*, pp.1-4.
188. Pfirschke, C., Engblom, C., Rickelt, S., Cortez-Retamozo, V., Garris, C., Pucci, F., Yamazaki, T., Poirier-Colame, V., Newton, A., Redouane, Y. and Lin, Y.J., 2016. Immunogenic chemotherapy sensitizes tumours to checkpoint blockade therapy. *Immunity*, 44(2), pp.343-354.
189. Phillips, E.H. and Illidge, T.M., 2020. Is it time to rethink checkpoint blockade therapy in non-Hodgkin lymphoma?.
190. Pinnix, C.C., Dabaja, B., Gunther, J.R., Fang, P., Wu, S.Y., Nastoupil, L., Strati, P., Nair, R., Ahmed, S., Steiner, R. and Westin, J., 2022. Response adapted ultra low dose radiation therapy for the definitive management of orbital indolent B-cell lymphoma. *International Journal of Radiation Oncology, Biology, Physics*, 114(3), pp.S2-S3.
191. Priya, V.T., Balasubramanian, N., Shanmugaiyah, V., Sathishkumar, P., Kannan, N.D., Karunakaran, C., Alfarhan, A. and Antonisamy, P., 2021. Partially purified lead molecules from *Dodonaea viscosa* and their antimicrobial efficacy against infectious human pathogens. *Journal of Infection and Public Health*, 14(12), pp.1822-1830.
192. Quah, B.J. and Parish, C.R., 2010. The use of carboxyfluorescein diacetate succinimidyl ester (CFSE) to monitor lymphocyte proliferation. *JoVE (Journal of Visualized Experiments)*, (44), p.e2259.
193. Rajamanickam, V., Rajasekaran, A., Anandarajagopal, K., Sridharan, D., Selvakumar, K. and Rathinaraj, B.S., 2010. Anti-diarrheal activity of *Dodonaea viscosa* root extracts. *International Journal of Pharma and Bio Sciences*, 1(4), pp.182-185.
194. Ramadass, V., Vaiyapuri, T. and Tergaonkar, V., 2020. Small molecule NF- κ B pathway inhibitors in clinic. *International journal of molecular sciences*, 21(14), p.5164.
195. Ramirez, E., Singh, R.R., Kunkalla, K., Liu, Y., Qu, C., Cain, C., Multani, A.S., Lennon, P.A., Jackacky, J., Ho, M. and Dawud, S., 2012. Defining causative factors contributing in the activation of hedgehog signaling in diffuse large B-cell lymphoma. *Leukemia research*, 36(10), pp.1267-1273.

196. Ramya, R., Sivasakthi, R., Senthilkumar, C., Anudeepa, J., Santhi, N. and Narayanan, R.V., 2011. Preliminary phytochemical and antifertility studies on *Dodonaea viscosa* Linn. *Asian Journal of Research in Pharmaceutical Science*, 1(3), pp.77-79.
197. Rani, M.S., Venkatesh, P., Pippalla, R.S. and Mohan, G.K., 2013. Biochemical and histological study of traditional plant: *Dodonaea viscosa* Linn extracts in diabetic rats. *The Journal of Phytopharmacology*, 2(4), pp.13-21.
198. Rapiti, E., Verkooijen, H.M., Vlastos, G., Fioretta, G., Neyroud-Caspar, I., Sappino, A.P., Chappuis, P.O. and Bouchardy, C., 2006. Complete excision of primary breast tumour improves survival of patients with metastatic breast cancer at diagnosis. *J clin oncol*, 24(18), pp.2743-2749.
199. Rashed, K., Meng, T.L., Lin-Tao, Z., Yong-Tang, Z., 2013. *Dodonaea viscosa* (L.) extracts as anti-human immunodeficiency virus type-1 (HIV-1) agents and phytoconstituents. *Peak J of Medicinal Plant Research*, 1, pp. 19-25.
200. Rehman, A., Fatima, I., Wang, Y., Tong, J., Noor, F., Qasim, M., Peng, Y. and Liao, M., 2023. Unveiling the multi-target compounds of *Rhazya stricta*: discovery and inhibition of novel target genes for the treatment of clear cell renal cell carcinoma. *Computers in Biology and Medicine*, 165, p.107424.
201. Ricci, M.S. and Zong, W.X., 2006. Chemotherapeutic approaches for targeting cell death pathways. *The oncologist*, 11(4), pp.342-357.
202. Rojas, A., Cruz, S., Ponce-Monter, H. and Mata, R., 1996. Smooth muscle relaxing compounds from *Dodonaea viscosa*5. *Planta medica*, 62(02), pp.154-159.
203. Rojas, A., Hernandez, L., Pereda-Miranda, R. and Mata, R., 1992. Screening for antimicrobial activity of crude drug extracts and pure natural products from Mexican medicinal plants. *Journal of ethnopharmacology*, 35(3), pp.275-283.
204. Rosolen, A., Perkins, S.L., Pinkerton, C.R., Guillerman, R.P., Sandlund, J.T., Patte, C., Reiter, A. and Cairo, M.S., 2015. Revised international pediatric non-Hodgkin lymphoma staging system. *Journal of clinical oncology*, 33(18), p.2112.
205. Rosen, R.D. and Sapra, A., 2021. TNM classification. *StatPearls [Internet]*.

206. Rowinsky, E.K. and Donehower, R.C., 1995. Paclitaxel (taxol). *New England journal of medicine*, 332(15), pp.1004-1014.
207. Saferdien, A., and Mowla, S. *Investigating the anti-cancer properties of Dodonaea viscosa, a traditional medicinal plant used by Cape Bush doctors*. PhD dissertation, University of Cape Town.
208. Salinas-Sánchez, D.O., Herrera-Ruiz, M., Pérez, S., Jiménez-Ferrer, E. and Zamilpa, A., 2012. Anti-inflammatory activity of hautriwaic acid isolated from *Dodonaea viscosa* leaves. *Molecules*, 17(4), pp.4292-4299.
209. Santagostino, S.F., Assenmacher, C.A., Tarrant, J.C., Adedeji, A.O. and Radaelli, E., 2021. Mechanisms of regulated cell death: current perspectives. *Veterinary Pathology*, 58(4), pp.596-623.
210. Sapkota, S. and Shaikh, H., 2023. Non-hodgkin lymphoma. In *StatPearls [Internet]*. StatPearls Publishing.
211. Saydah, S.H. and Eberhardt, M.S., 2006. Use of complementary and alternative medicine among adults with chronic diseases: United States 2002. *Journal of Alternative & Complementary Medicine*, 12(8), pp.805-812.
212. Schilter, B., Andersson, C., Anton, R., Constable, A., Kleiner, J., O'Brien, J., Renwick, A.G., Korver, O., Smit, F. and Walker, R., 2003. Guidance for the safety assessment of botanicals and botanical preparations for use in food and food supplements. *Food and Chemical Toxicology*, 41(12), pp.1625-1649.
213. Schmittlutz, K. and Marks, R., 2021. Current treatment options for aggressive non-Hodgkin lymphoma in elderly and frail patients: practical considerations for the hematologist. *Therapeutic Advances in Hematology*, 12, p.2040620721996484.
214. Schommers, P., Hentrich, M., Hoffmann, C., Gillor, D., Zoufaly, A., Jensen, B., Bogner, J.R., Thoden, J., Wasmuth, J.C., Wolf, T. and Oette, M., 2015. Survival of AIDS-related diffuse large B-cell lymphoma, Burkitt lymphoma, and plasmablastic lymphoma in the German HIV Lymphoma Cohort. *British Journal of Haematology*, 168(6), pp.806-810.
215. Sedeta, E., Ilerhunmwuwa, N., Wasifuddin, M., Uche, I., Hakobyan, N., Perry, J., Aiwuyo, H., Abowali, H. and Avezbakiyev, B., 2022. Epidemiology of Non-Hodgkin

Lymphoma: Global Patterns of Incidence, Mortality, and Trends. *Blood*, 140(Supplement 1), pp.5234-5235.

216. Seneviwickrama, M., Gunasekera, S., Liyanage, G., Heiyanthuduwa, W. and Jayakody, S., 2023. Availability of cytotoxic medicines in the WHO essential medicine list used in treating childhood malignancies in low-income and lower-middle-income countries: a systematic review protocol. *BMJ open*, 13(6), p.e071988.
217. Shafek, R.E., Shafik, N.H., Michael, H.N., El-Hagrassi, A.M. and Osman, A.F., 2015. Phytochemical studies and biological activity of *Dodonaea viscosa* flowers extract. *Journal of Chemical and Pharmaceutical Research*, 7(5), pp.109-116.
218. Shaheen, M.O.H.A.M.E.D., Borsanyiova, M.A.R.I.A., Mostafa, S.A.M.Y., Chawla-Sarkar, M.A.M.T.A., Bopegamage, S.H.U.B.H.A.D.A. and El-Esnawy, N.A.G.W.A., 2015. In vitro effect of *Dodonaea viscosa* extracts on the replication of coxsackievirus B3 (Nancy) and rotavirus (SA-11). *J Microbiol Antimicrob Agents*, 1(2), pp.47-54.
219. Shankland, K.R., Armitage, J.O. and Hancock, B.W., 2012. Non-hodgkin lymphoma. *The Lancet*, 380(9844), pp.848-857.
220. Sherr, C.J. and Bartek, J., 2017. Cell cycle–targeted cancer therapies. *Annual Review of Cancer Biology*, 1, pp.41-57.
221. Shi, X., Lan, X., Chen, X., Zhao, C., Li, X., Liu, S., Huang, H., Liu, N., Zang, D., Liao, Y. and Zhang, P., 2015. Gambogic acid induces apoptosis in diffuse large B-cell lymphoma cells via inducing proteasome inhibition. *Scientific reports*, 5(1), p.9694.
222. Shi, Y., 2004. Caspase activation, inhibition, and reactivation: a mechanistic view. *Protein science*, 13(8), pp.1979-1987.
223. Shiels, M.S., Pfeiffer, R.M., Gail, M.H., Hall, H.I., Li, J., Chaturvedi, A.K., Bhatia, K., Uldrick, T.S., Yarchoan, R., Goedert, J.J. and Engels, E.A., 2011. Cancer burden in the HIV-infected population in the United States. *Journal of the National Cancer Institute*, 103(9), pp.753-762.
224. Singh, R.R., Kim, J.E., Davuluri, Y., Drakos, E., Cho-Vega, J.H., Amin, H.M. and Vega, F., 2010. Hedgehog signaling pathway is activated in diffuse large B-cell lymphoma and contributes to tumour cell survival and proliferation. *Leukemia*, 24(5), pp.1025-1036.

225. Sisodiya, P.S., 2013. Plant derived anticancer agents: a review. *Int. J. Res. Dev. Pharm. Life Sci*, 2(2), pp.293-308.
226. Skerry, C., Harper, J., Klunk, M., Bishai, W.R. and Jain, S.K., 2012. Adjunctive TNF inhibition with standard treatment enhances bacterial clearance in murine model of necrotic TN granulomas. *PLoS one*, 7(6): e39680
227. Sofowora, A., 1996. Research on medicinal plants and traditional medicine in Africa. *The Journal of Alternative and Complementary Medicine*, 2(3), pp.365-372.
228. Song, K.W., Issa, S. and Batchelor, T., 2021. Primary central nervous system lymphoma: epidemiology and clinical presentation. *Annals of Lymphoma*, 5.
229. Soriano, V., Miró, J.M., García-Samaniego, J., Torre-Cisneros, J., Núñez, M., Del Romero, J., Martín-Carbonero, L., Castilla, J., Iribarren, J.A., Quereda, C. and Santin, M., 2004. Consensus conference on chronic viral hepatitis and HIV infection: updated Spanish recommendations. *Journal of Viral Hepatitis*, 11(1), pp.2-17.
230. South African National Biodiversity Institute. *Dodonaea viscosa var. angustifolia*. Available at: <http://pza.sanbi.org/dodonaea-viscosa-var-angustifolia>. [Accessed: 7 March 2021].
231. Spinner, M.A. and Advani, R.H., 2022. Current Frontline Treatment of Diffuse Large B-Cell Lymphoma. *Oncology (08909091)*, 36(1).
232. Subramanian, S., Duraipandian, C., Alsayari, A., Ramachawolran, G., Wong, L.S., Sekar, M., Gan, S.H., Subramaniyan, V., Seethalakshmi, S., Jeyabalan, S. and Dhanasekaran, S., 2023. Wound healing properties of a new formulated flavonoid-rich fraction from *Dodonaea viscosa* Jacq. leaves extract. *Frontiers in Pharmacology*, 14, p.1096905.
233. Sung, H., Ferlay, J., Siegel, R.L., Laversanne, M., Soerjomataram, I., Jemal, A. and Bray, F., 2021. Global cancer statistics 2020: GLOBOCAN estimates of incidence and mortality worldwide for 36 cancers in 185 countries. *CA: a cancer journal for clinicians*, 71(3), pp.209-249.

234. Susanibar-Adaniya, S. and Barta, S.K., 2021. 2021 Update on Diffuse large B cell lymphoma: A review of current data and potential applications on risk stratification and management. *American journal of hematology*, 96(5), pp.617-629.
235. Swerdlow, S.H., Campo, E., Pileri, S.A., Harris, N.L., Stein, H., Siebert, R., Advani, R., Ghielmini, M., Salles, G.A., Zelenetz, A.D. and Jaffe, E.S., 2016. The 2016 revision of the World Health Organization classification of lymphoid neoplasms. *Blood, The Journal of the American Society of Hematology*, 127(20), pp.2375-2390.
236. Tario, J.D., Conway, A.N., Muirhead, K.A. and Wallace, P.K., 2018. Monitoring cell proliferation by dye dilution: considerations for probe selection. *Flow cytometry protocols*, pp.249-299.
237. Tario Jr, J.D., Humphrey, K., Bantly, A.D., Muirhead, K.A., Moore, J.S. and Wallace, P.K., 2012. Optimized staining and proliferation modeling methods for cell division monitoring using cell tracking dyes. *JoVE (Journal of Visualized Experiments)*, (70), p.e4287.
238. Teshome, K., Gebre-Mariam, T., Asres, K. and Engidawork, E., 2010. Toxicity studies on dermal application of plant extract of *Dodonaea viscosa* used in Ethiopian traditional medicine. *Phytotherapy Research: An International Journal Devoted to Pharmacological and Toxicological Evaluation of Natural Product Derivatives*, 24(1), pp.60-69.
239. Thapa, B., Debes-Marun, C., Breckenridge, Z.M., Sandhu, I., Daly, A., Khan, F. and Chu, M.P., 2022. Predicting Response of CD19 Chimeric Antigen Receptor (CAR) T-Cell Therapy for Acute Lymphoblastic Leukemia (ALL) and Aggressive Non-Hodgkin Lymphoma (NHL) in ACIT001/EXC002, a Phase Ib Clinical Trial. *Blood*, 140(Supplement 1), pp.12681-12682.
240. Thawabteh, A., Juma, S., Bader, M., Karaman, D., Scrano, L., Bufo, S.A. and Karaman, R., 2019. The biological activity of natural alkaloids against herbivores, cancerous cells and pathogens. *Toxins*, 11(11), p.656.

241. Tong, J., Rufli, S. and Wong, W.W.L., 2023. Measuring Caspase Activity Using a Fluorometric Assay or Flow Cytometry. *JoVE (Journal of Visualized Experiments)*, (193), p.e64745.
242. Tong, Z.W., Gul, H., Awais, M., Saddick, S., Khan, F.S., Gulfraz, M., Afzal, U., Nazir, K., Malik, M.Y., Khan, S.U. and Khan, M.I., 2021. Determination of in vivo biological activities of *Dodonaea viscosa* flowers against CCL4 toxicity in albino mice with bioactive compound detection. *Scientific Reports*, 11(1), pp.1-15.
243. Tošić, I. and Frank, D.A., 2021. STAT3 as a mediator of oncogenic cellular metabolism: Pathogenic and therapeutic implications. *Neoplasia*, 23(12), pp.1167-1178.
244. Tsai, Y.F., Liu, Y.C., Yang, C.I., Chuang, T.M., Ke, Y.L., Yeh, T.J., Gau, Y.C., Du, J.S., Wang, H.C., Cho, S.F. and Hsu, C.M., 2021. Poor prognosis of diffuse large B-Cell lymphoma with hepatitis C infection. *Journal of Personalized Medicine*, 11(9), p.844.
245. Twilley, D., Rademan, S. and Lall, N., 2020. A review on traditionally used South African medicinal plants, their secondary metabolites, and their potential development into anticancer agents. *Journal of ethnopharmacology*, 261, p.113101.
246. Ulrickson, M., Press, O.W. and Casper, C., 2012. Epidemiology, diagnosis, and treatment of HIV-associated non-Hodgkin lymphoma in resource-limited settings. *Advances in hematology*, 2012.
247. United Nations. Lifestyle Diseases: An Economic Burden on the Health Services. Available: <https://www.un.org/en/chronicle/article/lifestyle-diseases-economic-burden-health-services#:~:text=Today%2C%20chronic%20diseases%20are%20a%20major%20public%20health,burden%20of%20disease%20were%20attributable%20to%20chronic%20diseases>. Accessed: 19 January 2023.
248. USDA, Agricultural Research Service, National Plant Germplasm System., 2022. Germplasm Resources Information Network (GRIN Taxonomy). National Germplasm Resources Laboratory, Beltsville, Maryland. Available at: <https://npgsweb.ars-grin.gov/gringlobal/taxon/taxonomydetail?id=14441>. [Accessed: 10 February 2022]

249. Van der Bij, G.J., Oosterling, S.J., Beelen, R.H., Meijer, S., Coffey, J.C. and van Egmond, M., 2009. The perioperative period is an underutilized window of therapeutic opportunity in patients with colorectal cancer. *Annals of surgery*, 249(5), pp.727-734.
250. Van Wyk, B.E. and Gericke, N., 2000. *People's plants: A guide to useful plants of Southern Africa*. Briza publications.
251. Vari, F., Arpon, D., Keane, C., Hertzberg, M.S., Talaulikar, D., Jain, S., Cui, Q., Han, E., Tobin, J., Bird, R. and Cross, D., 2018. Immune evasion via PD-1/PD-L1 on NK cells and monocyte/macrophages is more prominent in Hodgkin lymphoma than DLBCL. *Blood, The Journal of the American Society of Hematology*, 131(16), pp.1809-1819.
252. Vijayarathna, S. and Sasidharan, S., 2012. Cytotoxicity of methanol extracts of *Elaeis guineensis* on MCF-7 and Vero cell lines. *Asian pacific journal of tropical biomedicine*, 2(10), pp.826-829.
253. Voicu, V., Brehar, F.M., Toader, C., Covache-Busuioc, R.A., Corlatescu, A.D., Bordeianu, A., Costin, H.P., Bratu, B.G., Glavan, L.A. and Ciurea, A.V., 2023. Cannabinoids in Medicine: A Multifaceted Exploration of Types, Therapeutic Applications, and Emerging Opportunities in Neurodegenerative Diseases and Cancer Therapy. *Biomolecules*, 13(9), p.1388.
254. Wagner, H., Ludwig, C., Grotjahn, L. and Khan, M.S., 1987. Biologically active saponins from *Dodonaea viscosa*. *Phytochemistry*, 26(3), pp.697-701.
255. Waibel, M., Gregory, G., Shortt, J. and Johnstone, R.W., 2014. Rational combination therapies targeting survival signaling in aggressive B-cell leukemia/lymphoma. *Current Opinion in Hematology*, 21(4), pp.297-308.
256. Wang, H., Zhang, W., Yang, J. and Zhou, K., 2021. The resistance mechanisms and treatment strategies of BTK inhibitors in B-cell lymphoma. *Hematological Oncology*, 39(5), pp.605-615.
257. Wang, L., Hu, C. and Shao, L., 2017. The antimicrobial activity of nanoparticles: present situation and prospects for the future. *International journal of nanomedicine*, 12, p.1227.

258. Wang, L., Li, L.R. and Young, K.H., 2020. New agents and regimens for diffuse large B cell lymphoma. *Journal of Hematology & Oncology*, 13(1), pp.1-23.
259. Wang, Z., Zhang, R., Liu, L., Shen, Y., Chen, J., Qi, T., Song, W., Tang, Y., Sun, J., Lin, Y. and Xu, S., 2021. Incidence and spectrum of infections among HIV/AIDS patients with lymphoma during chemotherapy. *Journal of Infection and Chemotherapy*, 27(10), pp.1459-1464.
260. Wani, A.K., Akhtar, N., Mir, T.U.G., Singh, R., Jha, P.K., Mallik, S.K., Sinha, S., Tripathi, S.K., Jain, A., Jha, A. and Devkota, H.P., 2023. Targeting apoptotic pathway of cancer cells with phytochemicals and plant-based nanomaterials. *Biomolecules*, 13(2), p.194.
261. WebMD, 2021. Burkitt Lymphoma. Available: <https://www.webmd.com/cancer/lymphoma/burkitt-lymphoma-prognosis-diagnosis-treatments>. Accessed: 10 February 2024.
262. Weaver, B.A., 2014. How Taxol/paclitaxel kills cancer cells. *Molecular biology of the cell*, 25(18), pp.2677-2681.
263. Wei, T., Li, M., Zhu, Z., Xiong, H., Shen, H., Zhang, H., Du, Q. and Li, Q., 2021. Vincristine upregulates PD-L1 and increases the efficacy of PD-L1 blockade therapy in diffuse large B-cell lymphoma. *Journal of Cancer Research and Clinical Oncology*, 147, pp.691-701.
264. Wiernicki, B., Dubois, H., Tyurina, Y.Y., Hassannia, B., Bayir, H., Kagan, V.E., Vandenabeele, P., Wullaert, A. and Vanden Berghe, T., 2020. Excessive phospholipid peroxidation distinguishes ferroptosis from other cell death modes including pyroptosis. *Cell death & disease*, 11(10), p.922.
265. World Health Organization, 2013. *WHO traditional medicine strategy: 2014-2023*. World Health Organization.
266. World Health Organization, 2019. *WHO global report on traditional and complementary medicine 2019*. Available: <https://www.who.int/publications/i/item/978924151536>. Accessed: 19 January 2023.

267. World Health Organization, 2023. *Diabetes*. Available: <https://www.who.int/news-room/fact-sheets/detail/diabetes>. Accessed: 10 April 2023.
268. World Health Organization., 2021. *Cancer Fact Sheet*. Available at: <https://www.who.int/news-room/fact-sheets/detail/cancer>. [Accessed: 2 February 2022]
269. World Health Organization (WHO), 2022. *Noncommunicable disease*. Available: <https://www.who.int/news-room/fact-sheets/detail/noncommunicable-diseases>. Accessed: 19 January 2023.
270. Wu, Y., Dong, G. and Sheng, C., 2020. Targeting necroptosis in anticancer therapy: mechanisms and modulators. *Acta Pharmaceutica Sinica B*, 10(9), pp.1601-1618.
271. Xing, X., Wang, X., Liu, M., Guo, Q. and Wang, H., 2023. Ras interacting protein 1 facilitated proliferation and invasion of diffuse large B-cell lymphoma cells. *Cancer Biology & Therapy*, 24(1), p.2193114.
272. Xu, W., Berning, P. and Lenz, G., 2021. Targeting B-cell receptor and PI3K signaling in diffuse large B-cell lymphoma. *Blood, The Journal of the American Society of Hematology*, 138(13), pp.1110-1119.
273. Xu-Monette, Z.Y., Wu, L., Visco, C., Tai, Y.C., Tzankov, A., Liu, W.M., Montes-Moreno, S., Dybkær, K., Chiu, A., Orazi, A. and Zu, Y., 2012. Mutational profile and prognostic significance of TP53 in diffuse large B-cell lymphoma patients treated with R-CHOP: report from an International DLBCL Rituximab-CHOP Consortium Program Study. *Blood, The Journal of the American Society of Hematology*, 120(19), pp.3986-3996.
274. Yang, G., Zhang, Q., Kong, Y., Xie, B., Gao, M., Tao, Y., Xu, H., Zhan, F., Dai, B., Shi, J. and Wu, X., 2015. Antitumour activity of fucoidan against diffuse large B cell lymphoma in vitro and in vivo. *Acta biochimica et biophysica Sinica*, 47(11), pp.925-931.
275. Younes, A., Sehn, L.H., Johnson, P., Zinzani, P.L., Hong, X., Zhu, J., Patti, C., Belada, D., Samoilova, O., Suh, C. and Leppä, S., 2019. Randomized phase III trial of ibrutinib and rituximab plus cyclophosphamide, doxorubicin, vincristine, and prednisone in non-germinal center B-cell diffuse large B-cell lymphoma. *Journal of Clinical Oncology*, 37(15), p.1285.

276. Young, L., Sung, J., Stacey, G., and Masters, J.R., 2010. Detection of Mycoplasma in cell cultures. *Nature protocols*, 5(5), pp.929-934.
277. Young, R.M., Shaffer III, A.L., Phelan, J.D. and Staudt, L.M., 2015, April. B-cell receptor signaling in diffuse large B-cell lymphoma. In *Seminars in hematology* (Vol. 52, No. 2, pp. 77-85). WB Saunders.
278. Zahavi, D. and Weiner, L., 2020. Monoclonal antibodies in cancer therapy. *Antibodies*, 9(3), p.34.
279. Zhan, X.Z., Wei, T.H., Yin, Y.Q., Xu, J.Q., Yu, H., Chen, X.L., Kong, X.T., Sun, S.L., Li, N.G. and Ni, H.W., 2024. Determination and mechanism of Xiao-Ai Jie-Du decoction against diffuse large B-cell lymphoma: In silico and In vitro studies. *Journal of Ethnopharmacology*, 319, p.117271.
280. Zhang, B., Calado, D.P., Wang, Z., Fröhler, S., Köchert, K., Qian, Y., Koralov, S.B., Schmidt-Suppryan, M., Sasaki, Y., Unitt, C. and Rodig, S., 2015. An oncogenic role for alternative NF- κ B signaling in DLBCL revealed upon deregulated BCL6 expression. *Cell reports*, 11(5), pp.715-726.
281. Zhang, H., Chi, F., Qin, K., Mu, X., Wang, L., Yang, B., Wang, Y., Bai, M., Li, Z., Su, L. and Yu, B., 2021. Chidamide induces apoptosis in DLBCL cells by suppressing the HDACs/STAT3/Bcl-2 pathway. *Molecular Medicine Reports*, 23(5), pp.1-9.

Appendix A

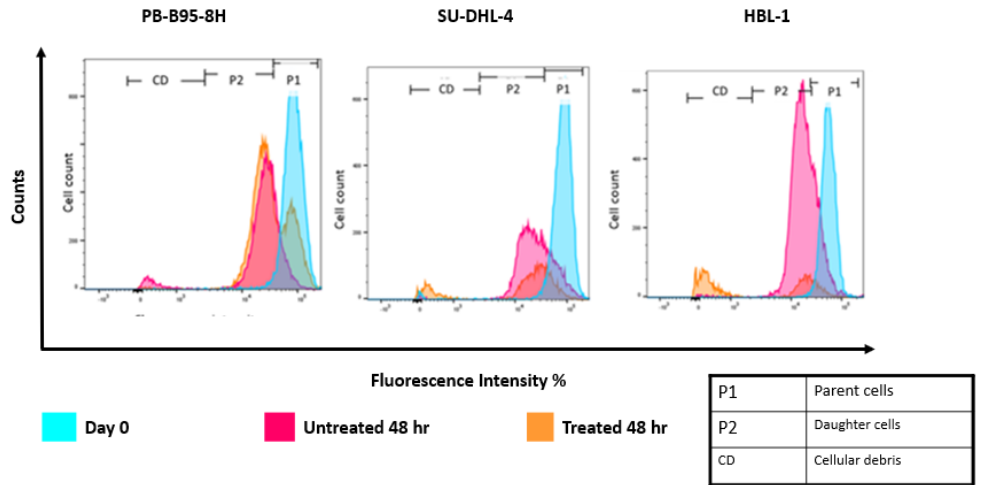


Figure A1. DVE slows down the proliferation of DLBCL cells in comparison to LCLs and induces cell death. DLBCL cell lines SU-DHL-4 and HBL-1 as well as a non-cancerous cell line PB-B95-8H were stained with 0.5 μ M CFSE Cell Trace dye, seeded and treated with either vehicle (PBS) (untreated – UT) or DVE (40 μ g/ml) (Treated -T). After 48 hours of treatment cells were fixed in 70% methanol and samples were examined using BD flow cytometry (FACSCalibur™, Becton Dickinson, USA). A T = 0 sample was included to track P1 (parental cell) generation and P2 (daughter cell generation). Analysis was performed using the FlowJo v10.9 software. The experiment was carried out twice.

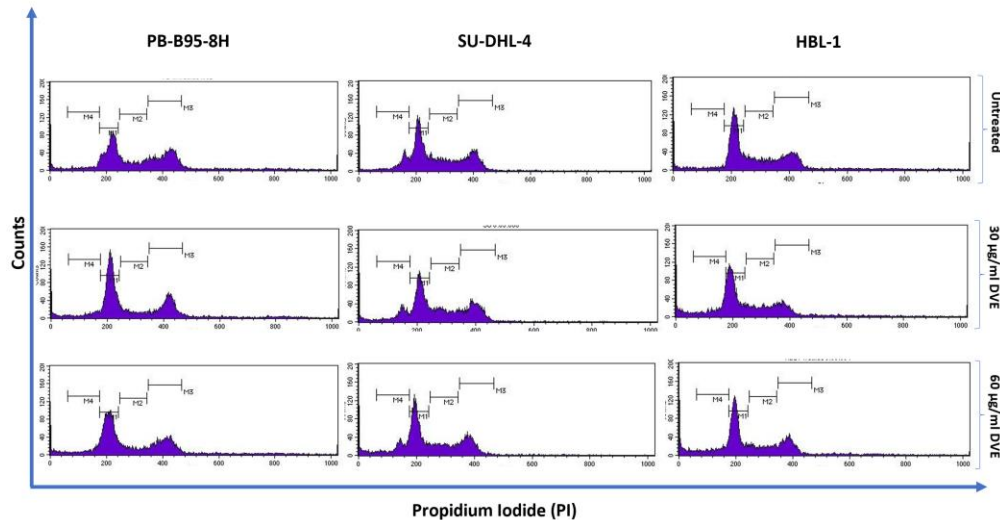


Figure A2. DVE does not modify the cell cycle profile of DLBCL cells and induces cell death. DLBCL cell lines SU-DHL-4 and HBL-1, as well as a non-cancerous cell line PB-B95-8H, were seeded, and treated with DVE (30 and 60 μ g/ml) or with 1x PBS (vehicle control-untreated (UT)) for 24 hours. Post-treatment, the

cells were stained with FxCycle™ PI/RNase and fixed using 70% methanol. Subsequently, the samples were analysed using BD Flow Cytometry (FACSCalibur™, Becton Dickinson, USA). The experiment was conducted at least three times.

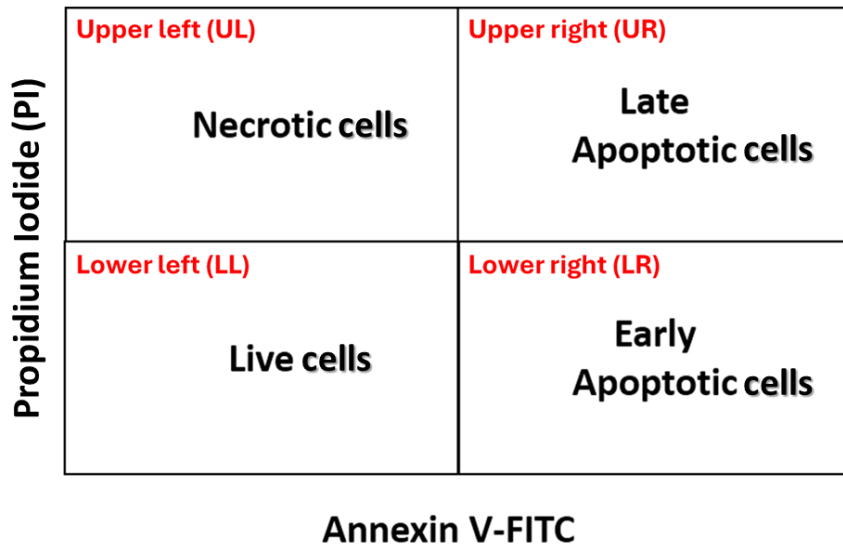


Figure A3. Schematic of the expected staining illustration of cell populations in Annexin V/PI assay experiment. (LL – lower left, LR – lower right, UL – upper left, UR – upper right).

Appendix B

Reagents

10% Ammonium persulfate (APS)

0.1 g of stock APS

1 ml of ddH₂O, store at 4°C

5% Bovine Serum Albumin (BSA) in phosphate-buffered Saline + 0.1% Tween (PBST)

5 g BSA

Up to 100 mL of PBS

Complete media for DLBCL cell lines (50 ml)

10% Foetal Bovine Serum (FBS) – 5 ml of FBS

1% Pen/Strep – 0.5 mL

Roswell Park Memorial Institute (RPMI) 1640 Medium – 44.5 ml

Complete media for the Lymphoblastoid Cell line (50 ml)

20% Foetal Bovine Serum (FBS) – 10 ml of FBS

1% Pen/Strep – 0.5 mL

Roswell Park Memorial Institute (RPMI) 1640 Medium – 39.5 ml

5% Fat-free milk in Tris-Buffered Saline + 0.1% Tween (TBST)

5 g Fat-free milk

Up to 100 mL of TSBT

Fixing solution (50 ml)

Glacial acetic acid: Methanol 1:3 (Keep at 4°C)

17 ml Glacial acetic acid

33 ml Methanol

Freezing medium (50 ml)

10% Foetal Bovine Serum (FBS) – 5 ml of FBS

10% Dimethyl sulfoxide (DMSO) – 5 ml of DMSO

Roswell Park Memorial Institute (RPMI) 1640 Medium – 40 ml

Mounting Fluid

Citric acid – disodium phosphate buffer

0.1 M Citric acid

0.2 M $\text{Na}_2\text{HPO}_4 \cdot 2\text{H}_2\text{O}$

pH 5.5, 4°C

1 X PBS-Tween

100 ml 10X PBS

0.5 ml Tween-20

Make up to 1 L with ddH₂O

10 X PBS

40 g NaCl

1 g KCl

1 g KH_2PO_4

5.75 g $\text{Na}_2\text{HPO}_4 \cdot 2\text{H}_2\text{O}$

2.1 g KH_2PO_4

Up to 500 ml with ddH₂O

pH of 7.4, autoclave

Ponceau S stain

0.1 g of Ponceau powder

95 ml of ddH₂O

5 ml of glacial acetic acid

7X Protease inhibitor

1 protease inhibitor tablet

2.5 ml 1X PBS

Store at -20°C

RIPA buffer

0.5 g (1%) deoxycholate powder in 40 ml ddH₂O

1.5 ml 5M NaCl (150 mM)

0.5 ml Triton X100 (1%)

0.25 ml 20% SDS (0.1%)

0.5 ml 1M Tris (pH 7.5) (10 mM)

Top up to 50 ml with ddH₂O

Store at 4°C

RIPA cell lysis buffer solution

423 µl RIPA buffer

71 µl 7X protease inhibitor

Store on ice until use

10 % SDS

10 g SDS

80 ml ddH₂O

Dissolve and make up to 100 ml ddH₂O

Gentle heat until the crystals disappear

5 X SDS Protein loading dye.

10% sodium dodecyl-sulphate (SDS) – 1 g

0.04% bromophenol blue – 0.004 g

4.83 ml of ddH₂O

1.5 M Tris (pH 6.8) - 1.67 ml

100% glycerol – 3 ml

0.5 ml β-mercaptoethanol

10X SDS-PAGE running buffer.

10 g SDS

30.3 g Tris

144.1 g glycine

800 ml ddH₂O

Adjust to 1 L of ddH₂O and store at room temperature.

1X SDS-PAGE running buffer.

100 ml of 10X SDS-PAGE running buffer stock

900 ml ddH₂O

Store at room temperature.

10X SDS-PAGE transfer buffer

38 g Tris

144 g glycine

800 ml ddH₂O.

Adjust volume to 1 L with ddH₂O and store at room temperature.

1X SDS-PAGE transfer buffer

100 ml 10X SDS-PAGE transfer buffer stock

700 ml ddH₂O

200 ml Isopropanol

Make in advance and store at 4°C.

30% acryl-bisacrylamide

29 g acrylamide

1 g N,N'-methylenebisacrylamide

60 ml ddH₂O

Heat the solution to 37°C.

Adjust volume to 100 ml and cover with foil to protect from light Store at 4°C.

8% Resolving gel (10 ml)

3.3 ml ddH₂O

30% acryl-bisacrylamide – 2.7 ml

1 M Tris pH 6.8 – 3.9 ml

10% SDS – 0.1 ml

10% APS – 0.1 ml

TEMED – 0.004 ml

15% Resolving gel (7.5 ml)

0.67 ml ddH₂O

30% acryl-bisacrylamide – 3.75 ml

1 M Tris pH 6.8 – 2.93 ml

10% SDS – 0.075 ml

10% APS – 0.075 ml

TEMED – 0.003 ml

5% Stacking gel (3 ml)

1.87 ml ddH₂O

30% acryl-bisacrylamide – 0.5 ml

1 M Tris pH 6.8 – 0.57 ml

10% SDS – 0.03 ml

10% APS – 0.03 ml

TEMED – 0/003 ml

Stripping buffer (100 ml)

0.5 M Tris HCL – 12.5 ml

10% SDS – 20 ml

2-mercaptoethanol – 0.8 ml

ddH₂O – 67.5 ml

Make in a fume hood

10 X TBS

12 g Tris

44 g NaCl

pH 7.6

Up to 500 ml ddH₂O, stock at 4°C

1 X TBS-Tween

100 ml 10X TBS

900 ml ddH₂O

0.5 ml Tween-20

Makeup to 1 L with ddH₂O

1 M Tris

121 g Tris base

800 ml ddH₂O

pH to 6.8, 7.5 or 8.8.

Make up to 1 L with ddH₂O, then autoclave.

Appendix C

Research Output by the MSc candidate during the research period.

1. Yekelo, B., and Mowla, S. Aqueous extracts of *Dodonaea viscosa* var. *angustifolia* induce potent and selective cytotoxicity against Diffuse large B cell lymphoma. Postgraduate Academic Training program, University of Cape Town, Faculty of Health Sciences. 7 July 2022. Oral presentation.
2. Yekelo, B., and Mowla, S. Aqueous extracts of *Dodonaea viscosa* var. *angustifolia* induce potent and selective cytotoxicity against Diffuse large B cell lymphoma. Annual Cell Biology Seminar, University of Cape Town, Faculty of Health Sciences. 14 September 2023. Oral presentation.
3. Yekelo, B., and Mowla, S. Aqueous extracts of *Dodonaea viscosa* var. *angustifolia* induce potent and selective cytotoxicity against Diffuse large B cell lymphoma. 15th Annual Haematology Symposium, Cape Town, South Africa. 16 September 2023. Oral presentation: Won best oral presentation.
4. Yekelo, B., and Mowla, S. Aqueous extracts of *Dodonaea viscosa* var. *angustifolia* induce potent and selective cytotoxicity against Diffuse large B cell lymphoma. 2023 Interdepartmental HUB/IBMS/Pathology (HIP) research day, University of Cape Town, Faculty of Health Sciences. Oral presentation: Won second-best oral presentation prize.

Appendix D



UNIVERSITY OF CAPE TOWN
Faculty of Health Sciences
Human Research Ethics Committee



E53-Room 46 Old Main Building
Groote Schuur Hospital
Observatory 7925

Email: hrec-enquiries@uct.ac.za

Website: <https://health.uct.ac.za/home/human-research-ethics>

30 October 2023

HREC REF: 813/2023

A/Prof S Mowla
Pathology/Haematology
Email PI: shaheen.mowla@uct.ac.za
Student: yklbab001@myuct.ac.za

Dear A/Prof Mowla

PROJECT TITLE: THE CYTOTOXIC EFFECT OF EXTRACTS OF DODONAEA VISCOSA, A TRADITIONAL HERBAL MEDICINE, ON NON-HODGKIN LYMPHOMA CELL

Thank you for submitting your study to the Faculty of Health Sciences Human Research Ethics Committee for review and approval.

It is a pleasure to inform you that the HREC has **formally approved** your Cell Line application as titled above.

*The HREC acknowledges that **Ms Babalwa Yekelo** will also be involved in the study:*

Please note that the ongoing ethical conduct of the study remains the responsibility of the principal investigator.

Please quote the above HREC Reference Number C001/2023 in all your correspondence.

Yours sincerely

A handwritten signature in black ink, appearing to read 'M. Blockman', written over a horizontal line.

PROFESSOR MARC BLOCKMAN
CHAIRPERSON, FACULTY OF HEALTH SCIENCES HUMAN RESEARCH ETHICS COMMITTEE